REDUCTIVE TRANSFORMATION OF 2,4,6-TRINITROTOLUENE BY *YARROWIA LIPOLYTICA* AN-L15 UNDER CONDITIONS OF DIFFERENT INITIAL pH OF THE CULTURE MEDIUM OR IN THE PRESENCE OF FERRIHYDRITE

by

Andy Joseph Pannier

A thesis submitted in partial fulfillment
of the requirements for the degree

of

Master of Science

in

Microbiology

MONTANA STATE UNIVERSITY
Bozeman, Montana

April 2009

APPROVAL

of a thesis submitted by

Andy Joseph Pannier

This thesis has been read by each member of the thesis committee and has been found to be satisfactory regarding content, English usage, format, citation, bibliographic style, and consistency, and is ready for submission to the Division of Graduate Education.

Dr. Robin Gerlach

Approved for the Department of Microbiology

Dr. Michael Franklin

Approved for the Division of Graduate Education

Dr. Carl A. Fox

STATEMENT OF PERMISSION TO USE

In presenting this thesis in partial fulfillment of the requirements for a master's degree at Montana State University, I agree that the Library shall make it available to borrowers under rules of the Library.

If I have indicated my intention to copyright this thesis by including a copyright notice page, copying is allowable only for scholarly purposes, consistent with "fair use" as prescribed in the U.S. Copyright Law. Requests for permission for extended quotation from or reproduction of this thesis in whole or in parts may be granted only by the copyright holder.

Andy Joseph Pannier

April 2009

TABLE OF CONTENTS

1. INTRODUCTION 1

2,4,6-Trinitrotoluene: A Xenobiotic, Nitroaromatic Compound 2
Yarrowia lipolytica AN-L15 6
Previous Work Pertaining to TNT Transformation 9
Biotic Transformation of TNT 9
Aromatic Ring Reduction of TNT 10
Nitro-Group Reduction of TNT 13
Combining Biotic and Abiotic Transformation of TNT 16
Goal of Research 17

2. MATERIALS AND METHODS 19

Yarrowia lipolytica AN-L15, Growth Media and Culturing Methods 19
Standards and Stocks 19
Growth Indicator Measurements 21
TNT-Metabolite Analysis 22
Iron Assay 23
Analysis of Nitrite and Nitrate 23
Experimental Setups 24
Reduction of TNT by *Y. lipolytica* AN-L15 at Different Initial pH of the Culture Medium 24
Reduction of TNT by *Y. lipolytica* AN-L15 in the Presence of Ferrihydrite 26

3. RESULTS 27

Effects on TNT Reduction by *Y. lipolytica* AN-L15 with Different Initial pH of the Culture Medium 27
Results from the Three Sets of Treatments with Different Initial pH Values 33
Changes in Patterns of Growth 34
Transformation of TNT and Formation of TNT-Metabolites 38
Reductive Transformation of TNT by *Y. lipolytica* AN-L15 in the Presence of Ferrihydrite 44
Growth Curves 45
Iron Analysis and pH Changes 46
Aromatic Ring Reduction, Products and Denitration 51
Formation of TNT-Metabolites via the Nitro-Group Reduction Pathway 59

TABLE OF CONTENTS CONTINUED

4. DISCUSSION 62

Reduction of TNT by *Y. lipolytica* AN-L15 with Different Initial pH of the Culture Medium 62
Reductive Transformation of TNT by *Y. lipolytica* AN-L15 in the Presence of Ferrihydrite 65
Future Work 71

5. SUMMARY 74

APPENDICES 76

APPENDIX A: Reduction of TNT by *Y. lipolytica* AN-L15 Under Constant Flow Conditions with an Initial pH of 4.5 77

APPENDIX B: Data Table for the Study of TNT Transformation by *Y. lipolytica* AN-L15 with Different Initial pH of the Culture Medium 95

APPENDIX C: Data Table for the Study of TNT Transformation by *Y. lipolytica* AN-L15 in the Presence of Ferrihydrite 113

APPENDIX D: Data Table for the Study of TNT Transformation by *Y. lipolytica* AN-L15 Under Constant Flow Conditions 140

REFERENCES CITED 146

LIST OF TABLES

Table Page

1. Physical and chemical properties of 2,4,6-trinitrotoluene 4

2. Retention times for TNT and TNT-metabolites 31

3. Stoichiometric balances of treatments from the study of *Y. lipolytica* AN-L15 in the presence of TNT and in the presence or absence of ferrihydrite 72

LIST OF FIGURES

Figure Page

1. 2,4,6-trinitrotoluene in crystalline form 2
2. Chemical structure of TNT 3
3. *Y. lipolytica* AN-L15 cells as viewed by microscopy and colonies growing on agar 8
4. Formation of 3-H^--TNT 10
5. Aromatic ring reduction pathway of TNT transformation 12
6. Nitro-group reduction pathway of TNT transformation 14
7. Condensation reaction resulting in formation of azoxy and azo compounds 15
8. Electron shuttling 16
9. Comparison, with Ziganshin et al. (2007), absorbance measurements 28
10. Chromatograms of metabolites from Ziganshin et al. (2007) and pH 7.0 original treatments 30
11. Comparison, with Ziganshin et al. (2007), of TNT reduction and TNT-metabolite formation 33
12. Absorbance measurements for the three sets of treatments with different initial pH 35
13. Fold change in growth (OD_{600}) of *Y. lipolytica* AN-L15 in the presence of absence of TNT 36
14. Change in pH over time for the three sets of treatments with different initial pH 37
15. Transformation of TNT and formation of TNT-metabolites for the three sets of treatments with different initial pH 40
16. Color changes of medium as hydride and dihydride-Meisenheimer complexes form 41

LIST OF FIGURES CONTINUED

Figure Page

17. Comparison of the formation of hydride and dihydride-Meisenheimer complexes for the three sets of treatments with different initial pH 43

18. Growth curves for the four sets of treatments in the ferrihydrite study 46

19. Changes in the concentrations of Fe(II), total Fe, and the pH values for the four sets of treatments in the ferrihydrite study 50

20. Color changes of medium as hydride and dihydride-Meisenheimer complexes form 52

21. TNT and 3-H^--TNT concentrations for the four set of treatments in the ferrihydrite study 54

22. Comparison of the formation of hydride and dihydride-Meisenheimer complexes for the four sets of treatments in the ferrihydrite study 57

23. Peak areas of 3,5-2H^--TNT-H^+ compared with nitrite formation 58

24. Formation of TNT-metabolites via the nitro-group reduction pathway for the four sets of treatments in the ferrihydrite study 61

25. Fold change in growth (protein) of *Y. lipolytica* AN-L15 in the presence of TNT and the presence or absence of ferrihydrite 67

26. Pathway of formation of nitrite and diarylamines 68

27. Schematic of the oxidation of 3-H^--TNT to TNT 70

28. Schematic of column set up 80

29. Absorbance measurements from the column study 84

30. pH values from the column study 86

LIST OF FIGURES CONTINUED

Figure Page

31. Transformation of TNT and formation of TNT-metabolites from the influent of the column study 89

32. Transformation of TNT and formation of TNT-metabolites from the effluent of the column study 90

33. Microscopy images from silicone tubing and glass bead 91

34. Protein concentrations throughout the disassembled columns 92

Nomenclature

ADNT – aminodinitrotoluene

AQDS – anthraquinone-2,6-disulfonate

Azo – tetranitroazotoluene

Azoxy – tetranitroazoxytoluene

DANT – diaminonitrotoluene

DNT – dinitrotoluene

EtOH – ethanol

Fe(II) – ferrous iron

Fe(III) – ferric iron

HADNT – hydroxylaminodinitrotoluene

HCl – hydrochloric acid

HPLC – high performance liquid chromatograph

NaOH – sodium hydroxide

NO-DNT - nitrosodinitrotoluene

OD – optical density

TAT – 2,4,6-triaminotoluene

TNT – 2,4,6-trinitrotoluene

UXO – unexploded ordnance

GLOSSARY

Azoxy – A compound having the general structure of R-N=N(O)-R' formed by the condensation of nitroso and hydroxylaminodinitrotoluene compounds.

Azo – A compound having the functional group R-N=N-R' (R and R' can be aryl or alkyl), formed from the reduction of azoxy compounds.

Cometabolic degradation – A process in which a substance may be degraded only in the presence of a primary source of carbon.

Hemiascomycetous – A class of fungi in the phylum Ascomycota, they do not have ascocarps (fruiting bodies).

Hydrocarbon – An organic compound consisting entirely of carbon and hydrogen.

Isomer – A chemical compound that has the same molecular formula but different structural formula.

Obligate aerobe – An organism that requires the presence of oxygen in its environment.

Ortho – substituents occupy positions next to each other (R and ortho in figure)

Para – substituents occupy positions opposite each other (R and para in figure)

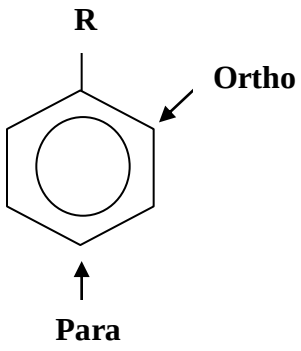

Recalcitrance – Compounds that are difficult to degrade under natural conditions.

Regioselectivity – A chemical reaction in which one structural isomer is favored over another.

Xenobiotic – Substances that are foreign to the entire biological system, often man made substances.

ABSTRACT

Batch and column studies were conducted to examine the difference in the transformation pathways of 2,4,6-trinitrotoluene (TNT) reduction by a hemiascomycetous yeast (*Yarrowia lipolytica* AN-L15) under conditions of different initial pH of the culture medium or in the presence or absence of ferrihydrite. Using high performance liquid chromatography (HPLC), it was observed that *Y. lipolytica* AN-L15 was able to transform TNT at three different initial proton concentrations of the culture medium: pH 7.0, pH 6.5, and pH 4.5. In the presence of TNT, *Y. lipolytica* AN-L15 showed preferential growth (OD_{600}) at the lower initial pH of 4.5. The increased growth (OD_{600}) resulted in increased reduction of TNT-metabolites in the culture medium with an initial pH of 4.5, as compared to, the culture medium with an initial pH of 6.5 or the culture medium with an initial pH of 7.0. TNT transformation via aromatic ring reduction was the major transformation pathway observed, with the major metabolite being 3-H^--TNT. 4-hydroxylaminodinitrotoluene (4-HADNT) was the major metabolite of the nitro-group reduction pathway. In the presence of ferrihydrite at a pH of 7.0, the transformation of TNT by *Y. lipolytica* AN-L15 showed a change in the transformation pathway. Nitro-group reduction was the major pathway of TNT transformation in the presence of ferrihydrite with 4-HADNT and 2-aminodinitrotoluene (4-ADNT) being the major metabolites formed. The time it took to reduce TNT was longer and the concentrations of TNT-metabolites were lower in the presence of ferrihydrite than in its absence. This may have been due to competition for available electrons between TNT and TNT-metabolites and Fe(III). It is also possible that some of the intermediate products of TNT transformation were oxidized back to TNT-metabolites by Fe(III) resulting in lower concentrations of TNT-metabolites and increased concentrations of Fe(II). This study demonstrates the complexity of the interactions of various environmental parameters, under controlled laboratory conditions, in the transformation of TNT by *Y. lipolytica* AN-L15.

INTRODUCTION

Xenobiotic, from the Greek ξένος (*xenox)* = foreign, βίος *(bios)* = life, in the context of environmental pollutants, refers to substances that are foreign to the entire biological system. For example, xenobiotics are chemicals that only exist in nature through the synthesis of the compound by man. Such compounds have a tendency to accumulate in nature due to the lack of adaptive degradative enzymes in organisms. Because the compounds are relatively new to the environment, the microorganisms in the environment have not developed the degradative pathway enzymes necessary to use these compounds as nutrient or energy sources. Often times, few microorganisms can use the compounds even cometabolically, which is to say they have difficulties degrading the initial compounds with their current repertoire of enzymes. Due to the quick adaptability of microorganisms, they are able to alter metabolic systems, drawing on pathways that have developed over long periods of time to derive new pathways that can begin to initiate the degradative cycle of the xenobiotic compounds (Rieger et al., 2002; Timmis and Piper, 1999). Of interest in this study is one of these xenobiotic compounds, 2,4,6-trinitrotoluene (TNT) (Figure 1).

Figure 1. 2,4,6-trinitrotoluene in its crystalline form. This TNT is 99% pure thus giving a clear coloration to the crystals; less pure TNT often has yellow crystals.

2,4,6-Trinitrotoluene: A Xenobiotic, Nitroaromatic Compound

The majority of nitroarenes present in the environment are xenobiotics. The compounds are used universally, throughout the world as explosives, pesticides, cleaning agents, and raw materials for synthesis of other products, such as dyes, pharmaceuticals, solvents, polyurethane, and numerous polymers (Stenuit et al., 2005). These chemicals proliferate throughout the environment due to their large-scale industrial and military use.

TNT is a trinitroaromatic, xenobiotic compound. It was synthesized in 1863 by the German chemist, Joseph Wilbrand to be used as a yellow dye. It was not until about

thirty years later that the explosive potential of TNT was realized. Wilbrand, speaking of his research, which led to the isolation of the symmetrical TNT compound, says:

> "The preparation of trinitrotoluene is very easy. Toluene is heated to about boiling temperature with a mixture of fuming nitric and sulphuric acids for a day. The acid mixture is agitated with water, and the residue is crystallized after washing with water and drying with alcohol" (Smith, 1918).

TNT is made by the sequential nitration of toluene by a mixture of nitric and sulfuric acids, a continuous process that uses counter flow of acids and an organic (toluene) phase. The 2,4,6-TNT isomer is purified from the asymmetrical TNT isomers with sodium sulfite in a process called selliting. Selliting produces water-soluble dinitrotoluenesulfonic acids as waste products that can be readily separated from TNT, which is present as oil in the production stream (Lewis et al., 2004).

Some other names used for TNT are: trinitrotoluol, 1-methyl-2,4,6-trinitrobenzene, methyltrinitrobenzene, tolit, trilit, alpha-trinitrotoluol, tolite, triton, tritol, trilite, and trinol. Its chemical composition is $C_6H_2(NO_2)_3CH_3$ (Figure 2).

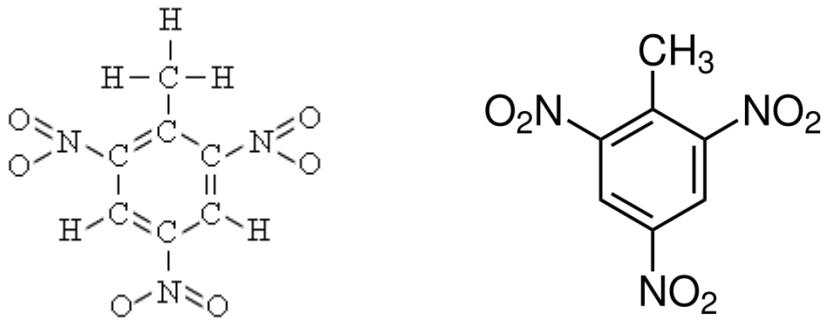

Figure 2. Chemical structure of TNT. The structure on the left is the complete structure. The structure on the right is the most common way to see it drawn.

TNT is classified as a secondary explosive because it is less susceptible to initiation than a primary explosive and requires a primary or initiating explosive for ignition. Also, TNT may be mixed with other explosives such as Cyclotrimethylenetrinitramine (RDX) and Octogen (HMX), and it is a constituent of many explosives, such as Amatol, Pentolite, Tetrytol, Torpex, Tritonal, Picratol, and Ednatol. The advantages of TNT include low cost, safety in handling, fairly high explosive power, good chemical and thermal stability, and compatibility with other explosives. It has a melting point significantly lower than its ignition point (Table 1), which allows it to be liquefied and molded into specific shape charges and blended with other explosives, adding pliability and stability to them. Various other physical and chemical properties of TNT are shown in Table 1.

Table 1. Physical and chemical properties of 2,4,6-trinitrotoluene.

Characteristic	Value
Molecular weight	227.13 g/mol
Density	1.654 at 4^{o} C
Melting point	81^{o} C
Ignition point	300^{o} C
Boiling point	240^{o} C
Solubility	25° C water solubility of 0.01%
Solubility in other than water	Soluble in alcohol, benzene, toluene, acetone
Physical structure	Clear or yellow crystal

TNT is one of the most widely used explosive compounds in the world and has been since World War I. The overarching reason it is in such demand as an explosive compound is the relative stability (insensitivity to friction and shock) of the compound. TNT is used as the standard of measure for all explosives; for example, a 1-kiloton bomb

has the explosive capacity of 1 kiloton of TNT. During World War II, Germany and the United States reached peak levels of TNT production. Germany produced 800,000 tons of TNT annually (Daun et al., 1998) throughout the war, and the United States annual production of TNT increased from 350,000 tons in World War I to 1.8 million tons in World War II (Croddy and Wirtz, 2005). This massive production led to the build up and disposal of large concentrations of waste laden with explosives. Additionally, the decommissioning of outdated armaments and the impure burning of explosives (duds) on training sites has led to significant contamination of the soils and ground water throughout the world. In the U. S., the Army has estimated the contamination of soils by explosives to exceed 1.2 million tons (Hampton et al., 1977). According to ATK Armament Systems, concern has been on the rise in the U. S. due to the initiation of the production of TNT in 2005. Production of TNT at military ammunition plants had been halted in 1980, but with the onset of the wars in Afghanistan and Iraq the need for explosives compounds has increased. This has led to restarting the production of TNT at three military ammunition plants in the U. S. since 2005 and public concern about further TNT contamination.

The recalcitrance of TNT is due to the protection of the π-electrons of the aromatic ring against oxidative and electrophilic mechanisms (Heiss and Knackmuss, 2002). The steric effects due to the symmetrical position of the three nitro groups also play a significant role in the recalcitrance of TNT (Stenuit et al., 2005).

Because of its abundant production, use, and its ability to act as a reservoir for contamination due to its recalcitrance, TNT is an environmental contaminant of concern.

It is listed on the Comprehensive Environmental Response, Compensation, and Liability Act (CERCLA) (Superfund) Priority List of Hazardous Substances, by the U. S. Department of Health and Human Services (2007 CERCLA). It is also listed by the United States Environmental Protection Agency (U. S. EPA) as a pollutant of concern. It enters the environment as a contaminant at production sites when waste is disposed of, and on military installations, where it is used in training and remains present in the form of unexploded ordinance (UXO). Additionally, the U. S. military has millions of kilograms of explosives that have reached the end of their shelf-life of about 20 – 50 years, but which are difficult to dispose of due to environmental concerns (Giles, 2004).

The toxicological effects of TNT are several. The U. S. EPA lists it as a Class C potential human carcinogen. TNT and the dinitrotoluene (DNT) isomers have been shown to be toxic and mutagenic (Honeycutt et al., 1996) and the DNT isomers are carcinogenic (Rosenblatt et al., 1991). TNT has been shown to inhibit the function of lymphocytes and monocytes in humans (Beltz et al., 2001; Bruns-Nagel et al., 1999). It has been shown to cause cytotoxic effects in the liver (Lui et al., 1992). TNT and some of its metabolites have also been shown to cause enlarged spleen, anemia, cataracts, hepatitis, and decreased fertility in males in laboratory rat studies (Army, 1976; Army, 1978; Dilley et al., 1982; Harkonen et al., 1983; Hathaway, 1985; Jiang et al., 1991; Morton et al., 1976).

Yarrowia lipolytica AN-L15

Yarrowia lipolytica AN-L15 (Figure 3) is a hemiascomycetous yeast; it is considered to be a "non-conventional" yeast species. It is an obligate aerobe (Ahlers et

al., 2000) and more closely related to the filamentous fungi than it is to the rest of the yeast species (Dujon et al., 2004). It is unique in that it has a haplo-diplontic cycle, i.e. it alternates between haploid and diploid phases. It is able to assimilate hydrocarbons and is often found in hydrocarbon rich environments, such as dairy and poultry waste processing, and petroleum rich environments (oil sludge). The yeast strain *Yarrowia lipolytica* AN-L15 was isolated in previous work (Zaripov et al., 2002) from an oil-polluted peat bog in Western Siberia. According to Ziganshin et al. (2007), *Y. lipolytica* AN-L15 is not able to grow using TNT as a sole nitrogen or carbon source. Thus, TNT conversion by *Y. lipolytica* AN-L15 is a cometabolic process. Remarkably, however, *Y. lipolytica* AN-L15 has been shown to have two reductive enzyme systems for TNT transformation: one for nitro-group reduction, and one for aromatic ring reduction (Jain et al., 2004; Ziganshin et al., 2007).

The described work used *Y. lipolytica* AN-L15 as the study system for the transformation of TNT. This system was studied under conditions of different pH and under conditions of the presence or absence of ferrihydrite.

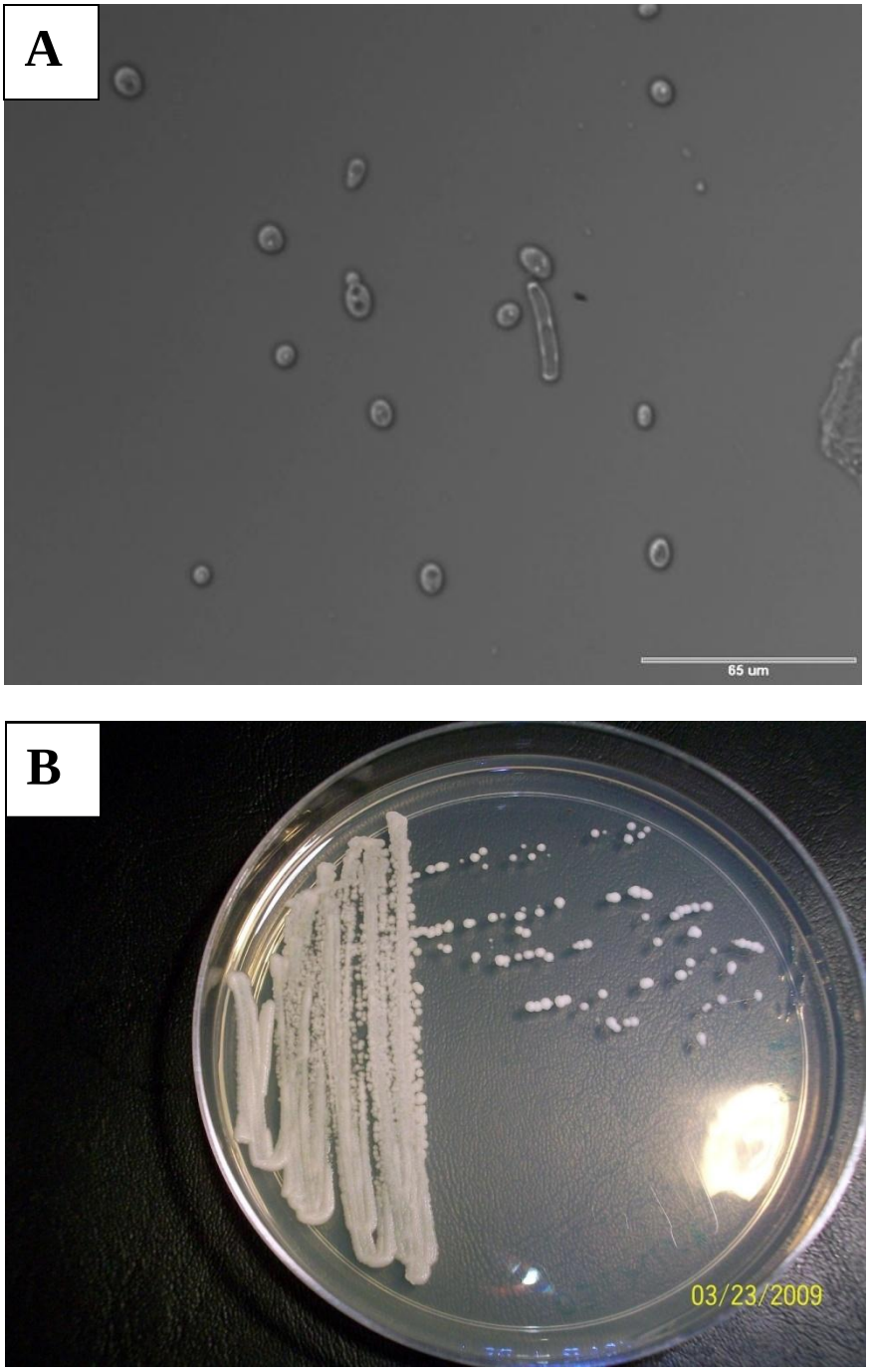

Figure 3. (A) Image of *Y. lipolytica* AN-L15, 600x magnification using a Nikon Eclipse E800 microscope with MetaVue (ver. 7.0r4) software. (B) *Y. lipolytica* AN-L15 growing on Sabouraud agar.

Previous Work Pertaining to TNT Transformation

There has been substantial research done in the area of TNT transformation both biotically and abiotically. The areas of research have spanned the gamut from molecular studies, to toxicological studies, to identification studies, to applied bioremediation studies, and have been funded by many sources. Understanding the TNT transformation pathway is important, since some metabolites may be more toxic than TNT. It is also important to understand the transformation of TNT for bioremediation, some metabolites may bind to soil particles more strongly or be more degradable under natural conditions. Covered in this thesis will be studies that pertain to the biotic and abiotic transformation of TNT and its associated metabolites within the context of the research conducted herein.

Biotic Transformation of TNT

Transformation of TNT through oxidative reactions is rare, but can occur at the methyl group as shown by Vanderberg et al. (1995). During oxidation of the methyl group, the typical products are alcohols, aldehydes, and carboxylic acid derivatives (Lewis et al., 2004). What has been shown most often is the transformation of TNT by nitroreduction. Complete nitroreduction leads to the formation of triaminotoluene (TAT), but this is rarely observed; the usual metabolite products are aminodinitrotoluenes (ADNTs) and diaminonitrotoluenes (DANTs), which are formed via transformation of HADNTs. More recently transformation of TNT by aromatic ring reduction has been the focus of study.

The aromatic ring reduction of TNT results in the appearance of hydride-Meisenheimer complexes, dihydride-Meisenheimer complexes, protonated dihydride-Meisenheimer complexes, and nitrite. Most of the microbial work that has been conducted in the area of TNT transformation has centered around the use of a select few bacterial species, with the focus being on finding a bacterium that could use TNT as a sole carbon and nitrogen source. None have been found so far. Some bacterial species have been found to be able to use TNT as a sole nitrogen source, but not as a sole carbon and energy source, this will be outlined later.

Aromatic Ring Reduction of TNT. 3-H^--TNT, formed by nucleophilic substitution of an aromatic carbon atom by a hydride ion (Lewis et al., 2004), is often the first product observed in the transformation of TNT along the aromatic ring reduction pathway (Figure 4). Further transformation often occurs resulting in 3-H^--TNT forming other hydride, dihydride, and protonated dihydride-Meisenheimer complexes. Ziganshin et al. (2007) showed that it is from one of these protonated dihydride-Meisenheimer complexes that nitrite is formed (Figure 5).

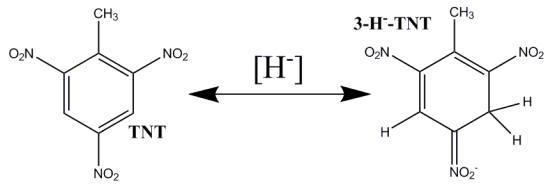

Figure 4. Formation of the C-3 H^--TNT complex from TNT.

French et al. (1998) have shown *Enterobacter cloacae* PB2 to be able to use TNT as a sole nitrogen source, through the formation of nitrite during reduction of TNT. The

hydride-Meisenheimer complex was also evidenced in a study using a *Mycobacterium* strain (Vorbeck et al., 1994), and one in which 2,4,6-trinitrophenol was reduced by *Rhodococcus erythropolis* (Rieger et al., 1999). In the latter study, it was noted that the media containing the picric acid turned red-orange upon formation of the hydride-Meisenheimer complex. Some studies have looked at the enzymes involved in this transformation process, particularly the family of enzymes known as the old yellow enzymes (OYE). These studies indicate that pentaerythritol tetranitrate (PETN) reductase (French et al., 1998; Khan et al., 2002), xenobiotic reductase B (XenB) (Blehert et al., 1999; Pak et al., 2000), and N-ethylmaleimide reductase (NemA) (Williams et al., 2004) are all enzymes capable of reducing TNT via the hydride-Meisenheimer complex (H^--TNT), the dihydride-Meisenheimer complex ($2H^-$-TNT), and the protonated dihydride-Meisenheimer complex ($2H^-$-TNT-H^+) (Figure 5). Aromatic ring reduction of TNT usually occurs at the C3 position on the aromatic ring resulting in the monohydride 3-H^--TNT (Ziganshin et al., 2007).

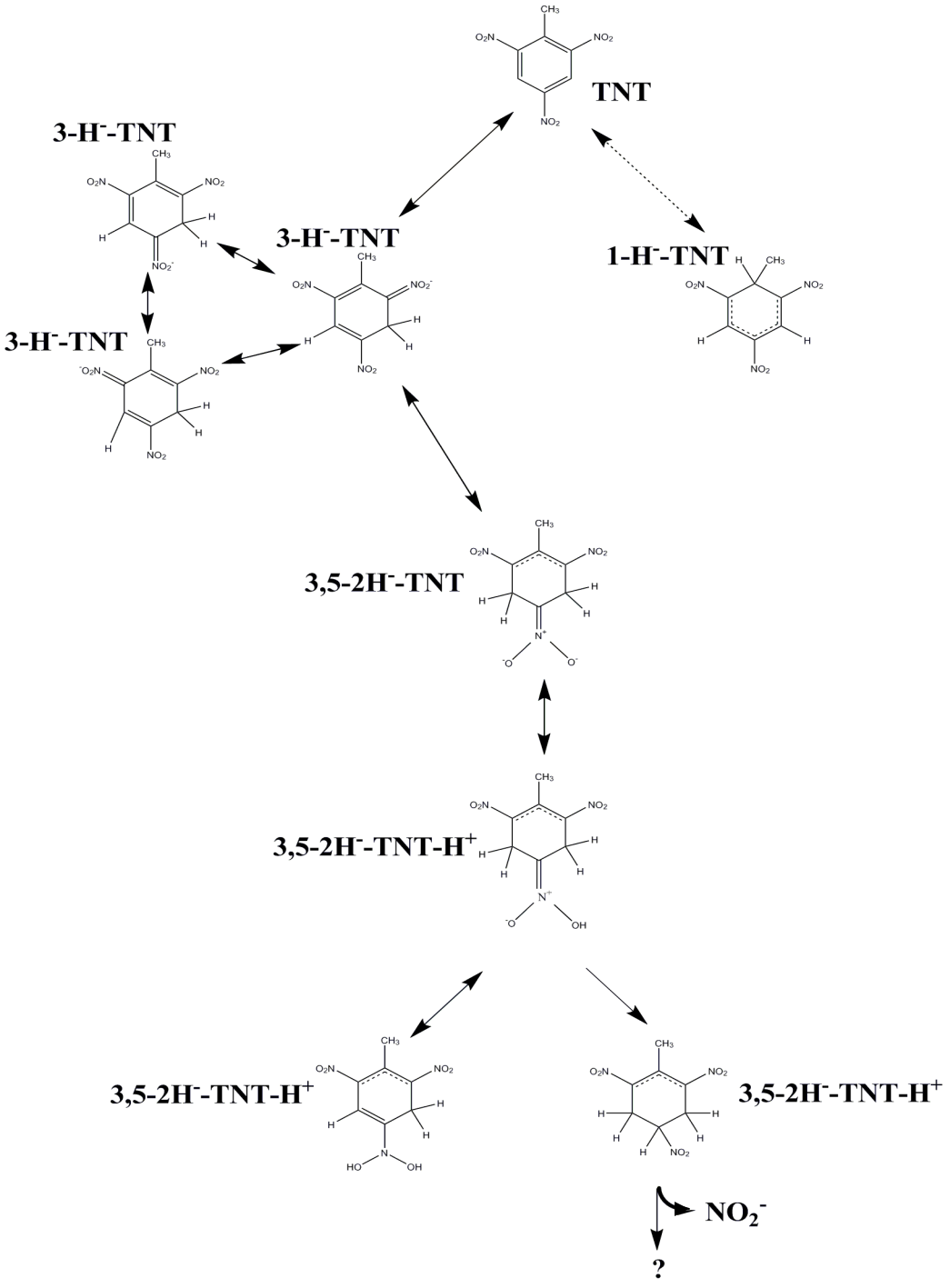

Figure 5. The pathway of TNT transformation via aromatic ring reduction. Illustrating the hydride-Meisenheimer complexes, dihydride-Meisenheimer complex, and protonated dihydride-Meisenheimer complexes.

Nitro-Group Reduction of TNT. Aromatic ring reduction of TNT via the hydride-Meisenheimer complex is not the only path to transforming TNT. Another pathway of TNT reduction by microbes is via the nitro-groups. The pathway of TNT transformation is dependent upon the organism and the enzymes it produces. During nitro-group reduction of TNT, there are two pathways that may be followed. One pathway is along the reduction of the para nitro-group and the other pathway is along the reduction of the ortho nitro-group. Biologically mediated nitro-group reduction has been shown to be at least somewhat regioselective for the para nitro-group reduction pathway (Borch et al., 2005; Elovitz and Weber, 1999; Leibzon et al., 2000) (Figure 6).

Due to the extremely unstable nature of the nitrosodinitrotoluenes (NO-DNTs) (Figure 6), this structure is difficult to detect and very short lived, thus the first products commonly detected along the nitro-group reduction pathway are HADNTs. The HADNTs are further reduced to ADNTs and the ADNTs to DANTs. The complete reduction of TNT would end with the transformation to TAT (Figure 6). Tetranitroazoxytoluene (azoxy) compounds can also be present and, most likely, form from hydroxylamino-nitroso condensation reactions (Wang et al., 2000); the azoxys can undergo further transformation resulting in the tetranitroazoxytoluene (azo) compounds (Figure 7). Azoxy compounds have the general structure of R-N=N(O)-R'; while the Azo compounds have the functional group R-N=N-R' (R and R' can be aryl or alkyl). In the context of this study, azo compounds are likely formed through the reduction of azoxy compounds.

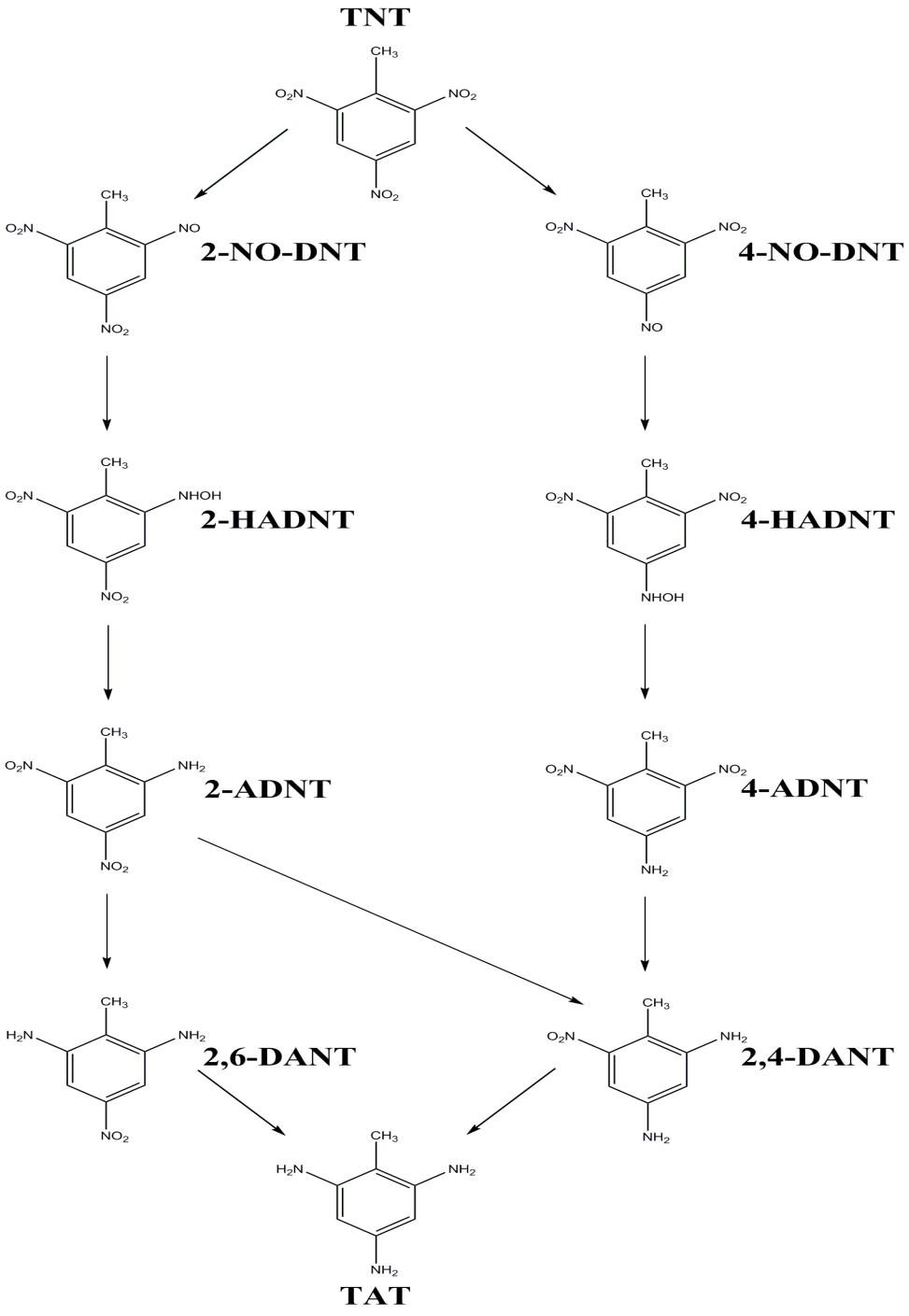

Figure 6. The transformation of TNT via nitro-group reduction. The ortho- and para-nitro-group reduction pathways are illustrated. The metabolites represented in the figure are: 2-nitroso-4,6-dinitrotoluene (2-NO-DNT), 4-nitroso-2,6-dinitrotoluene (4-NO-DNT), 2-hydroxylamino-4,6-dinitrotoluene (2-HADNT), 4-hydroxylamino-2,6-dinitrotoluene (4-HADNT), 2-amino-4,6-dinitrotoluene (2-ADNT), 4-amino-2,6-dinitrotoluene (4-ADNT), 2,6-diamino-4-nitrotoluene (2,6-DANT), and 2,4-diamino-6-nitrotoluene (2,4-DANT) .

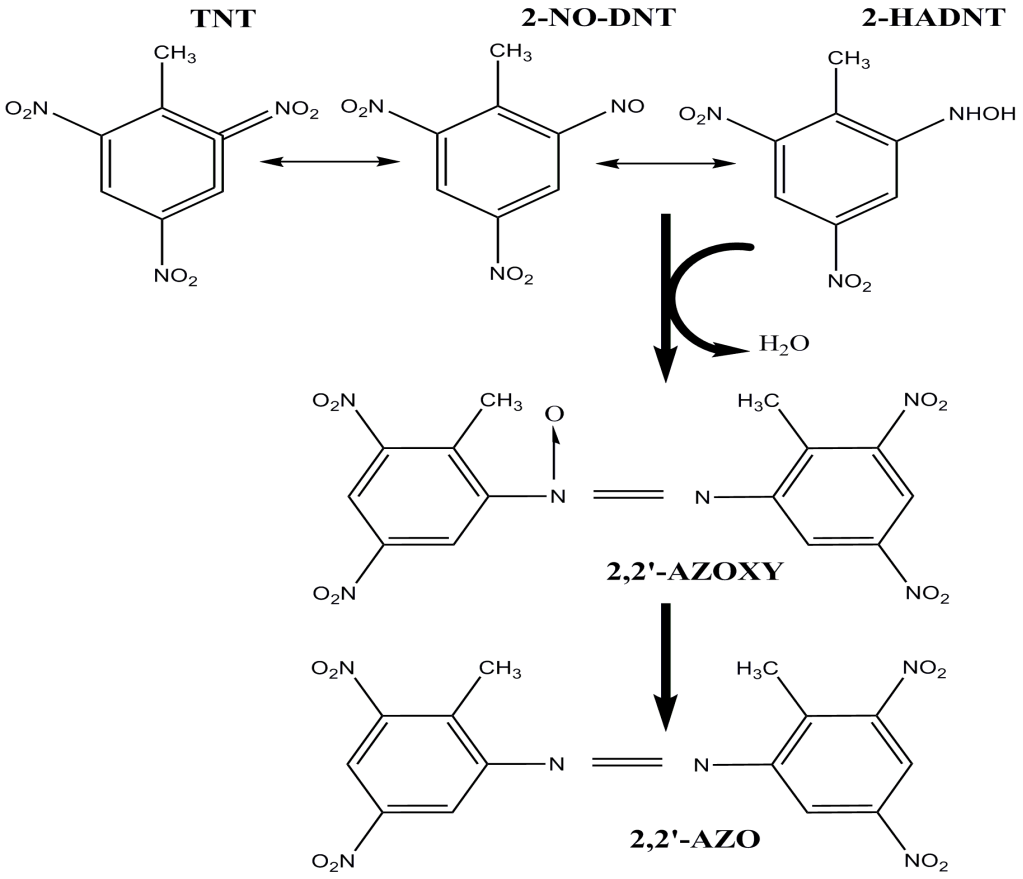

Figure 7. The condensation reaction of NO-DNT and HADNT compounds results in the formation of tetranitroazoxytoluene (azoxy) compounds. The azoxys can undergo further transformation resulting in the tetranitroazotoluene (azo) compounds. The reduction of NO-DNT to HADNT and the dimerization of azoxy and azo compounds can occur at the ortho- or para-positions. In this figure the formation of 4,4',6,6'-tetranitro-2,2'azoxytoluene (2,2'-AZOXY) and 4,4',6,6'-tetranitro-2,2'azotoluene (2,2'-AZO) are shown.

There has been evidence of *Phanerochaete chrysosporium*, a white rot fungus, being able to completely mineralize TNT to TAT, using the nitroreduction pathway, with approximately 40% efficiency (Hawari et al., 1999; Michels et al., 1995). Another characteristic that had been identified among fungi and yeasts is the ability of some species to degrade TNT via both the aromatic ring reduction pathway and the nitro-group reduction pathway. As noted earlier, *Y. lipolytica* AN-L15 is one yeast capable of doing

this. Ziganshin et al. (2007) published work that demonstrated the ability of *Y. lipolytica* AN-L15 to reduce TNT, predominantly, via the aromatic ring reduction pathway, and secondarily, through the nitro-group reduction pathway. The authors reported the formation of HADNTs, ADNTs, eight hydride complexes, and nitrite as reductive products of TNT.

Combining Biotic and Abiotic Transformation of TNT

Aside from biological electron donors, iron and sulfur are the most abundant natural reductants in soils (Stumm and Morgan, 1981). As is similar with quinones and iron porphyrins in biological systems, they can serve the role of electron carriers, (Figure 8) (Klausen et al. 1995, Schwarzenbach et al. 1990).

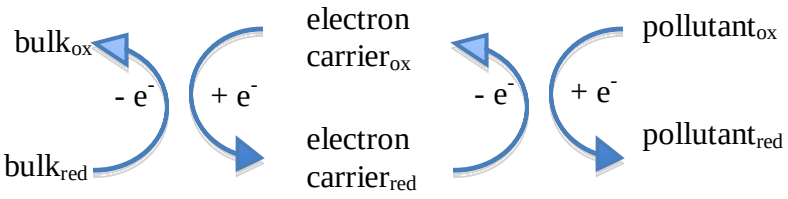

Figure 8. The electron carriers (be they biological or chemical) can act as shuttles for moving the reducing electrons from the bulk phase to the pollutants. Ideally, this results in reduced compounds that are less harmful to the environment, but this is not always the case.

Iron has been shown to have tremendous potential for reducing environmental contaminants, and in some studies, has been shown to produce more efficient TNT transformation than biotic components alone. Using zero valent iron (Fe^0) in TNT contaminated soils, Hundal et al. (1997) showed complete transformation of the TNT within eight hours. The resulting metabolites were monoaminodinitrotoluenes. They

also showed that Fe^0 treated TNT was more biodegradable than untreated TNT, resulting in greater mineralization of TNT. It was shown that ferrous iron (Fe(II)) present at the surface of goethite could reduce TNT (Hofstetter et al., 1999). Borch et al. (2005) looked at the effects of ferrihydrite and anthraquinone-2,6-disulfonate (AQDS) on TNT and showed that *Cellulomonas* sp. strain ES6, in the presence of ferrihydrite, resulted in an alteration in the TNT degradation pathway and a more rapid rate of TNT transformation.

In another study, Schwarzenbach et al. (1990) showed that in the presence of natural reductants in the soil coupled with small amounts of quinones or iron porphyrins the reduction of nitroaromatic compounds was accelerated significantly. They also identified the influence of pH on the reactions with the quinones present. Below pH ~7.0, the reactions were dependent on the type of quinone. Above pH ~7.0, the reactions were affected by the second-order rate for the reaction between nitroaromatic compounds and the quinones.

Goal of Research

Contamination of soils and ground water by TNT is of environmental significance due to the mutagenic nature of TNT and the carcinogenic and mutagenic nature of some of the metabolites resulting from the biotic and abiotic reduction of TNT. To develop appropriate, cost effective bioremediation techniques for the mineralization or immobilization of TNT and its reduced metabolites, it is important to understand the processes involved in the reduction pathways. This can lead to the increased efficiency of bioremediation techniques. *Y. lipolytica* AN-L15 has been shown to be a good

candidate for bioremediation of TNT, but there is more to know and understand about how it reduces TNT and the ideal conditions for maximizing its potential, as well as its functionality under environmental conditions.

The goal of this study was to determine the effect of various parameters on the reduction of TNT by *Y. lipolytica* AN-L15. This work was a continuation of work by Ayrat Ziganshin and Robin Gerlach. This research had three specific objectives:

1) Examine the effect of different initial pH values of the culture medium to determine if the reduction of TNT by *Y. lipolytica* AN-L15, via the aromatic ring pathway, was influenced by pH and enzyme activity or solely by enzyme activity.

2) Study the effect of the addition of ferrihydrite to the culture medium to determine whether the presence of ferrihydrite would affect the length of time to reduce TNT and the pathway of TNT transformation by *Y. lipolytica* AN-L15.

3) Simulate ground water flow conditions by use of a flow column to study the reduction of TNT by *Y. lipolytica* AN-L15 under continuous flow conditions.

Objectives 1 and 2 will be discussed in the main body of this thesis, while objective 3 will be discussed in Appendix A.

MATERIALS AND METHODS

Yarrowia lipolytica AN-L15, Growth Media and Culturing Methods

Y. lipolytica AN-L15, transferred from a culture maintained on Sabouraud agar (Ziganshin et al., 2007), was incubated aerobically for 24 hours at 30^{o}C on Sabouraud agar medium containing (per liter) 10 g of glucose, 10 g of peptone, 5 g yeast extract, 0.25 g sodium chloride (NaCl), and 20 g of granulated agar. *Y. lipolytica* AN-L15 cells were harvested, washed with 16 mM phosphate buffer (pH 7.0), and transferred into 250 mL Erlenmeyer flasks containing 50 mL of synthetic medium. The harvesting and washing consisted of: suspending the cells, which were grown on the agar, in the phosphate buffer, drawing them off, and centrifuging (Sorvall Instruments, RC5C) them at 4025 x g at, 4^{o} C at, for 6 minutes. The synthetic medium contained (per liter) 5.04 g glucose, 1.09 g potassium phosphate (KH_2PO_4), 1.14 g sodium phosphate (Na_2HPO_4), 1.00 g ammonium sulfate ($(NH_4)_2SO_4$), and 0.24 g magnesium sulfate ($MgSO_4$). The initial cell concentration was adjusted to an optical density (OD) of 0.2 as measured on a Spectronic GENESYS 5 spectrophotometer at a wavelength of 600 nm, using cell free synthetic medium as the reference.

Standards and Stocks

TNT (purity 99%) was purchased from ChemService (West Chester, PA) and was used to make the TNT/ethanol stock (360 mg TNT per 50 mL ethanol (EtOH) (95% purity) for a concentration of 7.2 g/L).

The standards used for the high performance liquid chromatography (HPLC) analysis were as follows: TNT (purity >99.0%), 2-amino-4,6-dinitrotoluene (2-ADNT) (purity >99.0%), 4-amino-2,6-dinitrotoluene (4-ADNT) (purity >99.0%), 2,4-diamino-6-nitrotoluene (2,4-DANT) (purity >99.0%), and 2,6-diamino-4-nitrotoluene (2,6-DANT) (purity >99.0%) were purchased from Supelco (Bellefonte, PA). 2-hydroxylamino-4,6-dinitrotoluene (2-HADNT) (purity 97.1%), 4-hydroxylamino-2,6-dinitrotoluene (4-HADNT) (purity 96%), 2,2',6,6'-tetranitro-4,4'-azoxytoluene (4,4'-Azoxy) (purity 98.8%), 2,2',6,6'-tetranitro-4,4'-azotoluene (4,4'-Azo) (purity 94.7%) and 4,4',6,6'-tetranitro-2,2'-azotoluene (2,2'-Azo) (purity 94.7%) were purchased from AccuStandard (New Haven, CT).

The standards used for ion chromatography were generated in the lab. All standards were made to an initial concentration of 10 mg/L and diluted with DI water as necessary. The chloride ion standard was made using sodium chloride (NaCl), the sulfate ion standard was made using sodium sulfate (Na_2SO_4) powder, the phosphate ion standard was made using sodium phosphate (Na_2HPO_4), the nitrite ion standard was made using sodium nitrite ($NaNO_2$), and the nitrate ion standard was made using sodium nitrate ($NaNO_3$).

The protein assay standards were made from bovine serum albumin (BSA), purchased from Thermo Scientific (Rockford, IL). The BSA had an initial concentration of 2 g/L.

Amorphous hydrous ferric oxide ($Fe_2O_3 \bullet XH_2O$) was synthesized by dissolving 3.4 g of ferric chloride ($FeCl_3$) in 100 mL deionized (DI) water. 6 N sodium hydroxide

(NaOH) was added drop wise over thirty-five minutes to normalize the pH to 7.0 (Lovley and Phillips, 1986).

The iron assay standards were made at an initial concentration of 1000 mg/L by dissolving 0.342 g of iron (II) ethylenediammonium sulfate ($FeC_2H_4(NH_3)_2(SO_4)_2*4H_2O$) in 50 mL 0.25 N HCl/0.25 N NH_2OH-HCl. 0.25 N HCl/0.25 N NH_2OH-HCl was used for standard set up, because the NH_2OH as a reductant helps to keep dissolved Fe in the form of Fe(II) (Lovley and Phillips, 1987).

Growth Indicator Measurements

Culture absorbance was monitored via measurements at a wavelength of 600 nm using the Spectronic GENESYS 5 spectrophotometer. Two 1 mL aliquots were drawn from each treatment. One aliquot was centrifuged at 14,000 x g for one minute, and then filtered through a 0.2 μm filter to serve as the reference. The other aliquot was compared spectrophotometrically to the reference.

During the experiments with iron hydroxide, growth curves were also constructed based upon the results of the Pierce-Coomassie assay. Samples (0.5 mL) were taken from each flask and processed as follows: 0.5 mL of 0.5 N NaOH was added in a microcentrifuge tube, vortexed for ten seconds, placed in 90^{o} C water bath (Fisher Scientific, IsoTemp 220) for ten minutes, allowed to cool to room temperature, 70 μL of hydrochloric acid (HCl) (6:10 dilution) were added, vortexed for ten seconds, and frozen. Twenty-four hours after the final time point was sampled, all the protein samples were thawed and assayed using the Pierce-Coomassie assay as follows: 50 μL of sample were

added to a 96 well plate, 150 μL of Pierce-Coomassie Reagent purchased from Thermo Scientific (Rockford, IL) were added, incubated at room temperature for fifteen minutes, then a Biotek Synergy HT was used to measure the absorbance at a wavelength of 595 nm. All standards were treated the same as the samples. Gen5 software (version 1.02) was used for the data collection.

TNT-Metabolite Analysis

Samples were centrifuged (Fisher Scientific, accuSpin Micro 17) at 14,000 x g for one minute and filtered through a 0.2 μm filter. During the pH variance experiments, detection of TNT and metabolites resulting from its transformation were conducted using an Agilent 1100 series High Performance Liquid Chromatograph (HPLC) equipped with an 1100 series temperature controlled (4^{o} C) autosampler, diode array detector, temperature controlled column compartment, Supelcosil LC-8 guard column (20 mm x 4.6 mm, 5 μm particle size), and a Supelcosil octyl LC-8 column (150 mm x 4.6 mm, 5 μm particle size). Using the method published by Borch and Gerlach (2004), separation was achieved at 36^{o} C. The metabolites were detected at 230, 254, 440, and 476 nm, as described in Ziganshin et al. (2007). Agilent ChemStation software (Rev A.10.02) was used for instrument control, data acquisition, and analysis.

For the iron hydroxide experiments, detection of TNT and the metabolites resulting from its transformation through both nitro-group reduction and the reduction of the aromatic ring was conducted using the Hewlett-Packard 1090 HPLC with an autosampler and diode array detector. The LC-8 guard column (20 mm x 4.6 mm, 5 μm

particle size) was used in conjunction with the Supelcosil octyl LC-8 column (150 mm x 4.6 mm, 5 μm particle size). Samples were centrifuged at 14,000 x g for one minute, and then filtered through a 0.2 μm filter. Using the method by Borch and Gerlach (2004) separation was achieved at 37^{o} C. The metabolites were detected at 230, 254, 440, and 476 nm, as described in Ziganshin et al. (2007). Agilent ChemStation software (Rev A.09.01) was used for controlling the HPLC, data acquisition, and analysis.

Iron Assay

To assay for the concentration of free Fe(II) in the media of each flask, 0.1 mL samples were taken and added to 0.4 mL of 0.5 N HCl, vortexed for ten seconds, and incubated at room temperature for ninety minutes. 20 μL of this solution were added to wells in a 96 well plate containing 200 μL of ferrozine in 50mM HEPES (pH 7.0), and the absorbance was read at 540 nm using the Biotek Synergy HT reader. Gen5 software (version 1.02) was used for the data collection. To assay for total Fe the procedure above was followed with the exception of adding 0.4 mL of 0.25 N hydroxylamine HCI in 0.25 N HCl in place of 0.4 mL of 0.5 N HCl. This method is similar to that previously published by Lovley and Phillips (1987).

Analysis of Nitrite and Nitrate

The analysis of nitrite and nitrate was conducted on a Dionex system with the following components: GP40 gradient pump, CD20 conductivity detector, AS40 autosampler, AS9A column, and 100 μL loop. PeakNet (version 5.2) software was used

for controlling the ion chromatography (IC) system, data collection, and analysis. 9 mM sodium carbonate (Na_2CO_3) was used as the eluent. The samples were prepared by pipetting 1.0 mL of medium from each flask, centrifuging (Fisher Scientific, accuSpin Micro 17) the samples at 14,000 x g for one minute and filtering them through a 0.2 μm filter. The treatments were then stored in the freezer. Within ninety-six hours after the final sampling time, all samples were thawed and analyzed, in succession, on the Dionex system.

Experimental Setups

Reduction of TNT by *Y. lipolytica* AN-L15 at Different Initial pH of the Culture Medium

For the initial part of this experiment, four 250 mL Erlenmeyer flasks were set up containing 50 mL of synthetic medium with a pH of 7.0 and were inoculated with *Y. lipolytica* AN-L15 and TNT (referred to as pH 7.0 original throughout the study). Two flasks were used for sampling and two flasks for medium transfer. Additionally, four control flasks were set up: two control flasks contained only medium and *Y. lipolytica* AN-L15 and the other two control flasks contained only medium and TNT/EtOH stock. The TNT/EtOH stock was added to a final concentration of 115.2 mg/L of TNT and 16 mL/L of ethanol. The flasks were incubated at 30^{o}C, without shaking. The pH 7.0 original flasks were sampled throughout the experiment as a means of comparing this experiment to the experiments by Ziganshin et al. (2007).

Six 250 mL Erlenmeyer flasks were set up for each of three pH values (pH 7.0, pH 6.5, and pH 4.5). Each flask contained 50 mL of synthetic medium at the respective

pH. Twenty-four hours into the study, the transformation of TNT to 3-H^--TNT was readily occurring in the pH 7.0 original treatments with *Y. lipolytica* AN-L15 and TNT, as indicated by the color change of the medium to deep red (Figure 16) and the HPLC data (Figure 1) (Ziganshin et al., 2007). At this time, transfers were made to the new media from the pH 7.0 original flasks set up for medium transfer. This allowed for transfer of the enzymes produced by *Y. lipolytica* AN-L15 and responsible for aromatic ring reduction of TNT. 5 mL of the pH 7.0 original treatments were pipetted from the flasks set up for medium transfer and added to each of four flasks for each initial pH value. TNT/EtOH stock was added to two of the flasks containing the transferred medium for each initial pH value. TNT/EtOH stock was also added to the two remaining flask containing only synthetic medium and no *Y. lipolytica* AN-L15 for each initial pH value. The TNT/EtOH stock was added to a final concentration of 115.2 mg/L of TNT and 16 mL/L of ethanol.

The final set up for the experiment consisted of six flasks for pH 7.0 original: two flasks containing medium and TNT, two flasks containing medium and *Y. lipolytica* AN-L15, and two flasks containing medium, TNT, and *Y. lipolytica* AN-L15 and six flasks for each pH 7.0, pH 6.5, and pH 4.5: two flasks containing medium and TNT, two flasks containing medium and transferred *Y. lipolytica* AN-L15, and two flasks containing medium, TNT, and transferred *Y. lipolytica* AN-L15. The flasks were incubated at 30^{o} C, without shaking.

All samples were taken using sterile techniques and were drawn under a laminar flow hood (SterilGARDHood Class II Type A/B3, Baker Company, Inc.) in an attempt to

minimize contamination. Additionally, all transfers of media were done under the laminar flow hood. Erlenmeyer flasks were shaken for twenty seconds prior to every sample being drawn.

Reduction of TNT by *Y. lipolytica* AN-L15
in the Presence of Ferrihydrite

Sixteen 250 mL Erlenmeyer flasks containing 50 mL of pH 7.0 synthetic medium were set up. Four contained *Y. lipolytica* AN-L15 and TNT, four contained *Y. lipolytica* AN-L15 and ferrihydrite, four contained ferrihydrite and TNT, and four contained *Y. lipolytica* AN-L15, ferrihydrite, and TNT. TNT/EtOH stock was added to a final concentration of 115.2 mg/L of TNT and 16 mL/L of ethanol. Ferrihydrite was added to a final concentration of 358 mg/L measured as Fe. The flasks were incubated at 30^{o} C without shaking.

Each flask was shaken for twenty seconds and sampled immediately. This was done in an effort to have a homogenous suspension of Fe(II) and Fe(III) in the medium.

All samples were taken using sterile techniques and drawn under a laminar flow hood in an attempt to minimize contamination. Additionally, all transfers of media were done under the laminar flow hood.

RESULTS

The results of the reduction of TNT by *Y. lipolytica* AN-L15 at different initial pH values and the reduction of TNT by *Y. lipolytica* AN-L15 in the presence and absence of ferrihydrite are displayed in the figures below. The different initial pH study was conducted in duplicates while the ferrihydrite study was conducted in triplicates. Error bars for all graphs indicate one standard deviation, positive and negative. Outliers on graphs are addressed within the corresponding text. Trends among treatments within a graph, or set of graphs, are identified and compared.

Effects on TNT Reduction by *Y. lipolytica* AN-L15 with Different Initial pH of the Culture Medium

Previously, Ziganshin et al. (2007) observed the reduction of TNT by *Y. lipolytica* AN-L15 in synthetic medium with an initial pH of 7.0. In that study, the authors identified a lag in the growth of *Y. lipolytica* AN-L15 in the presence of TNT. Figure 9 shows a comparison of the absorbance readings for treatments inoculated with *Y. lipolytica* AN-L15 in the absence of TNT and treatments inoculated with *Y. lipolytica* AN-L15 in the presence of TNT, between the Ziganshin et al. (2007) study and the pH 7.0 original treatments for this thesis. Both studies used an initial OD of 0.2. There was a lag in observable growth by approximately thirty-six hours for treatments with *Y. lipolytica* AN-L15 in the presence of TNT. This lag occurred in both studies. Also seen in both studies was a comparable cell density after ninety-six hours between the treatments with *Y. lipolytica* AN-L15 in the absence of TNT and the treatments with *Y.*

lipolytica AN-L15 in the presence of TNT, though the overall cell density was lower in the thesis study than in the study by Ziganshin et al. (2007).

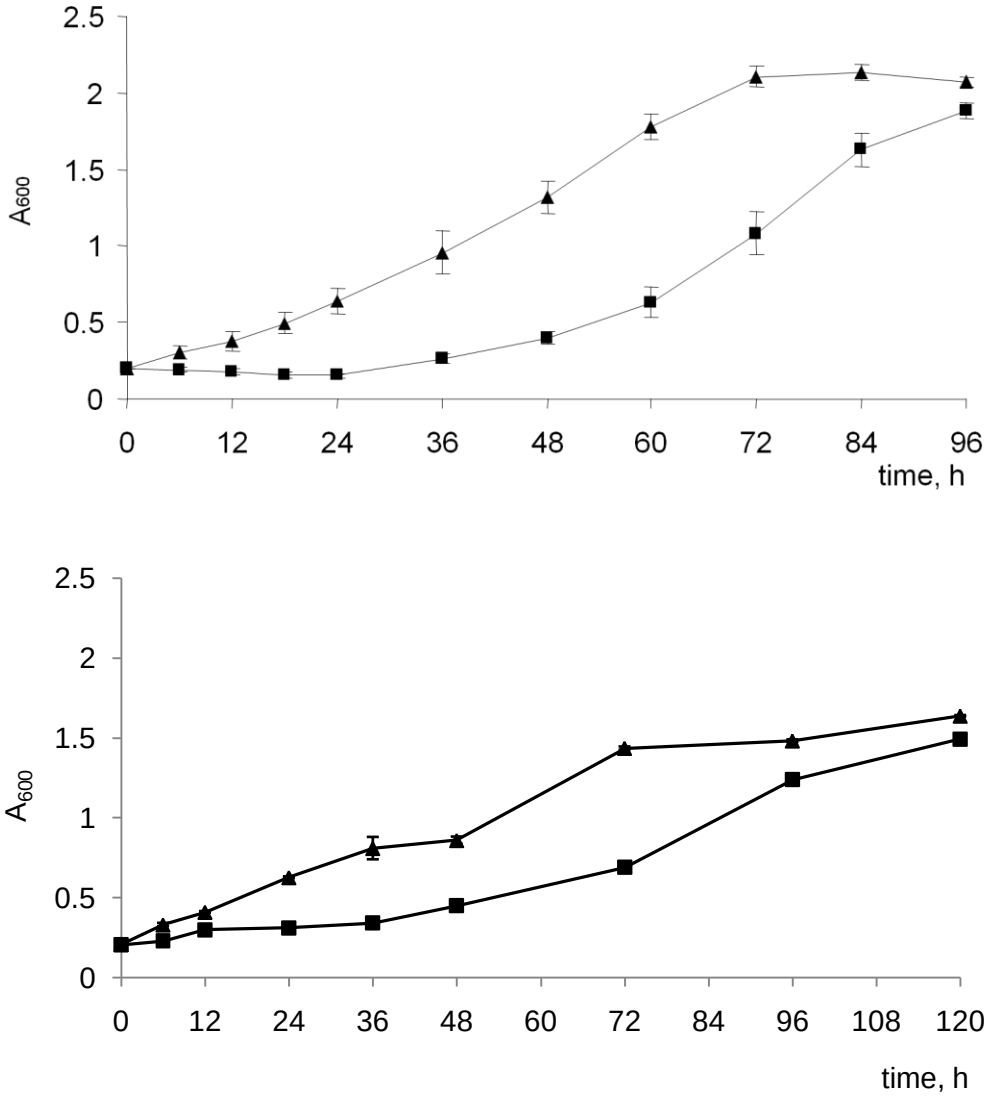

Figure 9. The graph on top shows absorbance over time for treatments without TNT (triangles) and treatments with TNT (squares) from the Ziganshin et al. (2007) study. The graph on the bottom shows absorbance over time for treatments without TNT (triangles) and treatments with TNT (squares) from the pH 7.0 original treatments for this thesis.

The identification of TNT and TNT-metabolites was based on the retention time and spectrum comparison to known standards and to the metabolites identified by

Ziganshin et al. (2007). Figure 10 shows four chromatograms: two chromatograms from a sample from the pH 7.0 original treatments with TNT, taken at thirty-six hours and two chromatograms from a similar sample from the Ziganshin et al. (2007) study taken at forty-two hours. The top chromatograms show metabolites detected at a wavelength of 254 nm measured as described in materials and methods, while the bottom chromatograms show metabolites detected at a wavelength of 476 nm measured as described in materials and methods. On the chromatograms, the metabolites are identified by numbers that correspond to Table 2. Both studies identified TNT, 2-HADNT, and 4-HADNT from nitro-group reduction. In the 476 nm chromatogram by Ziganshin et al. (2007), eight hydride complexes are identified; in the 476 nm chromatogram for the pH 7.0 original treatments, compounds 2 and 3 appear to have co-eluted thus giving only one peak. As can be seen in Table 2, the retention times for these two compounds are very close, 5.2 min. and 5.3 min., respectively. This makes separation of these peaks difficult, and only slight changes in the performance of the chromatography column, separation temperature, or composition of the solvents can lead to co-elution.

Table 2 corresponds to Figure 10 and shows the retention times of the compounds identified on the chromatograms in Figure 10. 2-ADNT and 4-ADNT are also listed in Table 2, though they do not appear on the chromatograms, because they did not occur at the same time as the eight hydride complexes.

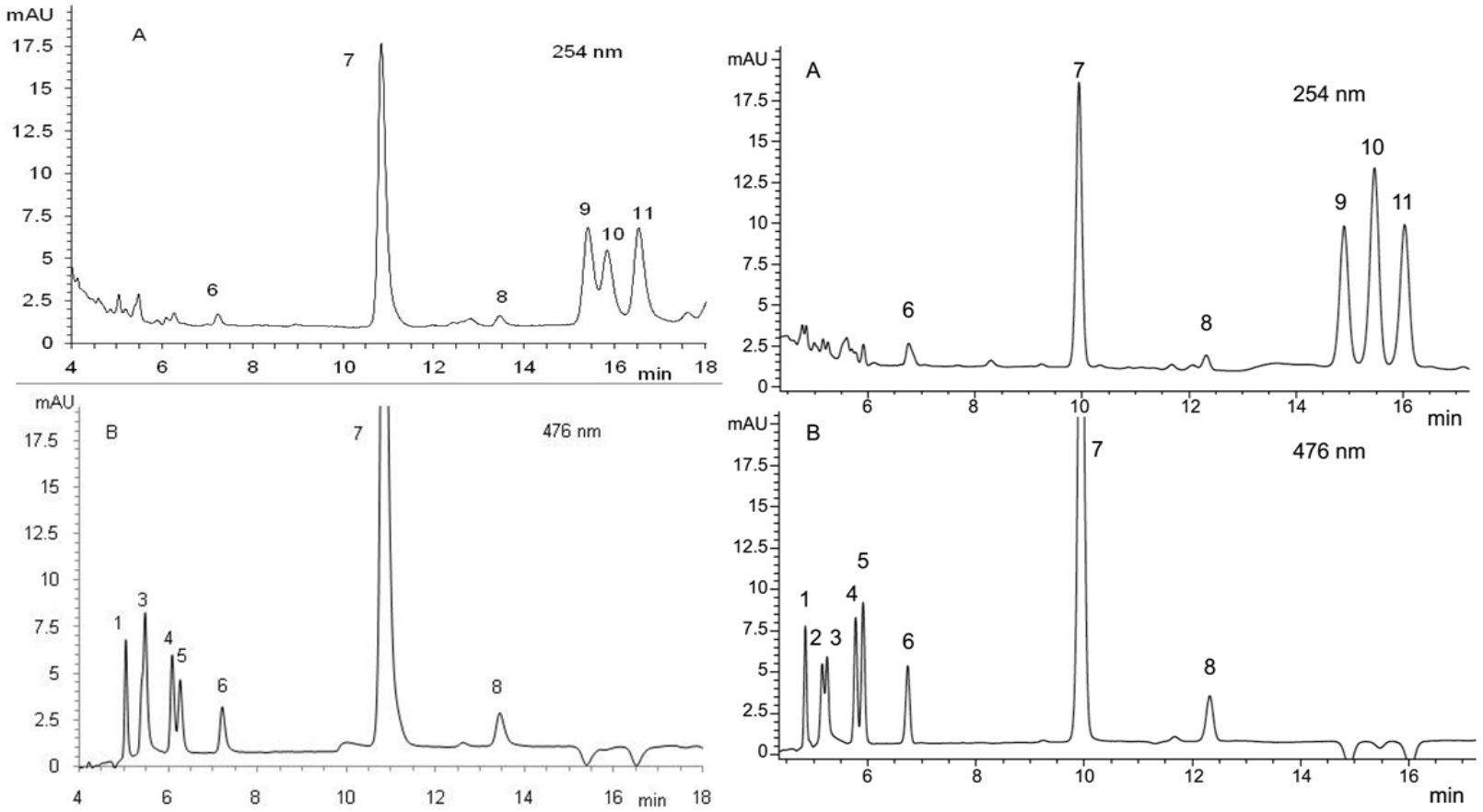

Figure 10. The chromatograms on the left are from the sample taken at thirty-six hours from the pH 7.0 original treatments. The chromatograms on the right are from the sample taken at forty-two hours from the Ziganshin et al. (2007) treatments. Chromatograms were acquired at 36°C, and absorbance was detected at (A) 254 nm and (B) 476 nm (reference wavelength, 360 nm). The numbers above the peaks correspond to the compounds shown in Table 2.

Table 2. The retention times for TNT and TNT-metabolites from both the nitro-group reduction and aromatic ring reduction pathways. Times are shown in minutes at a given temperature. Retention times for TNT and the TNT-metabolites from the nitro-group reduction pathway are based on the standards discussed in materials and methods. *Retention times for the TNT-metabolites from the aromatic ring reduction pathway are referenced from Ziganshin et al. (2007).

Number	Compound	Ret. time (min. at 36^{o} C)
1*	3-H^--TNT Isomer	4.8
2*	3,5-2H^--TNT-H^+ Isomer	5.2
3*	3,5-2H^--TNT-H^+ Isomer	5.3
4*	3,5-2H^--TNT	5.7
5*	3-H^--TNT Isomer	5.9
6*	3,5-2H^--TNT-H^+ Isomer	6.7
7*	3-H^--TNT Isomer	9.9
8*	1-H^--TNT	12.3
9	2-HADNT	13.01
10	TNT	13.47
11	4-HADNT	13.93
12	2-ADNT	14.99
13	4-ADNT	15.49

Figure 11 compares TNT, 2-HADNT, 4-HADNT, and 3-H^--TNT concentrations for the treaments with *Y. lipolytica* AN-L15 and TNT from the Ziganshin et al. (2007) study and the pH 7.0 original treatments in this thesis. TNT reached undetectable amounts between sixty and seventy-two hours in the Ziganshin et al. (2007) study and between sixty-six and ninety hours with the pH 7.0 original treatments for this thesis. Due to different sampling time points between the two studies, there were different windows for which TNT appeared to reach the undetectable levels. As shown in Figure 9, the growth of biomass (as estimated by OD_{600}) appeared to be slightly lower in the experiments described in this thesis, which could explain the slight delay in disappearance of TNT compared to the study by Ziganshin et al. (2007). 3-H^--TNT

concentrations reached approximately 260 μM after twenty-four hours in the Ziganshin et al. (2007) study and reached approximately 140 μM after twenty-four hours in the pH 7.0 original treatments for this thesis. This difference in the concentrations of 3-H^--TNT between the two studies could be due to the lower growth (OD_{600}) of *Y. lipolytica* AN-L15 observed in this study (Figure 9). The observed concentrations of 2-HADNT and 4-HADNT did not exceed 47 and 56 μM, respectively, for the Ziganshin et al. (2007) study. In the pH 7.0 original treatments for this thesis, the observed concentrations of 2-HADNT and 4-HADNT did not exceed 60 and 44 μM, respectively. Ziganshin et al. (2007) also saw 2-ADNT and 4-ADNT, though neither of these were seen in the pH 7.0 original treatments for this thesis. This lack of ADNT detection could again be due to the lower growth (OD_{600}) of *Y. lipolytica* AN-L15 observed in this study (Figure 9). Ziganshin et al. (2007) also analyzed the nitrite concentrations; this was attempted in the pH of 7.0 original treatments for this thesis, but due to equipment malfunction the results were lost.

During approximately the first fifty-four hours of TNT transformation, 3-H^--TNT was the primary metabolite, between fifty-four and sixty hours, this shifted and 4-HADNT became the primary metabolite (Figure 11).

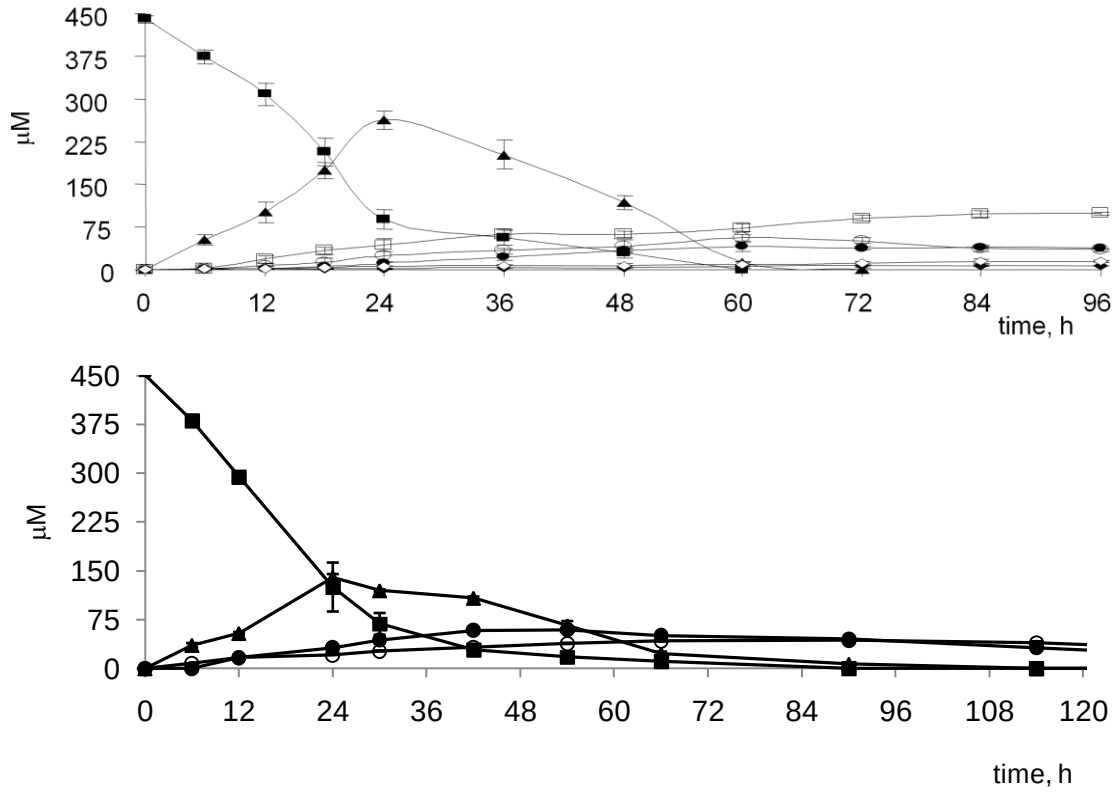

Figure 11. The two graphs compare the transformation of TNT and formation of 3-H⁻-TNT, 2-HADNT, and 4-HADNT over time by Ziganshin et al. (2007) (top graph) to the pH 7.0 original treatments (bottom graph). Filled squares represent TNT, filled triangles represent 3-H⁻-TNT, filled circles represent 2-HADNT, unfilled circles represent 4-HADNT, filled diamonds represent 2-ADNT, unfilled diamonds represent 4-ADNT, and unfilled squares represent nitrite.

Results from the Three Sets of Treatments with Different Initial pH Values

Comparison to Ziganshin et al. (2007) has helped to establish confidence that the inoculum used to inoculate the culture media with different initial pH values did indeed contain *Y. lipolytica* AN-L15 with active enzymes for aromatic ring reduction. It also established confidence that the procedures used in this thesis were similar to those already published by Ziganshin et al. (2007).

Changes in Patterns of Growth and pH Values. The patterns of growth (as estimated by OD_{600}) are shown in Figure 12. The two graphs compare the growth (OD_{600}) for the three sets of treatments with different initial pH values. The top graph shows the growth (OD_{600}) without TNT at each pH; the bottom graph shows the growth (OD_{600}) with TNT at each pH. Because these treatments were inoculated with 5 mL of the transferred culture medium, the initial OD for each treatment was lower than that seen in the pH 7.0 original treatments. The initial OD was approximately 0.003 for each treatment inoculated with the transferred culture medium. In the treatments without TNT, there was a lag period for the first twelve hours; this was most likely due to the lower initial cell concentrations. The lag period for the pH 4.5 treatments with TNT lasts for the first thirty-six hours, while the lag period for the pH 6.5 treatments and the pH 7.0 treatments lasts for the first seventy-two hours. In the treatments without TNT, the pH 7.0 treatments had the highest growth (OD_{600}), and the pH 4.5 treatments had the lowest growth (OD_{600}). In the treatments with TNT, the opposite was observed, the pH 4.5 treatments had the highest growth (OD_{600}), and the pH 7.0 treatments had the lowest growth (OD_{600}). In treatments with and without TNT, the pH 6.5 and the pH 7.0 treatments displayed similar growth (OD_{600}) until ninety-six hours, at which point they started to diverge.

In the presence of TNT, the initial pH value not only had an effect on the duration of the lag phase of the growth cycle, but also the overall level of growth (OD_{600}). *Y. lipolytica* AN-L15 grown at the pH of 4.5 appeared to have been the least affected by the addition of TNT. In the pH 4.5 treatments, there was a 6-fold increase in growth in the

absence of TNT, as seen in Figure 13. The pH 6.5 treatments and the pH 7.0 treatments both had a greater than 30-fold increase in growth in the absence of TNT (Figure 13).

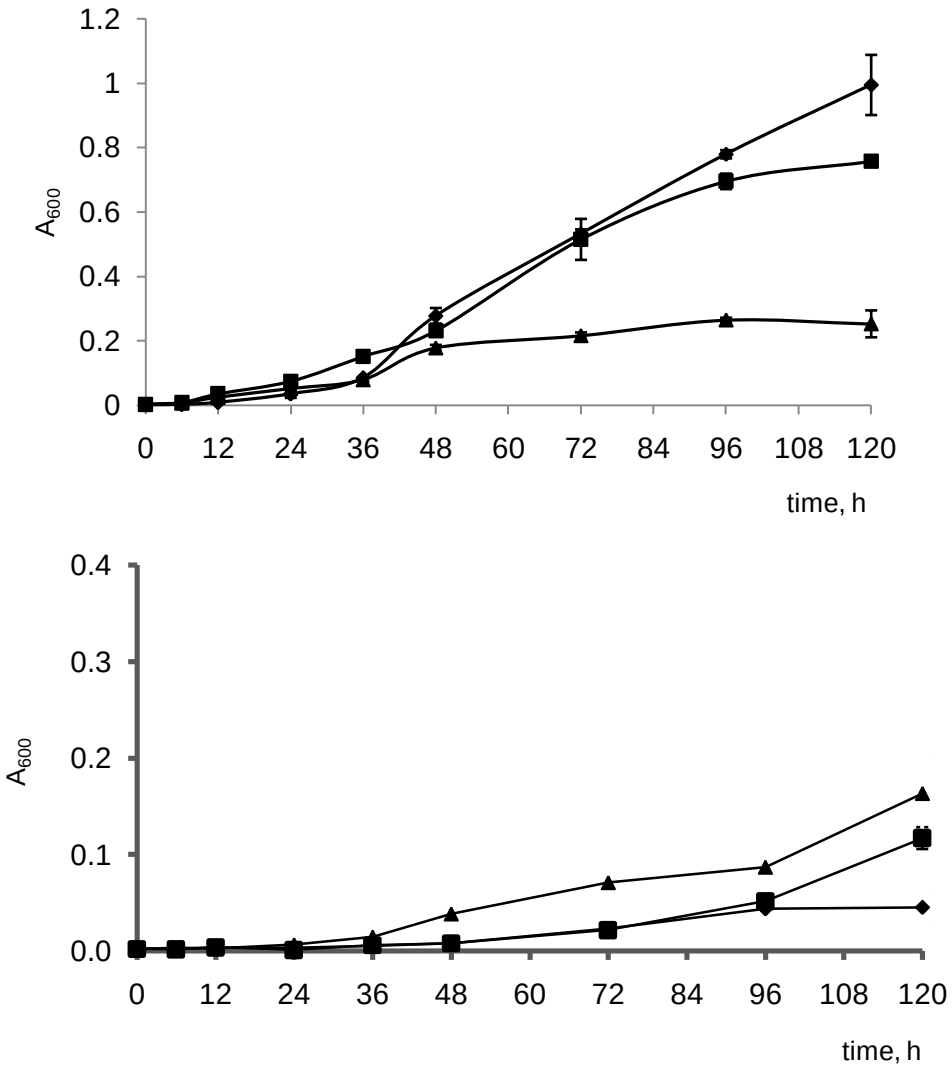

Figure 12. The top graph shows absorbance (600 nm) over time for the three sets of treatments with different initial pH values inoculated with *Y. lipolytica* AN-L15 in the absence of TNT. The bottom graph shows absorbance (600 nm) over time for the three sets of treatments with different initial pH values inoculated with *Y. lipolytica* AN-L15 in the presence of TNT. The diamonds represent the absorbance of pH 7.0 treatments, the squares represent the absorbance of pH 6.5 treatments, and the triangles represent the absorbance of pH 4.5 treatments. Note: scales differ.

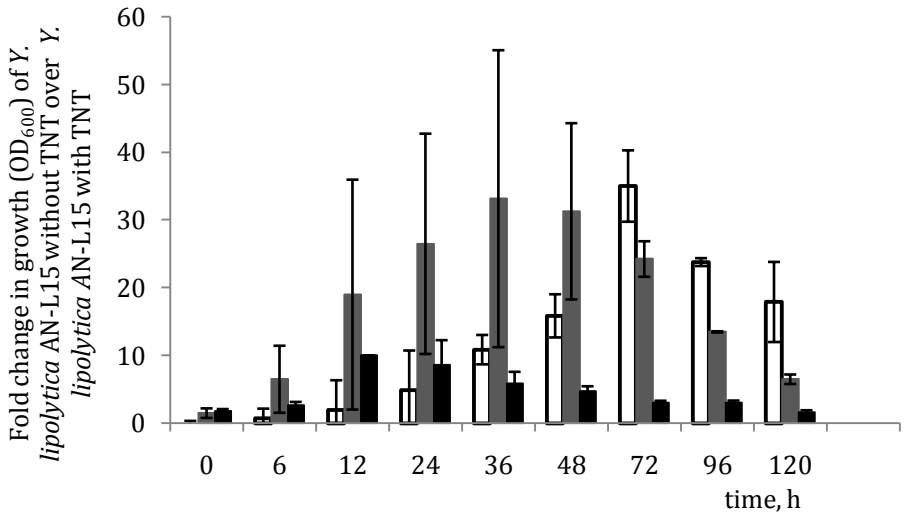

Figure 13. The bars show the relative increase in growth (OD_{600}) of *Y. lipolytica* AN-L15 in the absence of TNT versus in the presence of TNT. The white bars represent the pH 7.0 treatments, the grey bars represent the pH 6.5 treatments, and the black bars represent the pH 4.5 treatments.

The change in pH values over time is shown in Figure 14. The measurements are shown for treatments with and without TNT at initial pH values of 7.0, 6.5, and 4.5. The top graph shows the values for the treatments without TNT, and the bottom graph shows the values for the treatments with TNT. In all treatments, except the pH 6.5 treatments with TNT, the pH decreased throughout the experiment. For the pH 6.5 treatments with TNT the pH values decreased throughout the experiment, with the exception of the final time point. In all three sets of treatments, the pH values for the treatments without TNT decreased more than the pH values for the treatments with TNT. The higher pH values in the treatments with TNT may be attributed to the formation of the hydride and dihydride-Meisenheimer complexes which require the addition of $[H^+]$ to the compound being transformed. They may also be the result of a decrease in metabolic activity leading to lower production of organic acids.

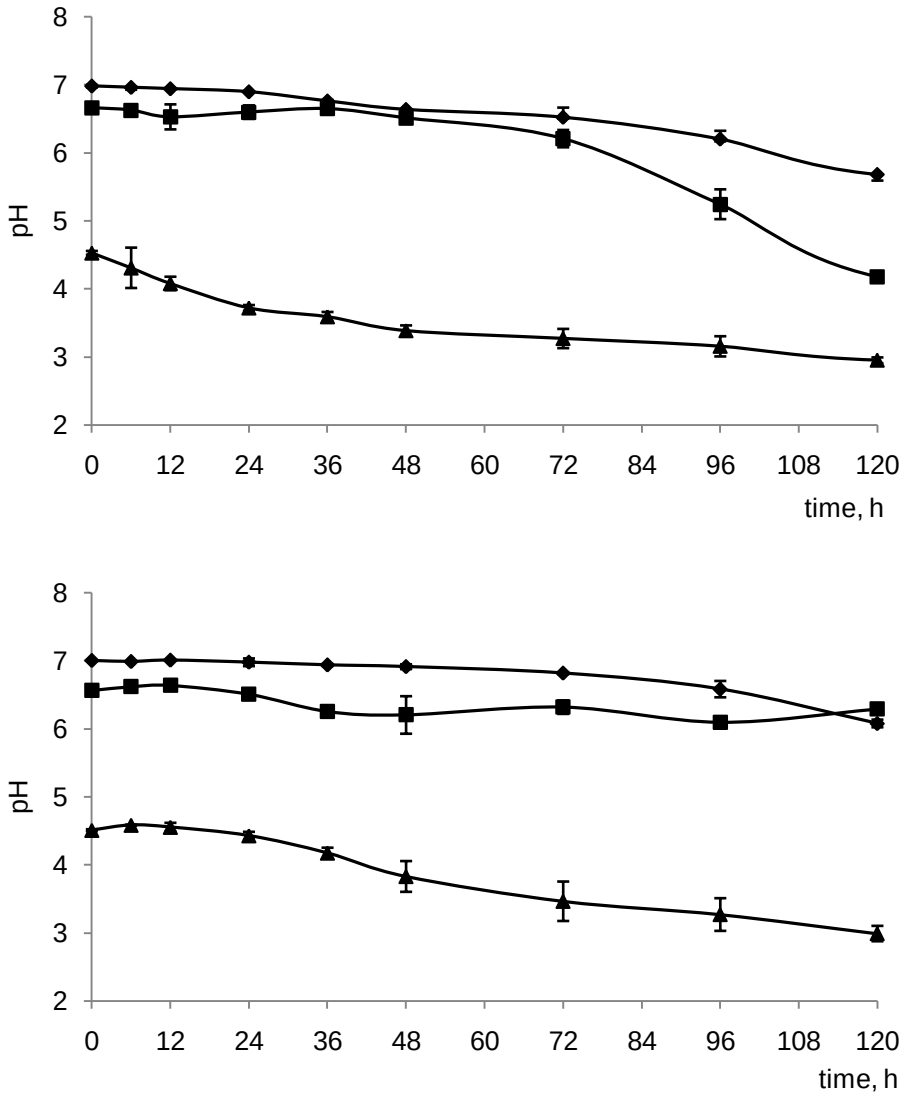

Figure 14. The change in pH values over time for the treatments without TNT (top graph) and with TNT (bottom graph). The three sets of treatments are represented on each graph. The diamonds represent the pH 7.0 treatments, the squares represent the pH 6.5 treatments, and the triangles represent the pH 4.5 treatments.

Transformation of TNT and
Formation of TNT-Metabolites

Figure 15 shows the reduction of TNT and formation of 2-HADNT, 4-HADNT, and 3-H^--TNT. TNT concentrations (Figure 15A) were similar throughout the study for all three sets of treatments, with the only significant difference being between thirty-six and sixty hours. During this time, the pH 4.5 treatments reached concentrations of about 50 μM less than the pH 6.5 treatments or the pH 7.0 treatments. Between sixty and seventy-two hours, the three sets of treatments once again reached similar concentrations. The final concentrations for the three sets of treatments were approximately: 50 μM for the pH 7.0 treatments, 55 μM for the pH 6.5 treatments, and 59 μM for the pH 4.5 treatments.

3-H^--TNT concentrations (Figure 15B) were similar among all three sets of treatments until seventy-two hours, at which time they began to diverge. The concentration of 3-H^--TNT in the pH 7.0 treatments began to decrease and continued to do so throughout the remainder of the study, reaching a final concentration of approximately 17 μM. The concentration of 3-H^--TNT in the pH 6.5 treatments slightly increased between seventy-two and ninety-six hours from approximately 64 μM to 69 μM. After ninety-six hours, the concentration of 3-H^--TNT decreased to a final concentration of, approximately, 30 μM. The concentration of 3-H^--TNT in the pH 4.5 treatments increased steadily between seventy-two and ninety-six hours from approximately 65 μM to 90 μM. After ninety-six hours, the concentration of 3-H^--TNT decreased to a final concentration of approximately 72 μM. The increase in hydride and

dihydride-Meisenheimer complexes may explain the decrease in 3-H^--TNT concentrations (Figures 16 and 17).

2-HADNT (Figure 15C) and 4-HADNT (Figure 15D) were observed in the pH 4.5 treatments twenty-four hours before they were observed in the pH 6.5 treatments. In both treatments, the HADNTs increased in concentration throughout the time they were observed. Neither HADNT was observed in the pH 7.0 treatments during this study.

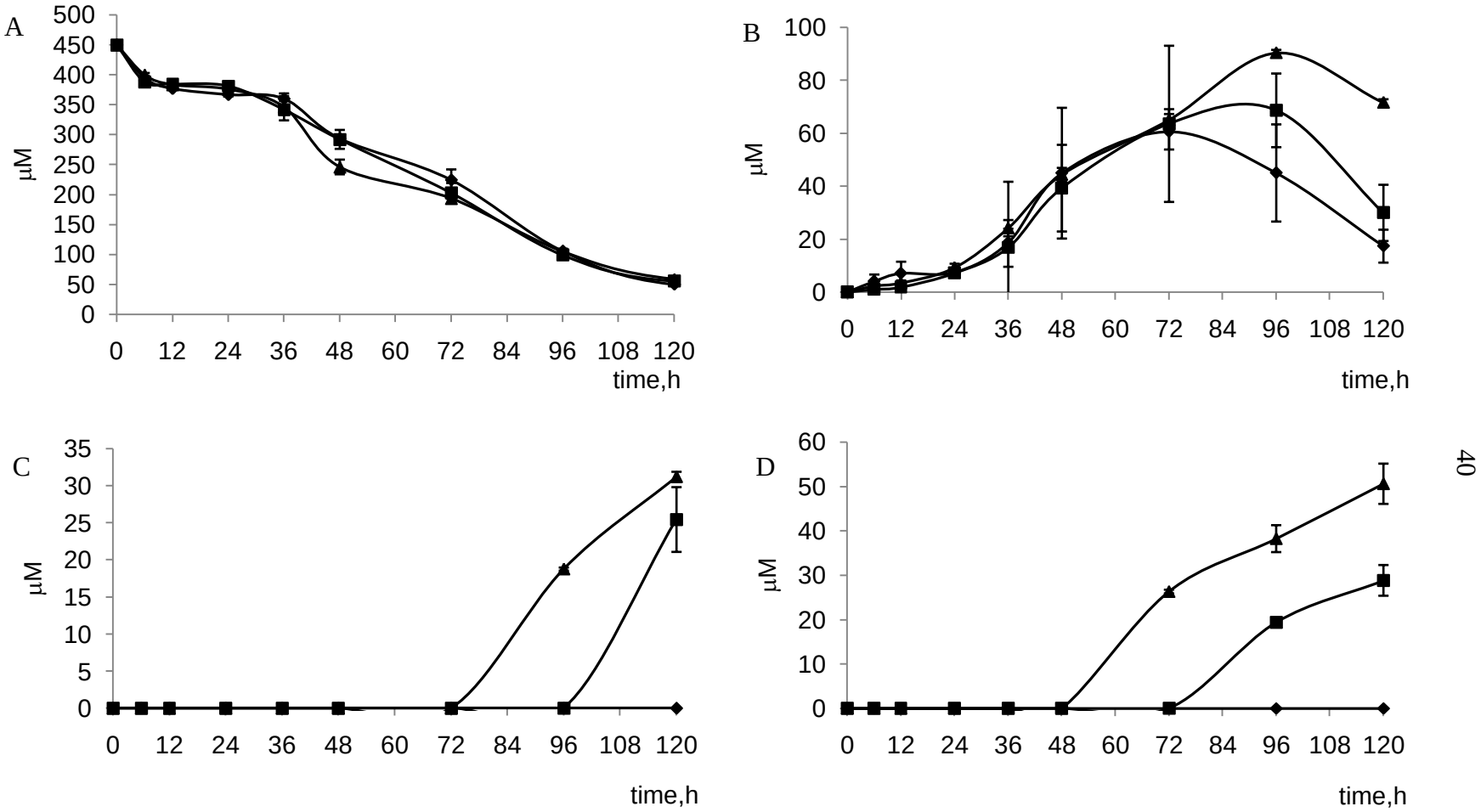

Figure 15. The transformation of TNT (Figure A) and formation of 3-H⁻-TNT (Figure B), 2-HADNT (Figure C), and 4-HADNT (Figure D) over time for treatments inoculated with *Y. lipolytica* AN-L15 in the presence of TNT. The three sets of treatments are represented on each graph. The diamonds represent the pH 7.0 treatments, the squares represent the pH 6.5 treatments, and the triangles represent the pH 4.5 treatments.

In addition to the 3-H^--TNT isomer identified above, the remaining two 3-H^--TNT isomers were observed, along with 3,5-$2H^-$-TNT and two isomers of 3,5-$2H^-$-TNT·H^+. The presence of these hydride and dihydride-Meisenheimer complexes was monitored by the color change of the medium (Figure 16) and by comparison of their spectrum and retention times with the hydride and dihydride-Meisenheimer complexes identified by Ziganshin et al. (2007). The medium changed from a colorless liquid to a deep red with the transformation of TNT to 3-H^--TNT and from deep red to yellow or orange with the transformation of 3-H^--TNT to dihydride and protonated dihydride-Meisenheimer complexes.

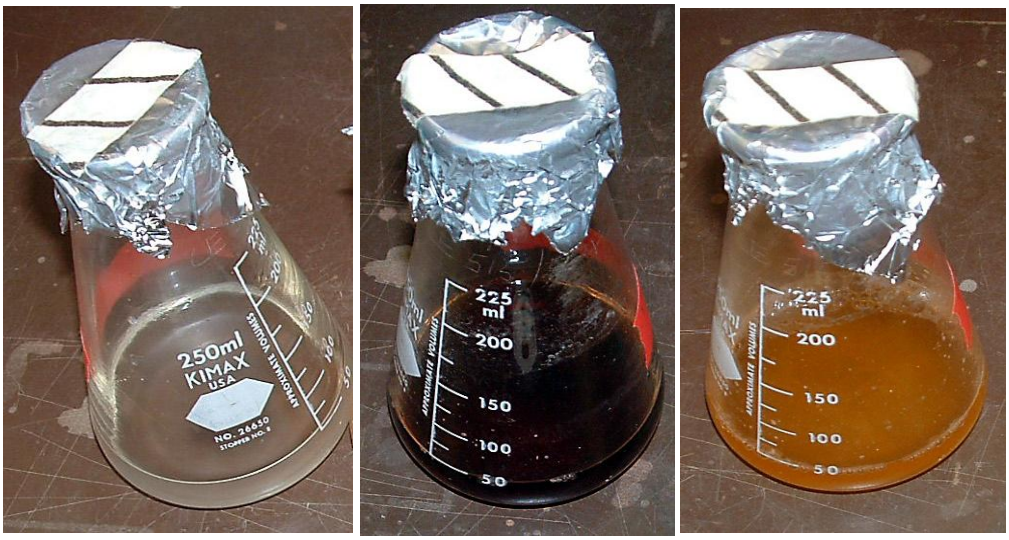

Figure 16. The photos are of the pH 4.5 medium inoculated with *Y. lipolytica* AN-L15 in the presence of TNT. From left to right, they were taken at the beginning of the study, at twenty-four hours, and at 120 hours, respectively. The red coloration of the medium in the middle photo is indicative of the transformation of TNT to 3-H^--TNT. The yellow coloration of the medium in the photo on the right is indicative of the transformation of 3-H^--TNT to dihydride-Meisenheimer and protonated dihydride-Meisenheimer complexes.

The concentrations of the two additional isomers of 3-H^--TNT, two isomers of 3,5-2H^--TNT·H^+, and 3,5-2H^--TNT are compared in Figure 17 as the sum total of the peak areas of 3-H^--TNT isomers, the sum total of the peak areas of 3,5-2H^--TNT·H^+ isomers, and the peak area of 3,5-2H^--TNT. For all three sets of metabolites, the pH 4.5 treatments had the highest concentration based on peak areas. In the pH 4.5 treatments, there was a sharp increase in peak areas for the 3-H^--TNT isomers between forty-eight and seventy-two hours, followed by a slight decrease over the remainder of the study. For the isomers of 3-H^--TNT and 3,5-2H^--TNT, the peak areas were similar between the treatments at pH 7.0 and the treatments at pH 6.5. The 3,5-2H^--TNT·H^+ isomers were observed to have higher cumulative peak areas in the pH 6.5 treatments than in the pH 7.0 treatments. None of the above-mentioned hydride or dihydride-Meisenheimer complexes were observed before forty-eight hours in any treatments; rather, all of them were first observed in the samples taken at forty-eight hours.

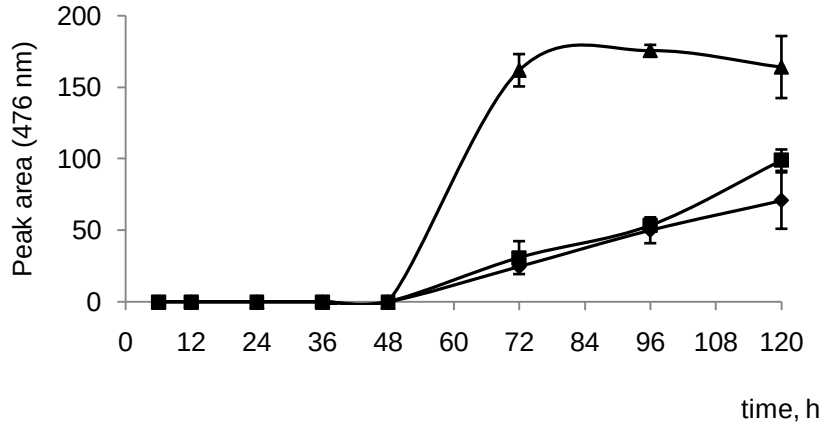

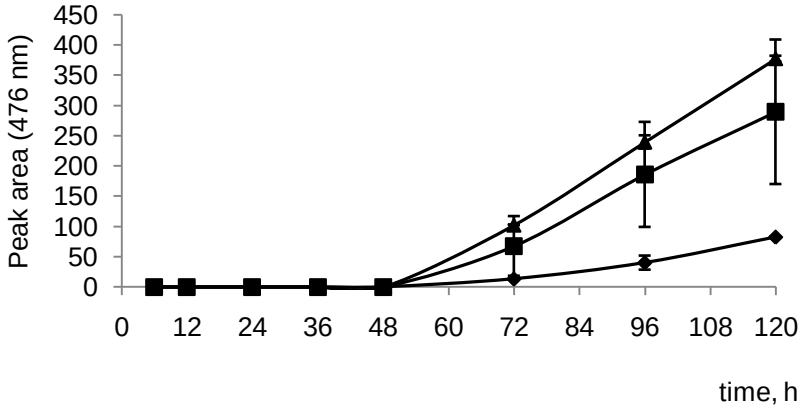

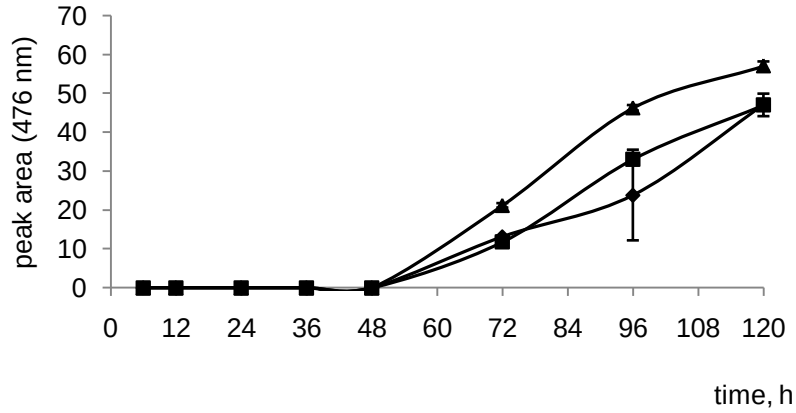

Figure 17. A comparison of the sum of the peak areas of two isomers of 3-H^--TNT (top left), of the sum of the peak areas of two isomers of 3,5-$2H^-$-TNT·H^+ (top right), and 3,5-$2H^-$-TNT (bottom) for the pH 7.0 treatments (diamonds), the pH 6.5 treatments (squares), and the pH 4.5 treatments (triangles).

Due to the instability of the hydride-Meisenheimer, dihydride-Meisenheimer, and protonated dihydride-Meisenheimer complexes, there are no standards available for comparison or calculations of the molar concentrations. Hence, the data are represented as peak area, with the exception of the isomer of 3-H^--TNT that is first observed in the transformation of TNT by *Y. lipolytica* AN-L15 (compound #7 in Table 2 and Figure 10). This isomer of 3-H^--TNT appears as the first metabolite in the aromatic ring reduction pathway and appears early. The approximate concentration of TNT and 4-HADNT are known at the six hour sampling time point. It was assumed the only other product formed at this early stage of transformation of TNT by *Y. lipolytica* AN-L15 was the 3-H^--TNT isomer. Based on this assumption, a one-point calculation was performed to determine the concentration of 3-H^--TNT; that concentration was used as the standard for the remaining calculations of concentrations of 3-H^--TNT (Ziganshin et al., 2007).

Reductive Transformation of TNT by *Y. lipolytica* AN-L15 in the Presence of Ferrihydrite

Due to the abundance of iron minerals in soils, it is likely that explosives contamination will occur in the presence of iron in the environment. It has been shown in previous work (discussed in the introduction) that the presence of iron in various mineral forms can enhance the reduction of TNT. To study the effects of iron on the transformation of TNT by *Y. lipolytica* AN-L15, medium was inoculated with *Y. lipolytica* AN-L15 in the presence of TNT, and in the presence or absence of ferric iron added as amorphous ferrihydrite. Throughout the study, the transformation of TNT was monitored according to the method described in the materials and methods. Additionally,

growth of *Y. lipolytica* AN-L15 was monitored in accordance with the protein assay protocol outlined in the materials and methods. Iron was assayed for total Fe and dissolved Fe(II) in accordance with the procedures outlined in the materials and methods.

Growth Curves

A Pierce-Coomassie assay was used to determine the growth of *Y. lipolytica* AN-L15, as estimated by protein concentrations. The results of the protein assays are shown in Figure 18. The greatest concentration of protein and shortest lag period, eighteen hours, was seen in the inoculated medium containing ferrihydrite in the absence of TNT. The inoculated medium with TNT and ferrihydrite had a longer lag period, forty-two hours, but similar protein concentrations were seen in both sets of treatments after sixty-six hours. The lowest concentration of protein was observed in the medium inoculated with *Y. lipolytica* AN-L15 and TNT. This treatment also had a lag period of forty-two hours. There was no increase in protein concentration in the uninoculated control containing ferrihydrite and TNT.

The presence of TNT in the culture medium acts as an initial hindrance on the growth (protein) of *Y. lipolytica* AN-L15, both in the presence and absence of ferrihydrite. Additionally, ferrihydrite causes an initial lag in the growth of *Y. lipolytica* AN-L15. Figure 18 shows that despite both TNT and ferrihydrite causing a lag in growth individually, the presence of both ferrihydrite and TNT together does not result in a greater lag in growth of *Y. lipolytica* AN-L15, than was observed only in the presence of TNT.

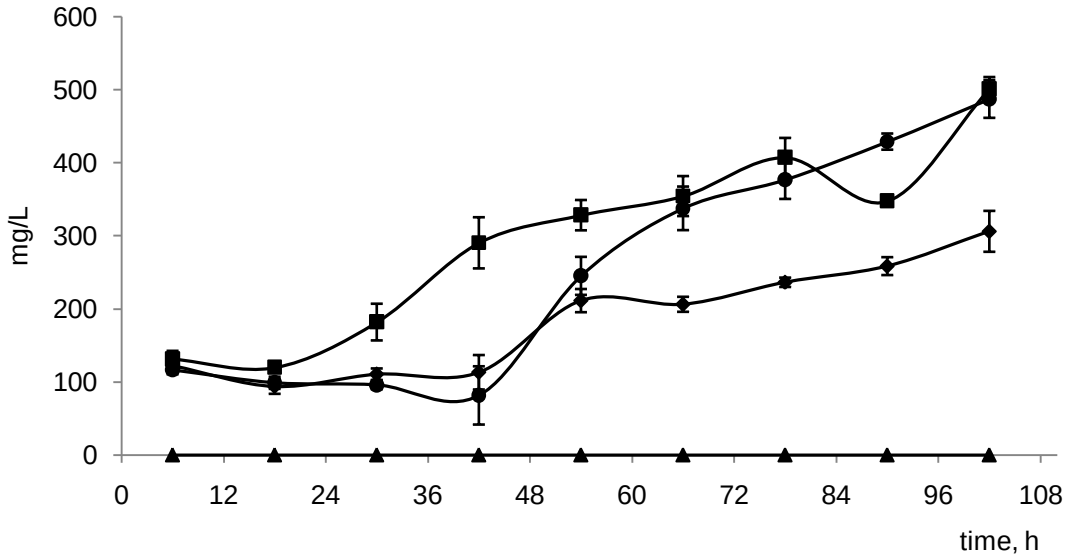

Figure 18. Growth curves, based on protein concentrations, are shown for the four different treatments used in this study. This graph shows the concentrations of protein over time. The four treatments are represented as follows: diamonds - *Y. lipolytica* AN-L15 and TNT, squares – *Y. lipolytica* AN-L15 and ferrihydrite, triangles – ferrihydrite and TNT, circles – *Y. lipolytica* AN-L15, ferrihydrite, and TNT.

Iron Analysis and pH Changes

Figure 19 shows the concentrations of Fe(II), total Fe, and the pH values over time. No Fe(II) or total Fe was detected in the control inoculated with *Y. lipolytica* AN-L15 in the presence of TNT, but not ferrihydrite. Also in the pH control medium containing only ferrihydrite and TNT, the pH values remained between 7.0 and 7.2 throughout the study.

The Fe(II) and total Fe profiles for the three remaining sets of treatments differed significantly. The treatment inoculated with *Y. lipolytica* AN-L15 in the presence of ferrihydrite, but not TNT, showed a general trend of increasing concentrations of Fe(II) throughout the study, with two exceptions. There was a decrease in Fe(II) concentrations in this treatment between eighteen hours and thirty hours. This decrease did not coincide

with a decrease in growth, but coincided with *Y. lipolytica* AN-L15 entering the exponential growth phase. It is possible that *Y. lipolytica* AN-L15 utilized a large portion of the dissolved Fe(II) as it entered exponential growth. In the treatment inoculated with *Y. lipolytica* AN-L15 in the presence of ferrihydrite and TNT, the exponential growth phase began at approximately forty-two hours. There was not a coinciding decrease in the concentration of Fe(II), as seen in the treatments above, but there was a significant decrease in the rate of Fe(II) formation during that time, which may support the statement that *Y. lipolytica* AN-L15 utilizes Fe(II) in the medium upon transition to exponential growth. The second decrease in Fe(II) concentrations in the treatment with *Y. lipolytica* AN-L15 in the presence of ferrihydrite, but not TNT, occurred between seventy-eight and ninety hours. This latter decrease in Fe(II) concentrations may be explained by a decrease in growth during the same time. The maximum observable concentration of Fe(II) for treatments with *Y. lipolytica* AN-L15 in the presence of ferrihydrite, but not TNT, was approximately 160 μM.

The treatments inoculated with *Y. lipolytica* AN-L15 in the presence of ferrihydrite and TNT showed the highest concentrations of Fe(II) throughout the study, with the largest increase being between thirty and forty-two hours. After forty-two hours, the increase leveled off. The leveling of the increase in concentrations of Fe(II) may be explained by the start of the exponential growth phase as hypothesized above. The maximum observable concentration of Fe(II) for treatments with *Y. lipolytica* AN-L15 in the presence of ferrihydrite and TNT was approximately 249 μM.

The uninoculated treatment with TNT and ferrihydrite showed fluctuating Fe(II) levels between thirty hours and the end of the study. The minimum observable concentration was approximately 12 μM, and the maximum observable concentration was approximately 81 μM, which was well below the values for treatments inoculated with *Y. lipolytica* AN-L15. Since no abiotic conversion of TNT was observed, it may be that ferrihydrite was reduced abiotically through media components.

The total Fe concentrations followed a similar pattern for the treatments with *Y. lipolytica* AN-L15 in the presence of ferrihydrite, but not TNT, and the treatments with *Y. lipolytica* AN-L15 in the presence of ferrihydrite and TNT, though the latter treatments were lower in concentration throughout the study. A sharp increase in total Fe concentrations was observed between sixty-six and ninety hours, followed by a sharp decrease between ninety hours and the end of the experiment. This pattern occurred in both sets of treatments. In the treatments with *Y. lipolytica* AN-L15 in the presence of ferrihydrite, but not TNT, there was a decrease in Fe(II) concentrations and a sharp decrease in protein concentrations that coincided with the sharp increase in total Fe. The sharp decrease in total Fe in this set of treatments also coincided with a sharp increase in protein concentrations. These changes in protein concentrations may indicate changes in growth and may explain the changes seen in the total Fe concentrations for this set of treatments. Similar occurrences in Fe(II) concentrations and growth were not observed in the treatments with *Y. lipolytica* AN-L15 in the presence of ferrihydrite and TNT, making it difficult to explain the changes in total Fe during the period of sharp increase. In the treatments with ferrihydrite and TNT only, total Fe was first observed between eighteen

and thirty hours. At thirty hours, total Fe was at its maximum concentration of approximately 993 μM and steadily decreased throughout the experiment to a final concentration of approximately 806 μM. Due to the inability to keep Fe suspended in the medium during sampling, there was some sampling error as identified by the larger error bars in Figure 19. This had some effect on the reliability of the total Fe data, but the trends still hold true even with the error bars.

There was a general trend of pH values decreasing over time for all treatments inoculated with *Y. lipolytica* AN-L15. The treatment with *Y. lipolytica* AN-L15 in the presence of ferrihydrite, but not TNT, and the treatment with *Y. lipolytica* AN-L15 in the presence of TNT, but not ferrihydrite, had very similar trends. The final pH values were 3.50 and 3.42, respectively, while the treatment with *Y. lipolytica* AN-L15 in the presence of ferrihydrite and TNT had a final pH value of 4.67. The lessened decrease in the pH values for treatments with *Y. lipolytica* AN-L15 in the presence of ferrihydrite and TNT may have been caused by the oxidation of Fe(II) to Fe(III) or by TNT-metabolites as discussed below.

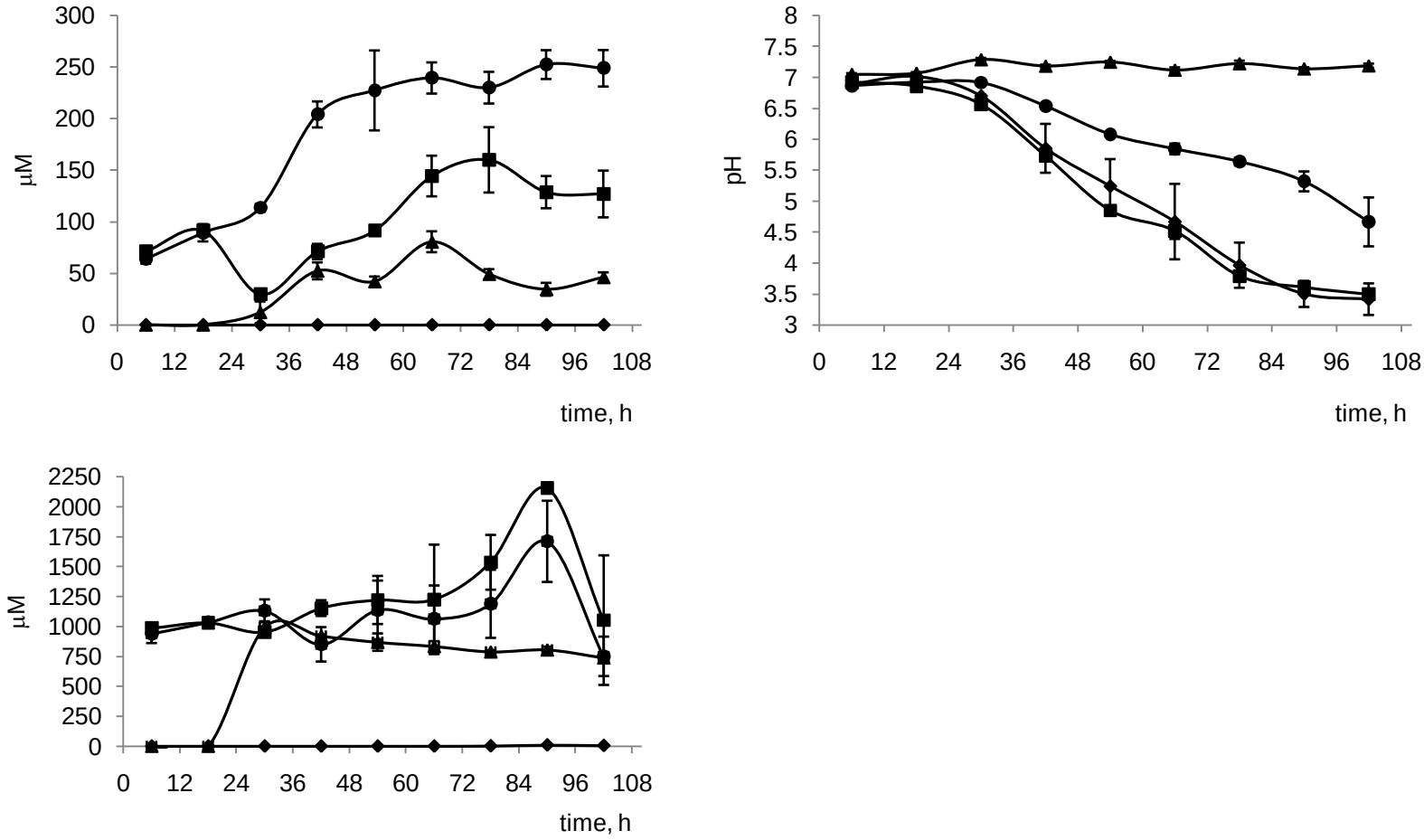

Figure 19: The top left graph shows Fe(II) concentrations for all four treatments. The bottom left graph shows total Fe concentrations for all four treatments. The top right graph shows pH values for all four treatments. The four treatments are represented as follows: diamonds - *Y. lipolytica* AN-L15 and TNT, squares – *Y. lipolytica* AN-L15 and ferrihydrite, triangles – ferrihydrite and TNT, and circles – *Y. lipolytica* AN-L15, ferrihydrite, and TNT.

Aromatic Ring Reduction Pathway, Products and Denitration

The transformation of TNT along the pathway of aromatic ring reduction was identified by color change of the media inoculated with *Y. lipolytica* AN-L15 in the presence of TNT, but not ferrihydrite, and of the media inoculated with *Y. lipolytica* AN-L15 in the presence of ferrihydrite and TNT. Figure 20 highlights the change in color of the media throughout the experiment for all four sets of treatments. The photos were taken at the beginning of the experiment (top left), at thirty hours (top right), at forty-two hours (bottom left), and at ninety hours (bottom right). The orange coloration of the media at the beginning of the study is due to the addition of ferrihydrite. The treatment on the far left of each photo shows *Y. lipolytica* AN-L15 in the presence of TNT, but not ferrihydrite. The medium changed from clear to deep red indicating the presence of 3-H^--TNT, predominantly. The maximum observable concentration of 3-H^--TNT in these treatments occurred at thirty hours. When comparing the photo on the top right (taken at thirty hours) and the photo on the bottom left (taken at forty-two hours), the photo on the top right shows a deeper, darker shade of red indicating higher concentrations of 3-H^--TNT than the photo on the bottom left. In the final photo, the color of the media changed from red to yellow indicating the transformation of 3-H^--TNT to dihydride-Meisenheimer complexes. Similar changes in color occurred in the flasks on the far right of each photo, treatments with *Y. lipolytica* AN-L15 in the presence of ferrihydrite and TNT. The top right photo for this treatment indicates small concentrations of 3-H^--TNT, based on the light red coloration. In the treatments second from the left in each photo, the change in

color can be explained by increased growth of *Y. lipolytica* AN-L15. These treatments became increasingly turbid throughout the study due to the increasing cell density.

Figure 20. The four treatments shown in each photo above, from left to right, are *Y. lipolytica* AN-L15 and TNT (YT), *Y. lipolytica* AN-L15 and ferrihydrite (YF), ferrihydrite and TNT (FT), and *Y. lipolytica* AN-L15, ferrihydrite, and TNT (YFT). The top left photo shows the four treatments at the beginning of the experiment. The top right photo shows the treatments at thirty hours. The red color of the medium for treatments YT and YFT was indicative of the presence of 3-H^--TNT. The bottom left photo taken at forty-two hours shows a change in color in the YFT treatment from red to orange this was indicative of the presence of a dihydride-Meisenheimer and protonated dihydride-Meisenheimer complexes. The change in color of the media from red to yellow, in treatments YT in the bottom right photo, was indicative of the presence of a dihydride-Meisenheimer and protonated dihydride-Meisenheimer complexes.

Figure 21 shows the decrease in concentrations of TNT and the transformation of 3-H^--TNT over time for the treatments inoculated with *Y. lipolytica* AN-L15 in the presence of TNT, and treatments inoculated with *Y. lipolytica* AN-L15 in the presence of ferrihydrite and TNT. In treatments inoculated with *Y. lipolytica* AN-L15 in the presence of TNT, TNT concentrations reached undetectable amounts between fifty-four and sixty-six hours. In the treatments with *Y. lipolytica* AN-L15 in the presence of ferrihydrite and TNT, TNT did not reach undetectable concentrations throughout the length of this study.

3-H^--TNT was observed in treatments inoculated with *Y. lipolytica* AN-L15 in the presence of TNT, between the beginning of the study and fifty-four hours. In these treatments, 3-H^--TNT concentrations increased between the beginning of the study and thirty hours; 3-H^--TNT reached a maximum concentration of approximately 59.0 μM at thirty hours. It then decreased until reaching undetectable concentrations at fifty-four hours. In treatments inoculated with *Y. lipolytica* AN-L15 in the presence of ferrihydrite and TNT, 3-H^--TNT was observed at thirty hours only. Its concentration at that time was approximately 10 μM. The lessened reduction of TNT and lower concentrations of 3-H^--TNT in treatments inoculated with *Y. lipolytica* AN-L15 in the presence of ferrihydrite and TNT may be a result of available electrons being used to reduce Fe(III) to Fe(II). The decrease in and eventual disappearance of 3-H^--TNT can be accounted for in the formation of other hydride and dihydride-Meisenheimer complexes and in the formation of nitrite.

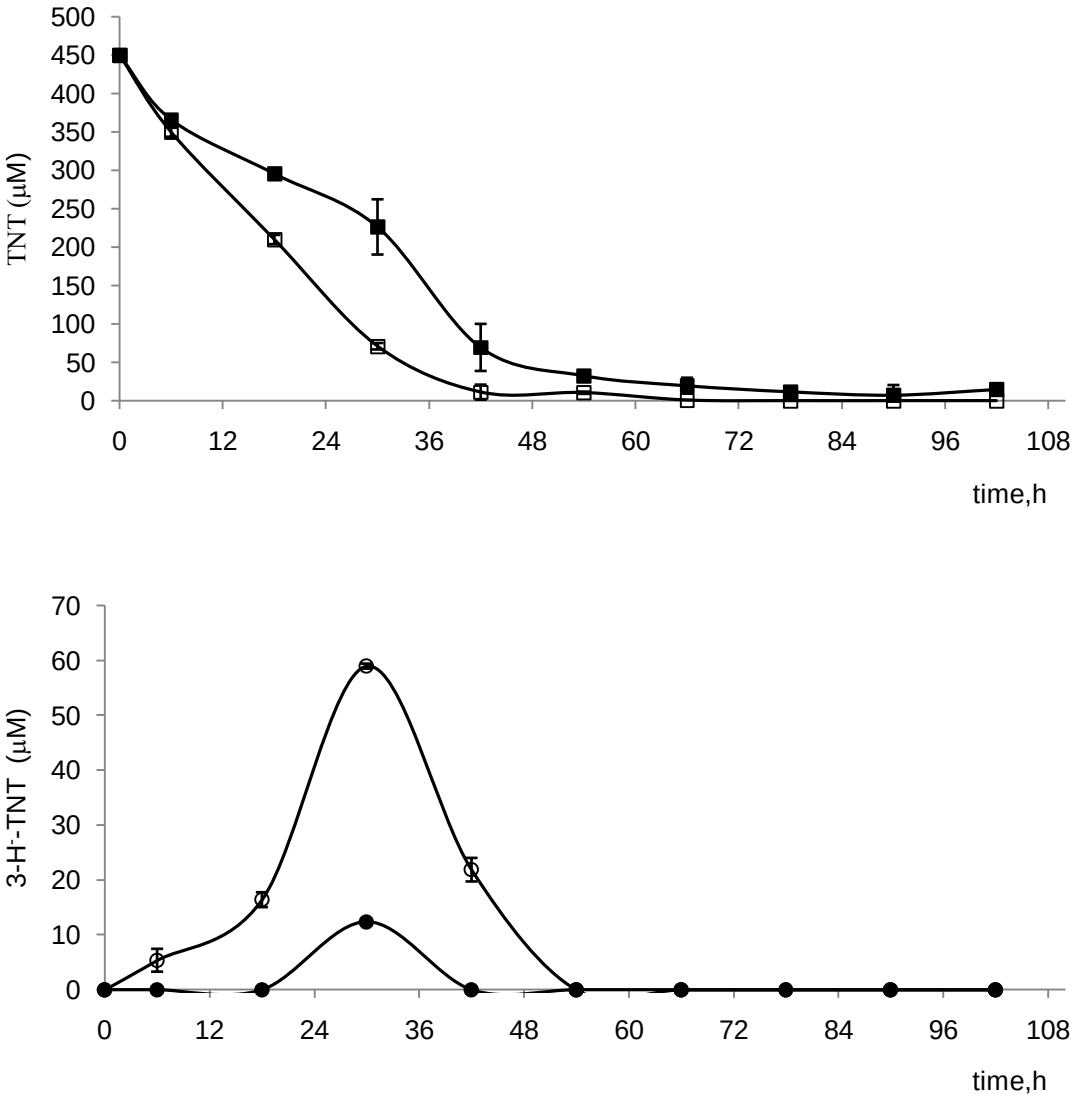

Figure 21. The top graph shows TNT concentrations over time for treatments inoculated with *Y. lipolytica* AN-L15 in the presence of TNT (unfilled squares) and for treatments inoculated with *Y. lipolytica* AN-L15 in the presence of ferrihydrite and TNT (filled squares). The bottom graph shows 3-H^--TNT concentrations over time for treatments inoculated with *Y. lipolytica* AN-L15 in the presence of TNT (unfilled circles) and for treatments inoculated with *Y. lipolytica* AN-L15 in the presence of ferrihydrite and TNT (filled circles).

In the treatments with *Y. lipolytica* AN-L15 in the presence of TNT, the 3-H^--TNT was transformed into the two remaining isomers of 3-H^--TNT, three isomers of 3,5-2H^--TNT·H^+, and 3,5-2H^--TNT (Figure 22). In the treatments with *Y. lipolytica* AN-L15

in the presence of ferrihydrite and TNT, the 3-H^--TNT was transformed into the one of the remaining two isomers of 3-H^--TNT, two isomers of 3,5-2H^--TNT·H^+, and 3,5-2H^--TNT (Figure 22). Figure 22 represents the sums of the isomers observed among the two sets of treatments. Not only were two more metabolites present in the treatments with *Y. lipolytica* AN-L15 in the presence of TNT than in the treatments with *Y. lipolytica* AN-L15 in the presence of ferrihydrite and TNT, but the metabolites present were in higher concentrations. This data, and the data shown in Figure 21, indicates that *Y. lipolytica* AN-L15 in the presence of ferrihydrite transforms less TNT through aromatic ring reduction than in the absence of ferrihydrite.

According to Ziganshin et al. (2007), nitrite can be released through denitration of 3,5-2H^--TNT·H^+ (compound #2 in Table 2 and Figure 10). Figure 23 shows the concentrations of 3,5-2H^--TNT·H^+ and nitrite over time for treatments with *Y. lipolytica* AN-L15 in the presence of TNT and treatments with *Y. lipolytica* AN-L15 in the presence of ferrihydrite and TNT. In treatments with *Y. lipolytica* AN-L15 in the presence of TNT, 3,5-2H^--TNT·H^+ was observed between eighteen and sixty-six hours. 3,5-2H^--TNT·H^+ was never observed in the treatments with *Y. lipolytica* AN-L15 in the presence of ferrihydrite and TNT.

Nitrite was observed in both sets of treatments. During the first forty-two hours, nitrite was present in similar concentrations between the two sets of treatments, with the *Y. lipolytica* AN-L15 in the presence of TNT treatments having slightly higher concentrations. Between forty-two hours and fifty-four hours, the concentrations of nitrite in the *Y. lipolytica* AN-L15 in the presence of ferrihydrite and TNT treatments

exceeded the concentrations of nitrite in the *Y. lipolytica* AN-L15 in the presence of TNT treatments. The concentrations of nitrite remained that way until just after seventy-eight hours, at which time the concentrations of nitrite were once again higher in the treatments with *Y. lipolytica* AN-L15 in the presence of TNT than in the treatments with *Y. lipolytica* AN-L15 in the presence of ferrihydrite and TNT. The decrease in concentrations of nitrite between thirty hours and forty-two hours in the treatments with *Y. lipolytica* AN-L15 in the presence of TNT coincide with a decrease in the concentrations of 3-H^--TNT and a decrease in the concentrations of 3,5-2H^--TNT·H^+. Similarly the decrease in concentrations of nitrite, in the treatments with *Y. lipolytica* AN-L15 in the presence of ferrihydrite and TNT, between thirty and forty-two hours coincide with the disappearance of 3-H^--TNT over the same time. These decreases in nitrite at this time may have been caused by sampling errors, since it would be expected for the nitrite concentrations to increase when the concentration of 3,5-2H^--TNT·H^+ and 3-H^--TNT are decreasing.

Given that nitrite was detected and 3,5-2H^--TNT·H^+ was not detected in the treatments with *Y. lipolytica* AN-L15 in the presence of ferrihydrite and TNT, this data indicates the possibility of additional pathways to the release of nitrite other than the pathway identified by Ziganshin et al. (2007). This hypothesis will be discussed in more detail in the discussion section of this thesis.

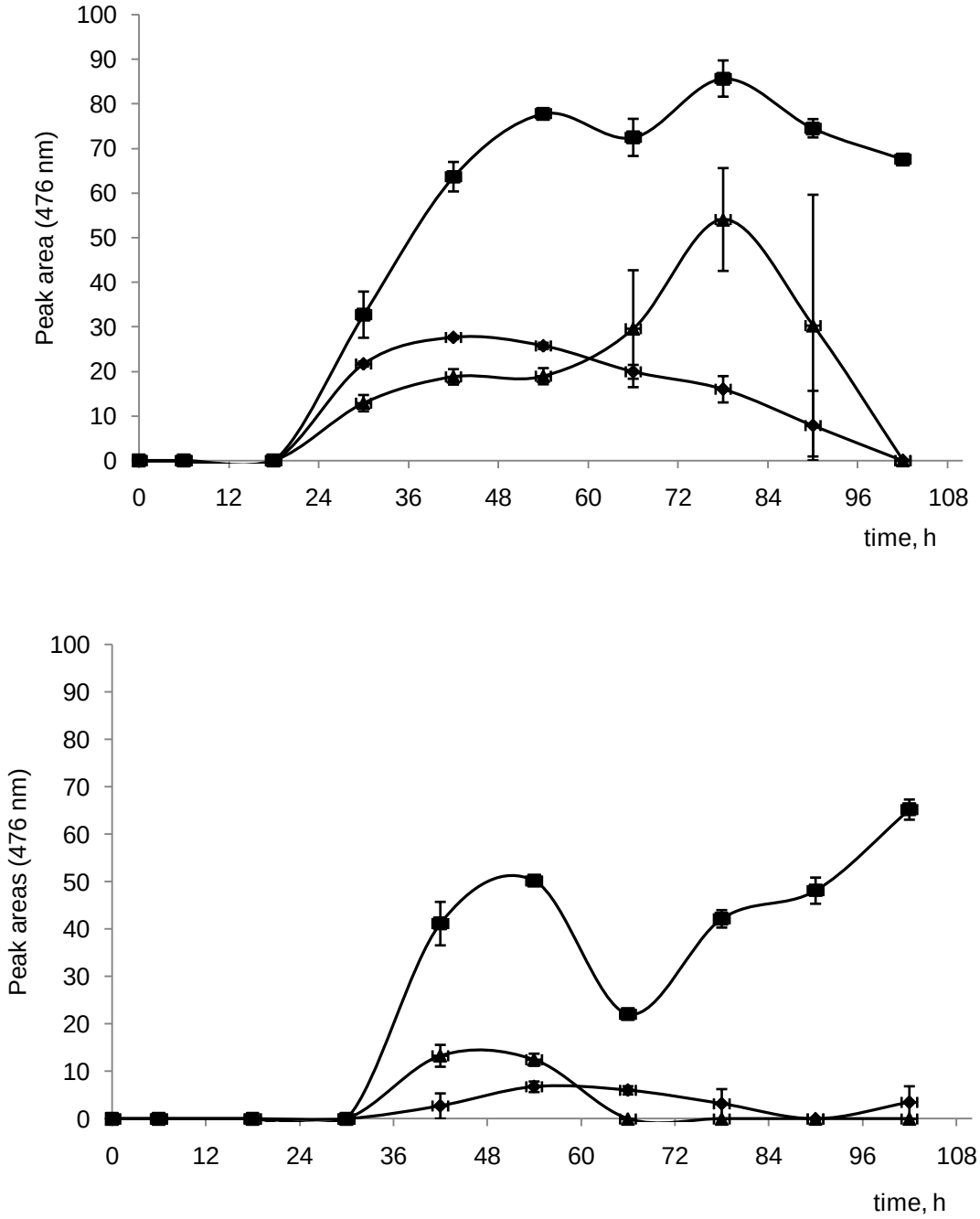

Figure 22. Peak areas of TNT-metabolites observed during the transformation of TNT via the aromatic ring reduction pathway. The top graph represents treatments inoculated with *Y. lipolytica* AN-L15 in the presence of TNT, and the bottom graph represents treatments inoculated with *Y. lipolytica* AN-L15 in the presence of ferrihydrite and TNT. Diamonds represent the sum of the peak areas of isomers of 3-H^--TNT, squares represent the sum of the peak areas of isomers of 3,5-2H^--TNT·H^+, and triangles represent the peak area of 3,5-2H^--TNT.

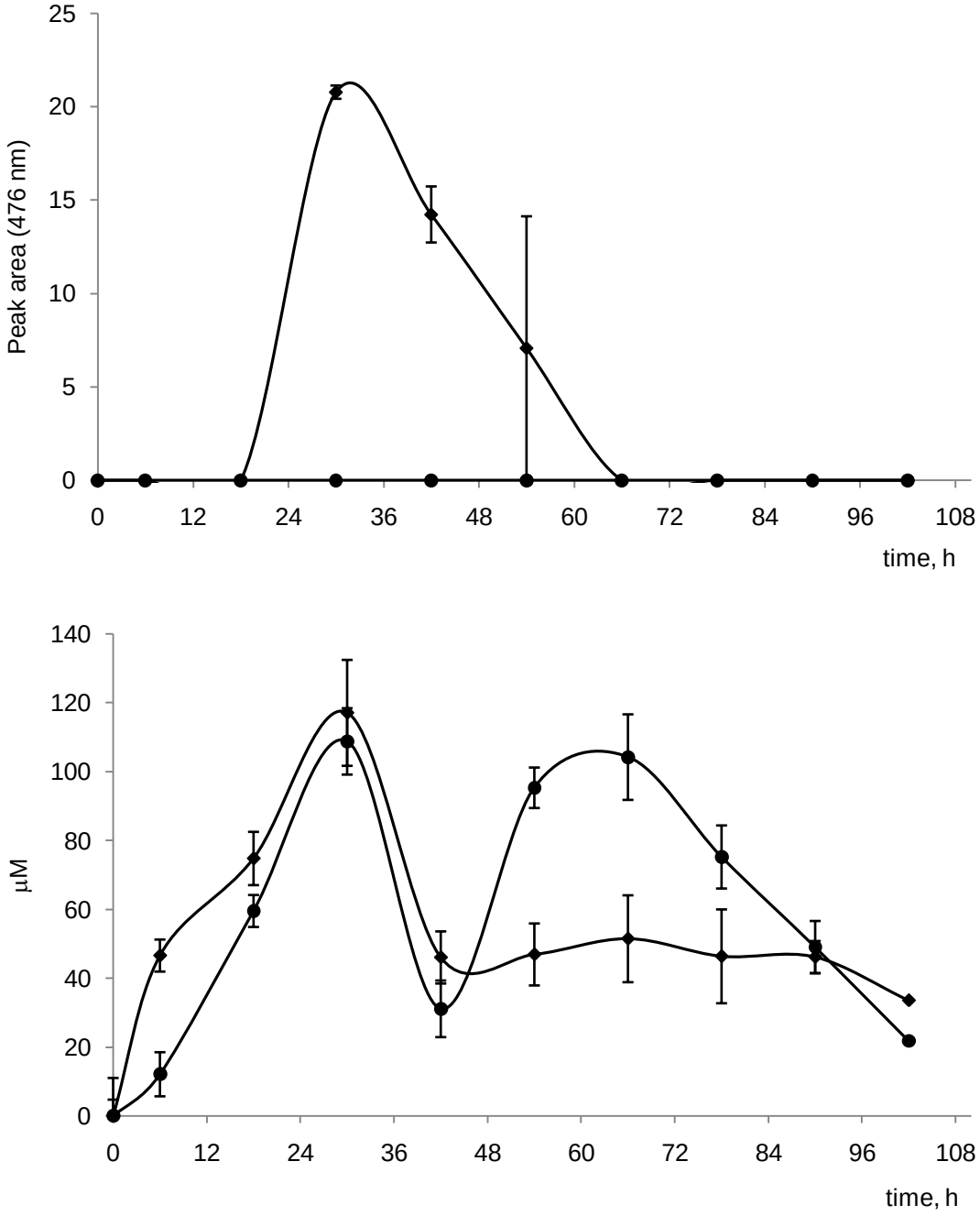

Figure 23. The top graph shows the peak areas detected for 3,5-2H$^-$-TNT·H$^+$ (compound #2 in table 2 and Figure 10). The bottom graph shows concentrations of nitrite detected throughout the study. Diamonds represent treatments inoculated with *Y. lipolytica* AN-L15 in the presence of TNT, and circles represent treatments inoculated with *Y. lipolytica* AN-L15 in the presence of ferrihydrite and TNT.

Formation of TNT-Metabolites via the
Nitro-Group Reduction Pathway

The transformation of TNT by *Y. lipolytica* AN-L15 in the presence and absence of ferrihydrite also formed TNT-metabolites via the nitro-group reduction pathway. The concentrations of these TNT-metabolites are shown in Figure 24. In the treatments inoculated with *Y. lipolytica* AN-L15 in the presence of TNT, the concentrations of 2-HADNT and 4-HADNT were higher throughout the study than in the treatments inoculated with *Y. lipolytica* AN-L15 in the presence of ferrihydrite and TNT (top graph, Figure 24). In the treatments with *Y. lipolytica* AN-L15 in the presence of TNT, concentrations of 2-HADNT increased steadily for the first forty-two hours, then leveled off for the remainder of the experiment. The final concentration of 2-HADNT was approximately 60 μM. In these same treatments, concentrations of 4-HADNT steadily increased for the first sixty-six hours, then leveled off. The final concentration of 4-HADNT was approximately 166 μM. In the treatments with *Y. lipolytica* AN-L15 in the presence of ferrihydrite and TNT, 2-HADNT was first observed at thirty hours, increasing in concentration until forty-two hours, after which time it decreased in concentration for the remainder of the study. The final concentration of 2-HADNT was approximately 17 μM. In these same treatments 4-HADNT had a more erratic pattern. It was first observed at thirty hours, increasing in concentration until forty-two hours, then decreasing in concentration until sixty-six hours. It again increased in concentration between sixty-six hours and seventy-eight hours, and then decreased in concentration for

the remainder of the experiment. The final concentration of 4-HADNT was approximately 71 μM.

For the two sets of experiments, the concentrations of 2-ADNT and 4-ADNT are shown on the bottom graph in Figure 24. Both 2-ADNT and 4-ADNT were observed for the same amount of time, and in similar concentrations, for both sets of treatments, throughout the experiment. For both metabolites, the trend was for the treatments with *Y. lipolytica* AN-L15 in the presence of ferrihydrite and TNT to have the higher concentrations before seventy-eight hours and lower concentrations beyond seventy-eight hours than the treatments with *Y. lipolytica* AN-L15 in the presence of TNT. The final concentrations for the treatments with *Y. lipolytica* AN-L15 in the presence of TNT were: 7.0 μM of 2-ADNT and 24 μM of 4-ADNT. The final concentrations for the treatments with *Y. lipolytica* AN-L15 in the presence of ferrihydrite and TNT were: 5 μM of 2-ADNT and 19 μM of 4-ADNT.

The fact that more 4-HADNT and 4-ADNT were produced than 2-HADNT and 2-ADNT supports the hypothesis that TNT transformation by *Y. lipolytica* AN-L15 is regioselective toward reduction along the para- pathway of nitro-group reduction. This pattern was also observed among the HADNTs of the previous study involving the different initial pH of the culture medium.

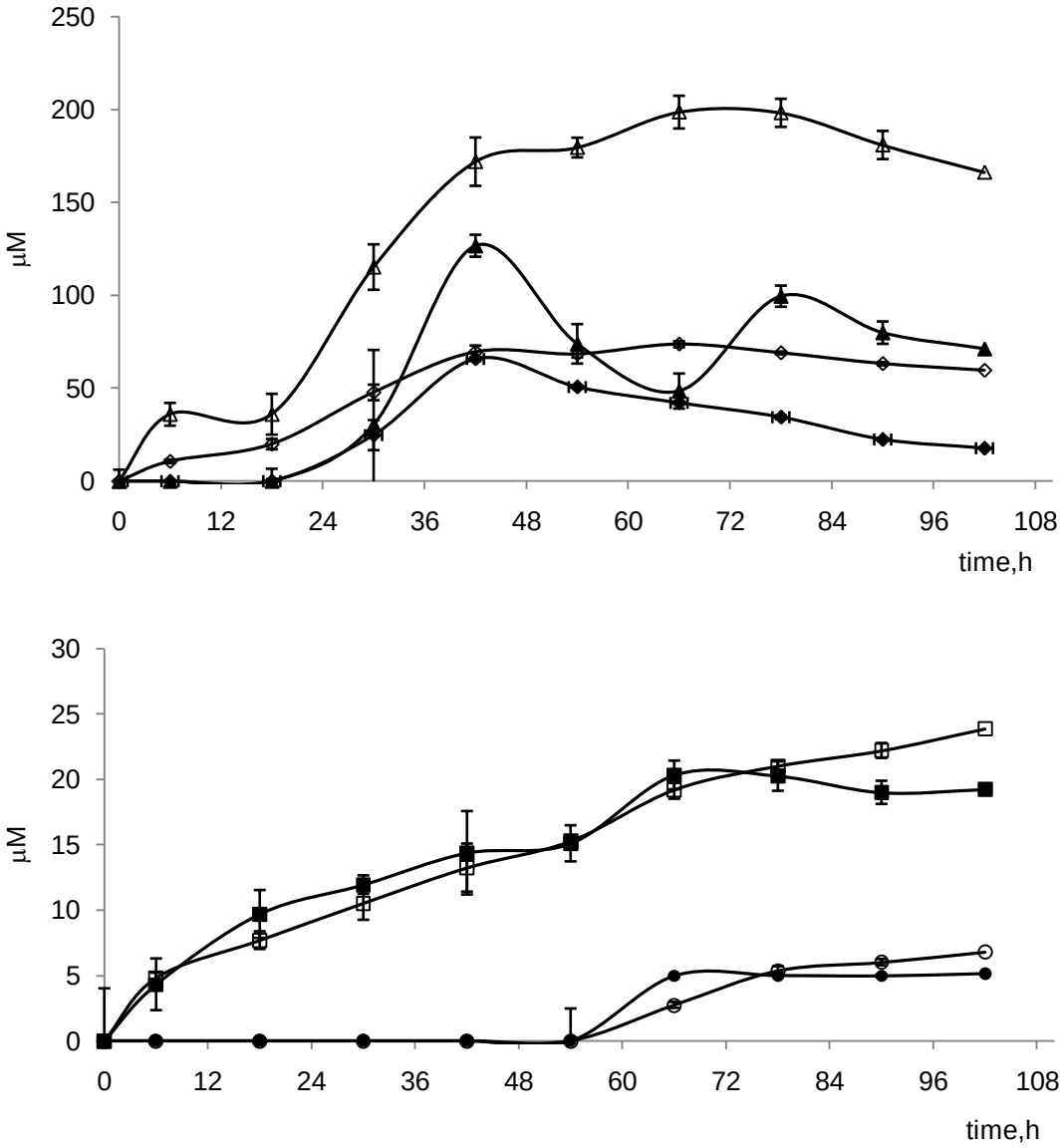

Figure 24. The top graph shows concentrations of 2-HADNT and 4-HADNT. The bottom graph shows concentrations 2-ADNT and 4-ADNT. Unfilled diamonds represent 2-HADNT for treatments inoculated with *Y. lipolytica* AN-L15 in the presence of TNT; filled diamonds represent 2-HADNT for treatments inoculated with *Y. lipolytica* AN-L15 in the presence of ferrihydrite and TNT. Unfilled triangles represent 4-HADNT for treatments inoculated with *Y. lipolytica* AN-L15 in the presence of TNT; filled triangles represent 4-HADNT for treatments inoculated with *Y. lipolytica* AN-L15 in the presence of ferrihydrite and TNT. Unfilled circles represent 2-ADNT for treatments inoculated with *Y. lipolytica* AN-L15 in the presence of TNT; filled circles represent 2-ADNT for treatments inoculated with *Y. lipolytica* AN-L15 in the presence of ferrihydrite and TNT. Unfilled squares represent 4-ADNT for treatments inoculated with *Y. lipolytica* AN-L15 in the presence of TNT; filled squares represent 4-ADNT for treatments inoculated with *Y. lipolytica* AN-L15 in the presence of ferrihydrite and TNT.

DISCUSSION

Reduction of TNT by *Y. lipolytica* AN-L15 with Different Initial pH of the Culture Medium

It is important to note a significant difference in the study conducted herein, and the study published by Ziganshin et al. (2007). Parts of this study were compared to Ziganshin et al. (2007), but in the Ziganshin et al. (2007) study, the initial culture medium had an OD of 0.2. In the section of this thesis addressing the different initial pH values of the culture medium, the initial OD was a result of adding only 5 mL of inoculum from the pH 7.0 original treatments, to 50 mL of synthetic medium for the three different pH treatments; this gave a starting OD of approximately 0.003. Therefore, the results of the main part of this study, the different initial pH values in the culture medium, should not be directly compared to Ziganshin et al. (2007). Direct comparison should be reserved only for the pH 7.0 original treatments, which had an initial OD of 0.2.

There is a positive correlation between lowering the pH value of the initial culture medium from a pH of 7.0 to a pH of 4.5 and the transformation of TNT. Since there was no observable transformation of TNT in the controls with TNT but without *Y. lipolytica* AN-L15, it can be assumed that pH does not have a direct effect on the transformation of TNT. Rather, it is apparent that *Y. lipolytica* AN-L15 in the presence of TNT has preferential growth (OD_{600}) at the lower pH of 4.5. The increase in growth (OD_{600}) leads to an increase in the concentration of available enzymes to reduce TNT, therefore, a decrease in TNT concentration and an increase in formation of TNT-metabolites from both the aromatic ring reduction pathway and the nitro-group reduction pathway. Not

only was there more growth (OD_{600}) of *Y. lipolytica* AN-L15 in the presence of TNT at the pH of 4.5, but the transition to exponential growth (OD_{600}) from the lag phase happened twenty-four hours earlier than in either the pH 7.0 treatments with TNT or the pH 6.5 treatments with TNT.

There was an increase in growth (OD_{600}) of *Y. lipolytica* AN-L15 in the presence of TNT in the pH 6.5 treatments from seventy-two hours until the end of the study that resulted in *Y. lipolytica* AN-L15 in these treatments being able to "catch up" to the growth (OD_{600}) of the *Y. lipolytica* AN-L15 in the presence of TNT in the pH 4.5 treatments. After seventy-two hours, the formation of 4-HADNT was observed in the pH 6.5 treatments and may be attributed to the increase in growth (OD_{600}).

2-HADNT and 4-HADNT were not observed in the pH 7.0 treatments throughout this study. In the pH 6.5 treatments, 2-HADNT and 4-HADNT each appeared twenty-four hours after they appeared in the pH 4.5 treatments. This may be due to the twenty-four hour difference between the two sets of treatments in exiting the lag phase. Also, in the pH 4.5 treatments and in the pH 6.5 treatments, 2-HADNT appeared within twenty-four hours of the appearance of 4-HADNT; this correlated with a 1.22 fold increase in the OD measurement for both sets of treatments over the same time period. In the pH 7.0 original treatments, 2-HADNT appeared within six hours of the appearance of 4-HADNT, which may be explained due to higher initial OD measurements equating to more cells initially, and a similar 1.22 fold increase was seen in the OD measurements for that time period. This may indicate a dependence on a specific ratio of active enzymes to be present in order for the transformation of TNT to use the ortho- as well as the para-

pathways of nitro-group reduction. It could also indicate the requirement of certain enzymes or cofactors that only become active or present in the presence of 4-HADNT.

The primary pathway of TNT reduction in all three sets of treatments was aromatic ring reduction. The aromatic ring reduction pathway of TNT followed an expected pattern, based on the growth (OD_{600}), of being greatest in the pH 4.5 treatments with TNT and least in the pH 7.0 treatments with TNT. The pH 4.5 treatments with TNT showed the greatest formation of the hydride-Meisenheimer, dihydride-Meisenheimer, and protonated dihydride-Meisenheimer complexes. There was a decrease in the concentration of 3-H^--TNT for all three treatments towards the end of the experiment. This may be explained by the increasing concentrations of the other hydride and dihydride-Meisenheimer complexes. It is likely that 3-H^--TNT was transformed into these other complexes.

It is also important to note that, throughout this set of experiments, there were complications with the analysis of the samples using the Agilent 1100 series HPLC. The composition of the medium was not ideal for analyzing the metabolite data on the 1100 series HPLC with the Supelcosil LC-8 column. The column would clog or the lines running from the column to the DAD would clog and cause the system to shut down due to high pressure errors. This led to downtime in analyzing samples, due to maintenance of the HPLC. During this time, samples were kept under refrigeration at 2^o C, but given the instability of some of the metabolites, especially those from the aromatic ring reduction pathway; it is possible that despite the samples being filtered to remove *Y. lipolytica* AN-L15, there was further transformation of TNT-metabolites. Ziganshin et al.

(2007) showed that 3-H^--TNT could transform back to TNT or further transform into other hydride-Meisenheimer complexes and dihydride-Meisenheimer complexes, abiotically. This abiotic conversion may have lead to altered values of TNT and some hydride-Meisenheimer complexes and dihydride-Meisenheimer complexes. This may explain some of the decrease in the 3-H^--TNT concentrations in all three sets of treatments from ninety-six hours until the end of the study.

Reductive Transformation of TNT by *Y. lipolytica* AN-L15 in the Presence of Ferrihydrite

The first part of this thesis described how one environmental parameter, pH change, could have an effect on the transformation of TNT by *Y. lipolytica* AN-L15. The change in pH did not appear to change the pathway of transformation of TNT; rather, the reduction time of TNT-metabolites changed possibly by creating more ideal growth conditions for *Y. lipolytica* AN-L15 or by decreasing the metabolic activity at the higher pH values. There are other environmental parameters to consider in the transformation of TNT by *Y. lipolytica* AN-L15: oxygen concentrations, mineral concentrations, ground water flow conditions, and microbial consortia, to name a few. The second major objective of this study was to look at the effect of ferrihydrite, another environmental parameter, on the transformation of TNT by *Y. lipolytica* AN-L15.

While cultures inoculated with *Y. lipolytica* AN-L15 in the presence of ferrihydrite and TNT or cultures inoculated with *Y. lipolytica* AN-L15 in the presence of ferrihydrite showed different growth patterns in the initial stages of the experiment, by sixty-six hours they showed similar growth patterns based on concentrations of proteins. In both

treatments, growth was enhanced by the addition of ferrihydrite as compared to the growth of *Y. lipolytica* AN-L15 in the presence of TNT without ferrihydrite. The initial lag in growth in treatments with *Y. lipolytica* AN-L15 in the presence of ferrihydrite and TNT was most likely due to the presence of TNT and TNT-metabolites.

The addition of ferrihydrite to the inoculated cultures resulted in a shift in the transformation pathway of TNT. TNT reduction in the presence of ferrihydrite was primarily along the nitro-group reduction pathway. TNT was never completely reduced in the presence of ferrihydrite, and all metabolites present were in lower concentrations than in the treatments without ferrihydrite, despite the 1.6 fold increase in growth of *Y.* lipolytica AN-L15 in treatments with ferrihydrite, between sixty-six hours and the end of the study (Figure 25). The lessened reduction of TNT and the lower concentrations of TNT-metabolites in the presence of ferrihydrite may be due to the loss of available electrons as they are used in the reduction of Fe(III) to Fe(II). Another reason for the lessened reduction of TNT and lower concentrations of TNT-metabolites may be due to the oxidation of TNT-metabolites to TNT in the presence of ferrihydrite.

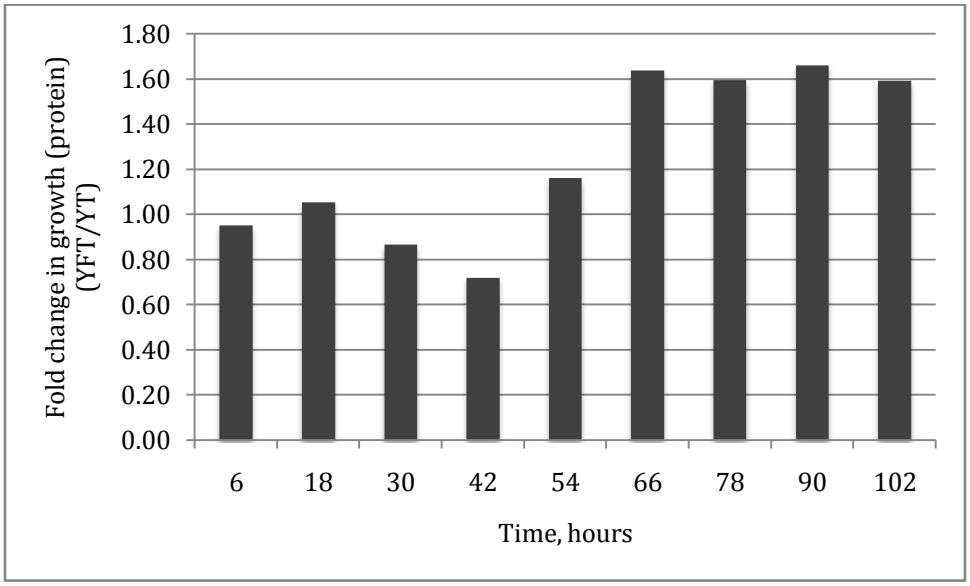

Figure 25. Fold change in the growth of *Y. lipolytica* AN-L15 in the presence of ferrihydrite and TNT (YFT) over *Y. lipolytica* AN-L15 in the presence of TNT (YT). Growth is based on protein concentrations.

Interestingly, the concentrations of nitrite were similar for the two treatments from the beginning of the experiment through forty-two hours, but between forty-two hours and ninety hours, the treatments with ferrihydrite had a higher concentration of nitrite than the treatments without ferrihydrite. It was assumed that the formation of nitrite from the reduction of TNT occurred from the transformation of one of the isomers of 3,5-$2H^-$-TNT-H^+ (compound #2 in Table 2 and Figure 10), but the lack of observable concentrations of this metabolite from the aromatic ring reduction pathway in treatments with ferrihydrite did not support this. There have been several papers published since the start of this thesis that support a different argument for the formation of nitrite. van Dillewijn et al. (2008), Wittich et al. (2008), and Wittich et al. (2009) propose that nitrite is formed from the rearomatization of dihydride-Meisenheimer complexes through the

condensation with HADNTs. The resulting products are nitrite and secondary diarylamines (Figure 26).

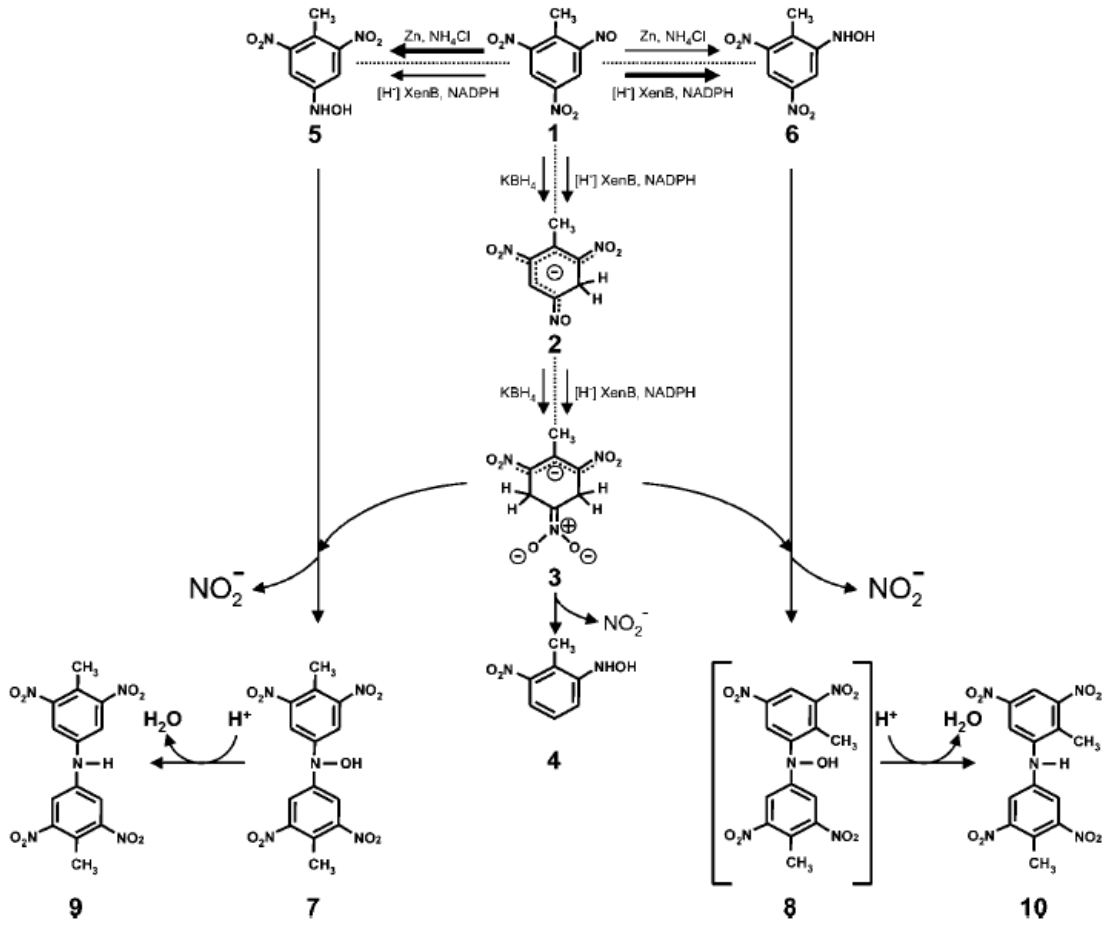

Figure 26. This figure shows the pathways that lead to the release of nitrite and diarylamines (compounds 9 and 10) via the rearomatization of dihydride-Meisenheimer complexes through the condensation of HADNTs. Compound 1 is TNT, compound 2 is a monohydride-Meisenheimer complex, compound 3 is a dihydride-Meisenheimer complex, compound 4 is 2-hydroxylamino-6-nitrotoluene, compound 5 is 4-HADNT, compound 6 is 2-HADNT, compound 7 is symmetric N,N-bis(3,5dinitrotolyl)hydroxylamine, compound 8 is identified only as a hydroxylamine precursor, compound 9 is symmetric N,N-bis(3,5-dinitrotolyl)amine, and compound 10 is *N*-(2-methyl-3,5-dinitrophenyl)-4-methyl-3,5-dinitroaniline. Reprinted with permission from Wittich R., A. Haidour, P. van Dillewijn, and J. Ramos. 2008. OYE flavoprotein reductases initiate the condensation of TNT-derived intermediates to secondary diarylamines and nitrite. Environ. Sci. Technol. 42:734-739. Copyright 2008 American Chemical Society.

Wittich et al. (2008) shows the formation of approximately 200 μM of nitrite from approximately 850 μM of TNT in 150 minutes. These studies were done with the addition of 0.02 mL of XenB reductase added to 0.85 mL of TNT saturated potassium phosphate buffer, as opposed to this thesis which used whole organisms growing in synthetic medium, therefore, the decrease in TNT concentration and the increase in TNT-metabolite formation in the studies above are much faster than those of this thesis. Their argument for the pathway of nitrite production is supported by their evidence of a decrease in the concentrations of HADNT and isomers of 3,5-$2H^-$-TNT-H^+ while observing an increase in the concentrations of secondary diarylamines and nitrite. The authors mention that 3,5-$2H^-$-TNT-H^+ is being formed from 3-H^--TNT much faster than 3-H^--TNT is being formed from TNT. The authors also observed only small quantities of dihydride-Meisenheimer complexes. If this additional pathway for nitrite formation is correct, then it may explain the concentrations of nitrite in the treatments with ferrihydrite, despite no observable concentrations of the isomer of 3,5-$2H^-$-TNT-H^+ (compound #2 in Table 2 and Figure 10) discussed by Ziganshin et al. (2007), lower concentrations of hydride and dihydride-Meisenheimer complexes, and lower concentrations of HADNTs.

This thesis did not take into account the formation of diarylamines, which have a very low solubility. Since only aqueous phase samples were analyzed, their formation might have been missed. Further work will need to be conducted to determine if diarylamines are indeed formed during the transformation of TNT by *Y. lipolytica* AN-L15 in the presence and absence of ferrihydrite.

Another reason for the slower reduction of TNT and the lower concentrations of TNT-metabolites in the presence of ferrihydrite could be due to the competition for electrons between TNT and TNT-metabolites and Fe(III). Both TNT and its metabolites and Fe(III) are potential electron acceptors for the electrons generated from the metabolism of glucose by *Y. lipolytica* AN-L15. By adding ferrihydrite to the culture medium containing TNT, it creates an additional electron acceptor and is likely competing for electrons that could have been used in the reduction of TNT.

There were periods of decreasing concentrations of Fe(II) and periods of increasing concentrations of total Fe during this thesis study. This may have occurred due to some TNT-metabolites being transformed in a reverse direction along their respective pathways, using Fe(II) as an electron donor (Figure 27). Illustrated in Figure 27 is the oxidation of 3-H^--TNT to TNT. This could also occur from other intermediates oxidizing back to previous metabolites. This would result in lower concentrations of metabolites, decreased overall TNT transformation, and a decrease in Fe(II) formation, all of which were observed in this study.

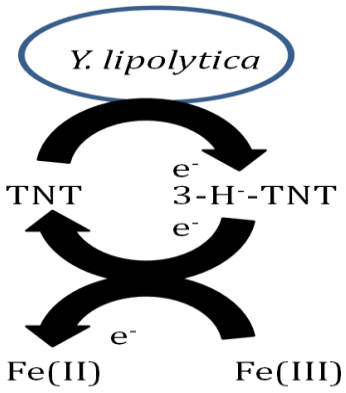

Figure 27. A schematic diagram showing the transfer of electrons from *Y. lipolytica* AN-L15 to TNT resulting in the reduction of TNT to 3-H^--TNT. 3-H^--TNT is then oxidized by Fe(III) resulting in the formation of Fe(II) and the oxidation 3-H^--TNT to TNT.

Future Work

There are several areas of future work to consider. The first of which would be to conduct a study of the flow of N throughout the transformation of TNT in the presence and absence of ferrihydrite. This type of study is beyond both the scope of this thesis, and the scope of the author's knowledge on analytical techniques to use for such a study, but it would assist in understanding the transformation pathways, especially in regard to the production of nitrite. Table 3 shows the stoichiometric balances from the study involving *Y. lipolytica* AN-L15, ferrihydrite, and TNT. The balances are not closed partly due to not having standards to measure the hydride and dihydride-Meisenheimer complexes. There is also the possibility of the formation of other metabolites that have yet to be identified. ^{14}C-labeled TNT could be used in the future to improve the mass balance and identify unknown metabolites. Other than the isomer of 3-H$^-$-TNT previously mentioned, the remaining complexes do not appear in the balance since they were only represented by peak areas. IC analysis of nitrite and nitrate production could be performed again for the three treatments with different initial pH of the culture medium, since the data was lost due to equipment malfunctions.

Table 3. The concentrations of 2-HADNT, TNT, 4-HADNT, 2-ADNT, 4-ADNT, 3-H$^-$-TNT, NO_2^-, and NO_3^- expressed in μM for treatments with *Y. lipolytica* AN-L15 and TNT (top table) and for treatments with *Y. lipolytica* AN-L15, ferrihydrite, and TNT (bottom table) The bolded column on the right of each table shows the stoichiometric balance at each sampling time.

***Y. lipolytica* AN-L15 and TNT**

Time	2-HADNT	TNT	4-HADNT	2-ADNT	4-ADNT	3-H$^-$-TNT	NO2$^-$	NO3$^-$	**Balance**
0	0	450	0	0	0	0	0	0	**450**
6	11	350	36	0	5	5	47	5	**458**
18	20	210	36	0	8	16	75	8	**373**
30	48	71	115	0	11	59	117	8	**429**
42	70	11	172	0	13	22	46	7	**341**
54	68	11	180	0	15	0	47	6	**327**
66	74	0	199	3	19	0	51	7	**353**
78	69	0	198	5	21	0	46	14	**354**
90	63	0	181	6	22	0	46	18	**337**
102	60	0	166	7	24	0	34	22	**312**

***Y. lipolytica* AN-L15, ferrihydrite, and TNT**

Time	2-HADNT	TNT	4-HADNT	2-ADNT	4-ADNT	3-H$^-$-TNT	NO2$^-$	NO3$^-$	**Balance**
0	0	450	0	0	0	0	0	0	**450**
6	0	366	0	0	4	0	12	5	**388**
18	0	296	0	0	10	0	60	8	**373**
30	25	227	30	0	12	12	109	6	**420**
42	66	70	127	0	14	0	31	2	**310**
54	51	33	74	0	15	0	95	4	**272**
66	42	20	49	5	20	0	104	4	**244**
78	34	12	100	5	20	0	75	6	**252**
90	22	8	80	5	19	0	49	5	**188**
102	18	15	71	5	19	0	22	5	**155**

Another area of study would be to add AQDS to the system with ferrihydrite and observe the effects. The capacity of AQDS to act as an electron shuttle in the presence of ferrihydrite may alter the transformation rates and pathways of TNT and TNT-metabolites. The results of such a study may alter bioremediation strategies.

A third area of work would be to repeat the transformation of TNT under continuous flow conditions (see Appendix A). This work was incomplete and could lead to valuable information about the transformation of TNT by *Y. lipolytica* AN-L15 under simulated ground water conditions. This would be in preparation for the next step, which would be to monitor the transformation of TNT by *Y. lipolytica* AN-L15 in a meso-scale field study.

In addition to the aforementioned future work, a thorough examination of the genome of *Y. lipolytica* should be undertaken. This should include a close study of the enzymes and pathways present for nitrogen metabolism and carbon metabolism.

SUMMARY

The large scale manufacture and use of explosives compounds, especially TNT, has resulted in the contamination of soils and ground water. TNT and some TNT-metabolites show negative effects on the environment and health, thus, are of importance for remediation. Bioremediation has become an environmentally friendly, cost-effective alternative to past remediation approaches such as incineration. *Y. lipolytica* AN-L15 has the potential to be a bioremediator of TNT largely due to its capacity to transform TNT along the aromatic ring reduction pathway and the nitro-group reduction pathway. However, the pathways of TNT and TNT-metabolite transformation by *Y. lipolytica* AN-L15 in heterogeneous systems are not well understood.

This thesis aimed to study some of the conditions *Y. lipolytica* AN-L15 could experience in the natural environment while transforming TNT. The two major goals were to observe the transformation of TNT by *Y. lipolytica* AN-L15 in culture medium with different initial pH values, and to observe the transformation of TNT by *Y. lipolytica* AN-L15 in the presence and absence of ferrihydrite. It was observed that *Y. lipolytica* AN-L15 was able to transform TNT at three different initial proton concentrations of the culture medium: pH 7.0, pH 6.5, and pH 4.5. *Y. lipolytica* AN-L15 showed preferential growth and demonstrated increased formation of TNT-metabolites in culture medium of an initial pH of 4.5 as compared to culture medium of an initial pH of 6.5 or culture medium of an initial pH of 7.0. Aromatic ring reduction was the major transformation

pathway observed with the major metabolite being 3-H^--TNT. 4-HADNT was the major metabolite of the nitro-group reduction pathway.

In the presence of ferrihydrite at a pH of 7.0, transformation of TNT by *Y. lipolytica* AN-L15 showed a change in the transformation pathway. Nitro-group reduction was the major pathway with 4-HADNT and 4-ADNT being the major metabolites formed. Using ion chromatography, it was observed that *Y. lipolytica* AN-L15 in the presence of ferrihydrite formed greater concentrations of nitrite from the transformation of TNT-metabolites between thirty and ninety hours than in cultures without ferrihydrite. The lower concentrations of TNT-metabolites and difference in concentrations of nitrite could be explained by one or a combination of the following: (i) nitrite could be formed from the rearomatization of dihydride-Meisenheimer complexes through the condensation with HADNTs, resulting in the formation of nitrite and secondary diarylamines, (ii) there could be competition for electrons between TNT and TNT-metabolites and Fe(III), (iii) some of the TNT-metabolites could be oxidized back to previous TNT-metabolites using Fe(III) as an electron acceptor.

APPENDICES

APPENDIX A

REDUCTION OF TNT BY *Y. LIPOLYTICA* AN-L15 UNDER CONSTANT FLOW CONDITIONS WITH AN INITIAL pH OF 4.5

Introduction

The reduction of TNT by *Y. lipolytica* AN-L15 was observed under constant flow conditions using stainless steel columns. This experiment was only conducted once and had several flaws that will be discussed in this appendix. It is an area of future work, but worthy of discussion now to avoid similar mistakes and have a more efficient system.

It is of importance that the reduction of TNT by *Y. lipolytica* AN-L15 under simulated ground water flow conditions be studied and understood if *Y. lipolytica* AN-L15 is to have commercial viability as a bioremediator. As discussed in the thesis introduction, TNT contamination often occurs in the soil and in the groundwater. Though TNT has a low solubility in water, it can still be transported by the ground water and act as reservoirs for contamination in places of deposition. In addition, some of the metabolites of TNT can be more water-soluble and become health concerns for those using the water.

Materials and Methods

To conduct this study, stainless steel columns were used as flow reactors. The columns were filled with sintered glass beads (1-2 mm diameter, 55-60% pore volume, 60-300 μm pore diameter) and connected to peek tubing with an inner diameter 0.04 inches (Western Analytical Products, Wildomar, CA) on the influent end. An Omnifit 3-way valve connector (Supelco, Bellefonte, PA) was inserted into the influent line to be used as a sampling port. The effluent end was connected to peek tubing (inner diameter 0.04 in.). The peek tubing was connected to an Omnifit 3-way valve connector which

was then connected to silicone tubing that drained into a waste container (Figure 28). A syringe pump (KD Scientific model 780230, Holliston, MA) was used to pump medium through the system at constant flow. Using a dye tracer test, the volume of the bead filled columns was determined to be approximately 40 mL. The initial flow rate was 5 mL/day, but was later increased to 10 mL/day for reasons explained in the discussion section.

Sterile 60 mL syringes were used as medium vessels to hold the medium as it was pumped into the columns. All syringes were filled in a laminar flow hood. A 0.2 μm filter was installed between the syringe and the influent sampling port to prevent contamination in the medium source syringe (Figure 28). The initial pH of the medium in the columns was 4.5. Initially two columns were set up: column 1 was inoculated with *Y. lipolytica* AN-L15 and column two was inoculated with *Y. lipolytica* AN-L15 in the presence of TNT. 105 hours into the study, two additional columns were added: column 3 was inoculated with *Y. lipolytica* AN-L15 in the presence of TNT, and column 4 contained TNT only. Columns 1 and 4 were controls. Columns 1, 2, and 3 were filled with culture medium, inoculated with *Y. lipolytica* AN-L15, having an initial OD of 0.2 and were allowed to incubate at room temperature for twenty-four hours before starting the flow of medium into the columns. This was done to allow for a biofilm to begin to form if, in fact, *Y. lipolytica* AN-L15 could form a biofilm.

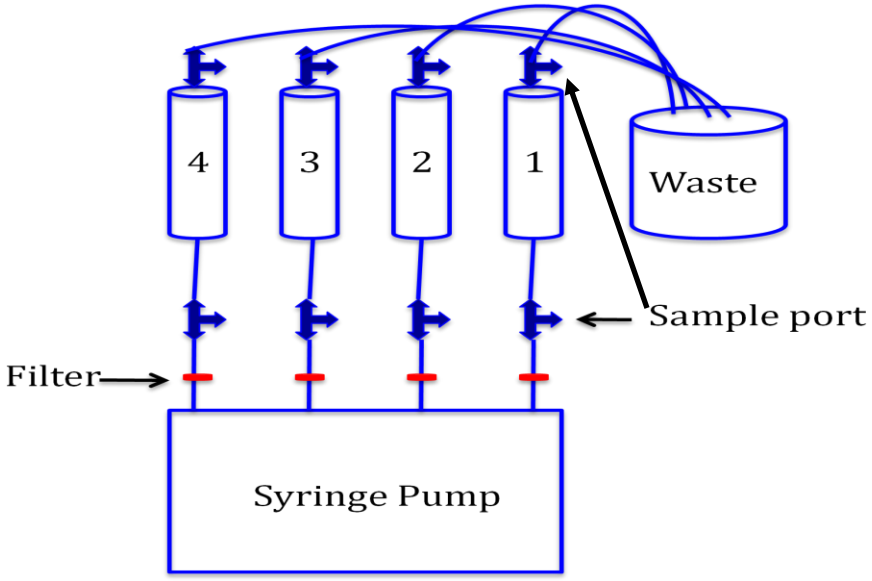

Figure 28. Schematic of column set up. The columns were positioned vertically on a steel framed structure. 0.2 µm filters were used between the syringe pump and the influent sampling port.

Sampling was conducted under as sterile of conditions as possible. The sampling ports being constructed of T-valves allowed for flow into the column to be redirected at sampling times thus reducing the opportunity for contamination. The sampling ports were covered with aluminum foil when not being used for sampling, and they were sterilized with a flame before and after each sampling. The sample port opening was of a Luer-Loc design, in order to allow a sterile syringe to be attached to the port to withdraw the sample. During sampling, 1 mL was taken from the effluent side and then 1 mL from the influent side of each column. Initially, samples were taken twice per day, but this was switched to once per day on day four to allow for column recharge between sampling events. During the first 180 hours, samples from the influent side were taken by opening flow between the bottom of the column and the sampling port. This was changed after 180 hours; samples from the influent side were then taken by opening flow between the

syringe pump and the sampling port. The sampling technique was changed in order to monitor what was flowing into the column and check for possible contamination. As will be addressed in the discussion section, this sampling technique should be modified. Samples were processed for pH, absorbance, and metabolite formation using the same procedures, standards, and equipment used in the different initial pH of the culture medium study described earlier.

On day thirty-eight, the columns were disassembled. The same procedure was used for each column. The beads were removed and separated into top, middle, and bottom column beads. 2 g of beads were placed into each of three sterile vials to be used for the protein assay, metabolite analysis, and serial dilution and plating, respectively. An additional 2 g of beads were placed in a sterile serum tube to be used for microscopy. A 2 cm section of the silicone tubing was removed and stored in a serum bottle to be used for microscopy.

The beads that were set aside for protein assay were processed in accordance with the procedure outlined for the Pierce-Coomassie assay in the materials and methods of the main part of this thesis. The procedure outlined in the materials and methods is meant to be applied to 0.5 g samples. Therefore, all amounts of solutions used for this technique were quadrupled since the sample from the column was 2 g.

The desorption of *Y. lipolytica* AN-L15 from the beads for serial dilution was accomplished using a procedure similar to that described by Camper et al. (1985). The beads were placed into a desorption solution (0.01 M Tris, pH 7, 0.01% peptone, 10^{-6} M Zwittergent 3-12, 10^{-3} M EGTA), vortexed for thirty seconds, shaken (150 rpm,

horizontal) at room temperature for three hours, vortexed for thirty seconds, allowed to settle and the supernatant drawn off. The dilutions plated were 10^{-5}, 10^{-6}, and 10^{-7}.

Extractions were performed according to EPA Method 8330, modified to one hour ultrasound aided extraction in acetonitrile. 2 g of beads were placed in a wide mouth bottle, 4 mL of acetonitrile should have been added, the sample was vortexed for one minute, and placed in a cooled ultrasonic bath for one hour. This procedure was followed, but a critical mistake was made. Acetone was used instead of acetonitrile. This rendered the samples unusable for HPLC analysis, therefore no data was collected.

The beads were viewed, with and without staining, using the Nikon Eclipse E800 microscope with MetaVue (ver. 7.0r4) software. Calcofluor White MR2 (Molecular Probes, Eugene, OR) was used as the cell stain. Approximately ten beads were placed on a slide. 0.1 mL of DI water was added to the slide followed by adding 25 μM of Calcofluor White M2R. The slide was allowed to incubate at room temperature in the dark for fifteen minutes. It was then viewed at 600x magnification using the above mentioned microscope and a DAPI filter.

The 2 cm piece of silicone tubing was split open lengthwise and viewed under the microscope. The inside of the tubing was scraped with a metal spatula. The scraping was added to a slide and suspended in DI water. The samples were viewed, with and without, staining. Following the procedure above, Calcofluor White M2R was used for staining and a DAPI filter was used when viewing stained cells.

Results

Absorbance measurements above zero for the first 180 hours are due to the sampling technique of taking influent samples from the bottom of the column. The higher absorbance seen in column 1 as compared to column 2 for the first 180 hours may be due to the absence of TNT in column 1. Growth (OD_{600}) of *Y. lipolytica* AN-L15 in column 2 may have been inhibited due to the presence of TNT in the medium. Since the remainder of the influent samples were taken from flow directed from the syringe pump, but after the in-line filter, the growth (OD_{600}) seen in the influent samples may be explained by *Y. lipolytica* AN-L15 being present in the sampling line or by possible contamination. The data for column 2 and 3 overlay each other on the graph from 105 hours until the end of the study, therefore, only one data symbol is visible. Column 4, the uninoculated control, had detectable absorbance measurements between 105 and 180 hours in the influent samples; this may have been due to contamination.

The absorbance data for the effluent of all four treatments indicates growth (OD_{600}) in all four columns. The highest absorbance occurred in column 1. It showed a maximum OD of 0.18, measured at 600 nm, at 323 hours, then started to decrease. Columns 2 and 3 showed two patterns of a period of increase, followed by a period of decrease. In column 4, the control column with TNT only, the final absorbance measurement was an OD of approximately 0.1 (Figure 29).

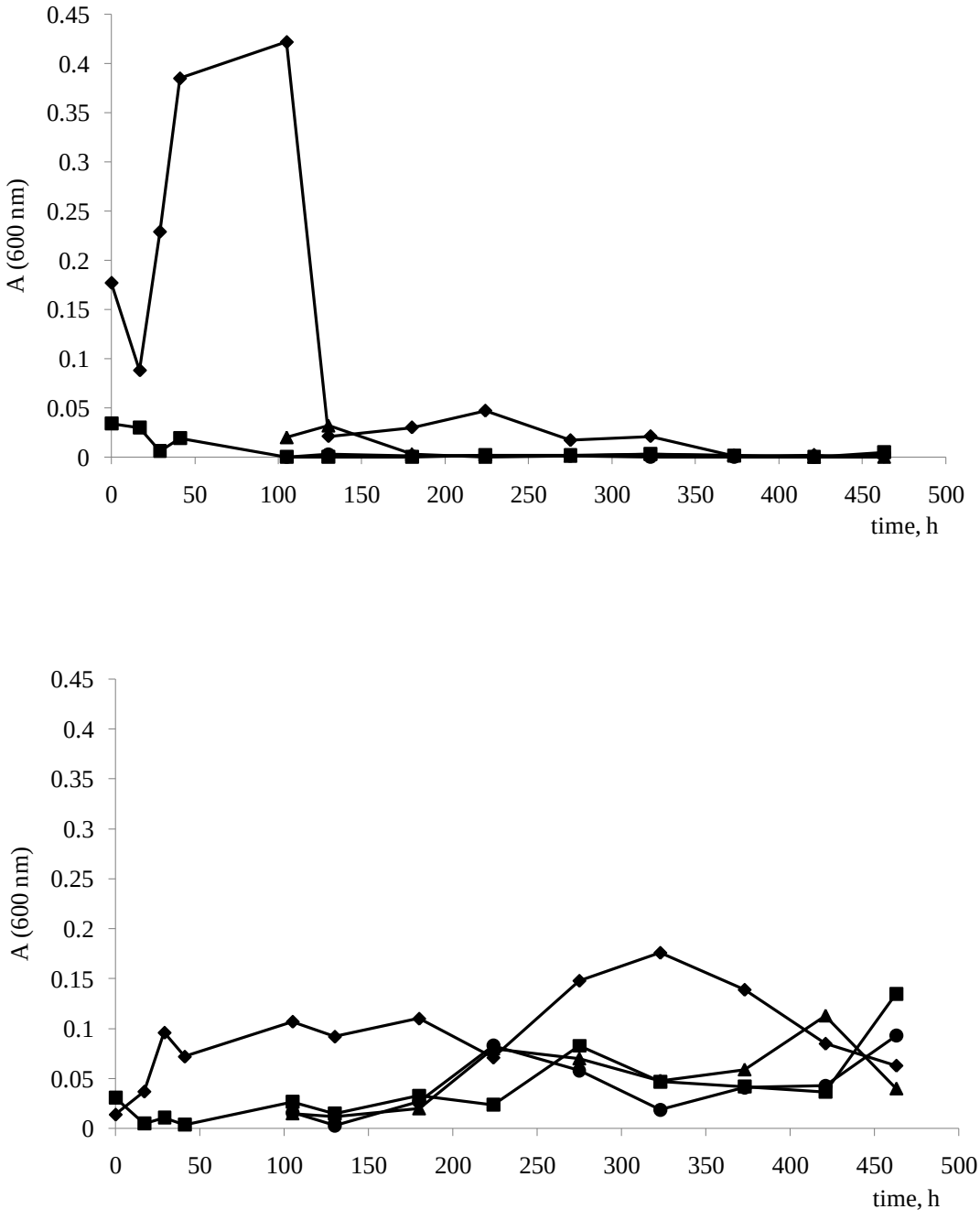

Figure 29. The top graph shows the absorbance measurements of the influent sampling for the four columns over time. The bottom graph shows the absorbance measurements of the effluent sampling for the four columns over time. Column 1 (*Y. lipolytica* AN-L15) - diamonds, Column 2 (*Y. lipolytica* AN-L15 and TNT) - squares, Column 3 (*Y. lipolytica* AN-L15 and TNT) - triangles, Column 4 (TNT) - circles.

There was a decrease in pH in the influent during the first 180 hours that can be attributed to sampling from the bottom of the column. As was seen in the previous studies in this thesis, there was a trend of decreasing pH in medium inoculated with *Y. lipolytica* AN-L15 in the presence and absence of TNT. After the technique was changed to sampling the influent from the flow direction of the syringe pump, the pH values in all four columns remained steady around a pH of 4.5. pH values of the effluent for columns 1 and 4 fluctuated between 4.5 and 4.0 for the entire study. pH values for the effluent from columns 2 and 3 followed similar trends to each other. The pH in both of these columns decreased steadily from 4.5 to approximatley 3.23 over a period of 100 hours and then remained steady around 3.23 for the remainder of the study (Figure 30).

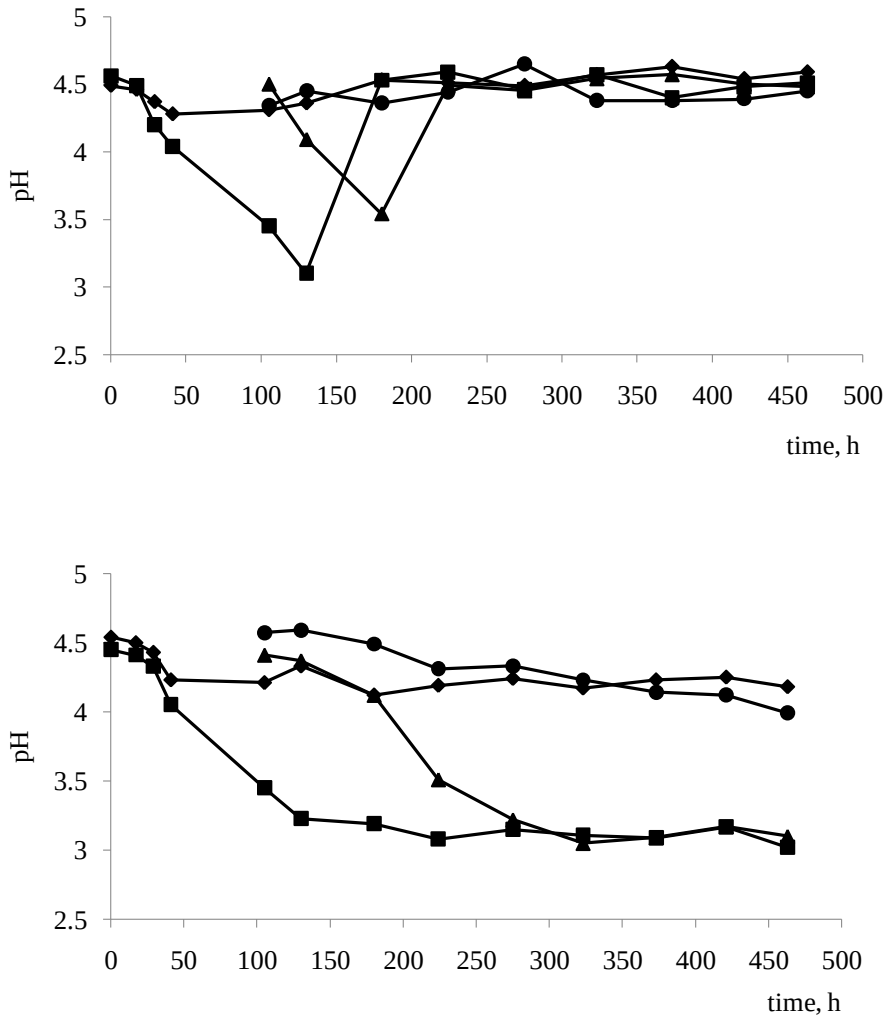

Figure 30. The top graph shows the pH values of the influent sampling for the four columns over time. The bottom graph shows the pH values of the effluent sampling for the four columns over time. Column 1 (*Y. lipolytica* AN-L15) - diamonds, Column 2 (*Y. lipolytica* AN-L15 and TNT) - squares, Column 3 (*Y. lipolytica* AN-L15 and TNT) - triangles, Column 4 (TNT) - circles.

Figure 31 shows the concentrations of TNT, 3-H-TNT, 2-HADNT, and 4-HADNT over time for column 2, column 3, and column 4, influent samples. Column 1 was inoculated with *Y. lipolytica* AN-L15 in the absence of TNT , therefore no TNT or TNT-metabolites were detected in column 1 (data not shown). Because the samples were

taken from either the bottom of the column (from the beginning of the study until 180 hours) or from the flow from the syringe pump, between the filter and the bottom of the column (after 180 hours until the end of the study), the media flowing into the column was always exposed to *Y. lipolytica* AN-L15. This may explain the fluctuation in TNT concentrations and the observation of 3-H$^-$-TNT and 4- HADNT in the influent of columns 2 and 3. There was no 2-HADNT observed in either column in the influent samples. There were no metabolites observed in the influent samples of column 4, but there was still a fluctuation in the concentrations of TNT. This is difficult to explain since the flow of medium from the syringe pump had a TNT concentration of 450 μM. It was possible that some of the TNT was adsorbing to the syringe, the peek tubing, or the filter.

Figure 32 shows the concentrations of TNT, 3-H$^-$-TNT, 2-HADNT, and 4-HADNT over time for column 2, column 3, and column 4, effluent samples. TNT concentrations were lower in the effluent than in the influent for columns 2 and 4. No TNT or TNT-metabolite concentrations were observed from the effluent of column 3, at this time, there is no known explanation for this. The concentrations of 3-H$^-$-TNT were lower than the concentrations of 4-HADNT in the effluent of column 2, which was the opposite of what was observed in the influent of column 2. Depending on whether the flow rate of the medium was 5 mL/day or 10 mL/day, there was a difference of ninety-six to 192 hours between when medium entered the column, and when it exited the column. As was seen in the previous studies in this thesis, initially the transformation of TNT by *Y. lipolytica* AN-L15 resulted in higher concentrations of 3-H$^-$-TNT than 4-HADNT, but

over time, there was a change, and the concentrations of 4-HADNT surpassed those of 3-H^--TNT. This may explain why the concentrations of 3-H^--TNT were higher than the concentrations of 4-HADNT in the influent of column 2 and lower in the effluent of column 2. The presence of 3-H^--TNT and 4-HADNT, along with the absorbance reading mentioned earlier, indicated that column 4 was contaminated.

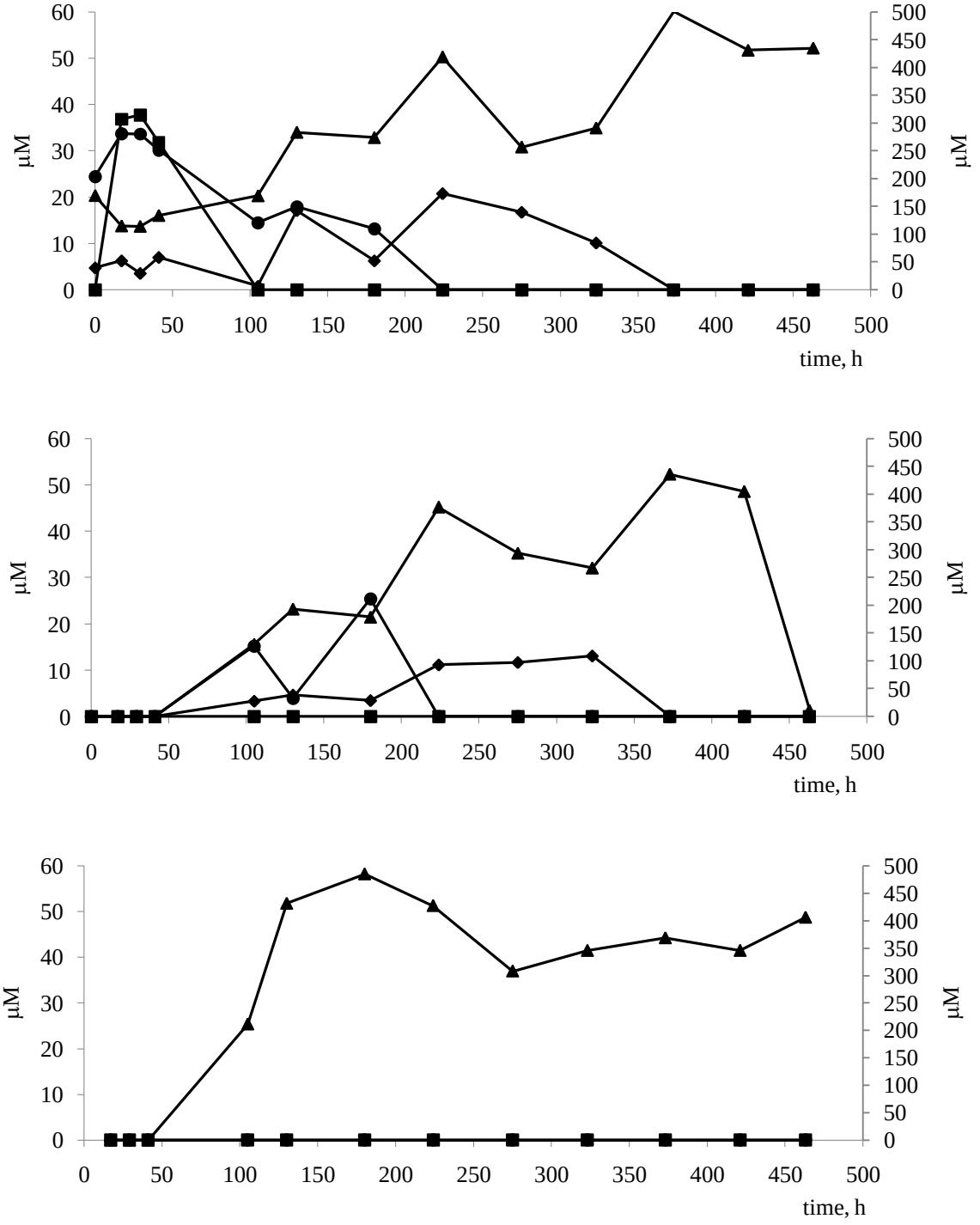

Figure 31. The transformation of TNT (triangles) and formation of 3-H-TNT (diamonds), 2-HADNT (squares), and 4-HADNT (circles). The graphs represent influent samples. The top graph represents column 2, *Y. lipolytica* AN-L15 and TNT. The middle graph represents column 3, *Y. lipolytica* AN-L15 and TNT. The bottom graph represents column 4, TNT only. The left axis represents TNT-metabolite concentrations. The right axis represents TNT concentrations.

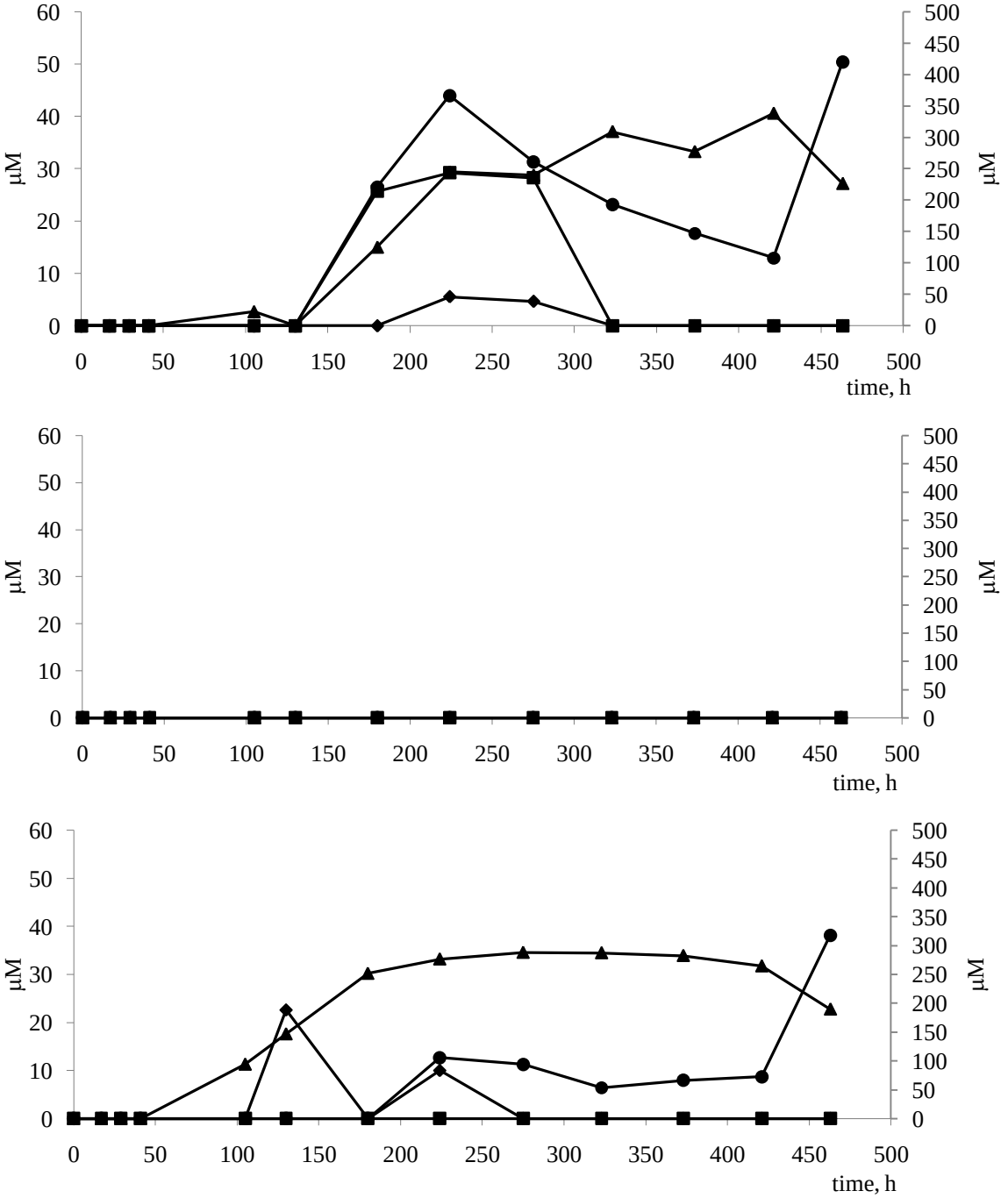

Figure 32. The transformation of TNT (triangles) and formation of 3-H$^-$-TNT (diamonds), 2-HADNT (squares), and 4-HADNT (circles). The graphs represent effluent samples. The top graph represents column 2, *Y. lipolytica* AN-L15 and TNT. The middle graph represents column 3, *Y. lipolytica* AN-L15 and TNT. The bottom graph represents column 4, TNT only. The left axis represents TNT-metabolite concentrations. The right axis represents TNT concentrations.

Figure 33 shows two microscopy images taken from samples from column 2. The photo on the left shows cells taken from the scraping of the silicon tubing. The photo on the right shows a layer of what might be extra-polysaccharide on one of the glass beads; further study is required to determine if this was, in fact, biofilm.

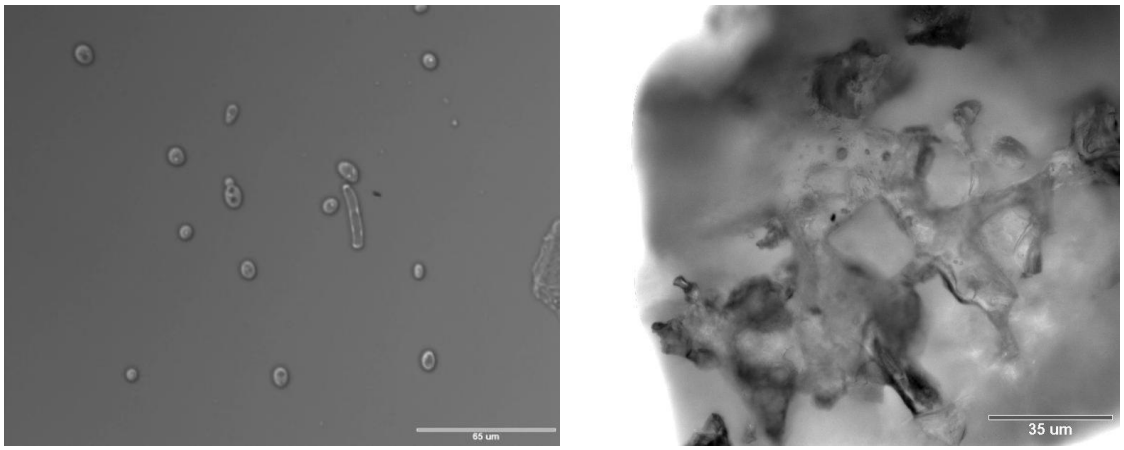

Figure 33. The image on the left is of cells of *Y. lipolytica* AN-L15 taken from silicone tubing, at 600x magnification using a Nikon Eclipse E800 microscope with MetaVue (ver. 7.0r4) software. The image on the right is of some material, possibly biofilm, on a glass bead from column 2. The bead was removed from the column at the end of the experiment and imaged at 600x magnification using a Nikon Eclipse E800 microscope with MetaVue (ver. 7.0r4) software.

There was no growth on the serial dilution plates after forty-two hours of incubation at 30^{o} C. This may have been due to overexposure of *Y. lipolytica* AN-L15 to the desorption solution (three hours instead of the recommended thirty minutes).

The protein assay showed growth based on protein concentrations in all four columns. Column one had less growth in the middle of the column; this is potentially due to an oxygen gradient in the column, preferentially directed flow paths in the middle of the column versus either end, or it may be due to the buildup of toxic by-products or intermediates. Columns 2 and 3 showed lower concentrations of protein than column one, which may be explained due to the inhibition TNT has on the growth of *Y. lipolytica*

AN-L15. Column 4 was the uninoculated control. It showed higher concentrations of protein at the top of the column than in the middle or bottom, possibly indicating that the contamination came from the effluent end of the column (Figure 34).

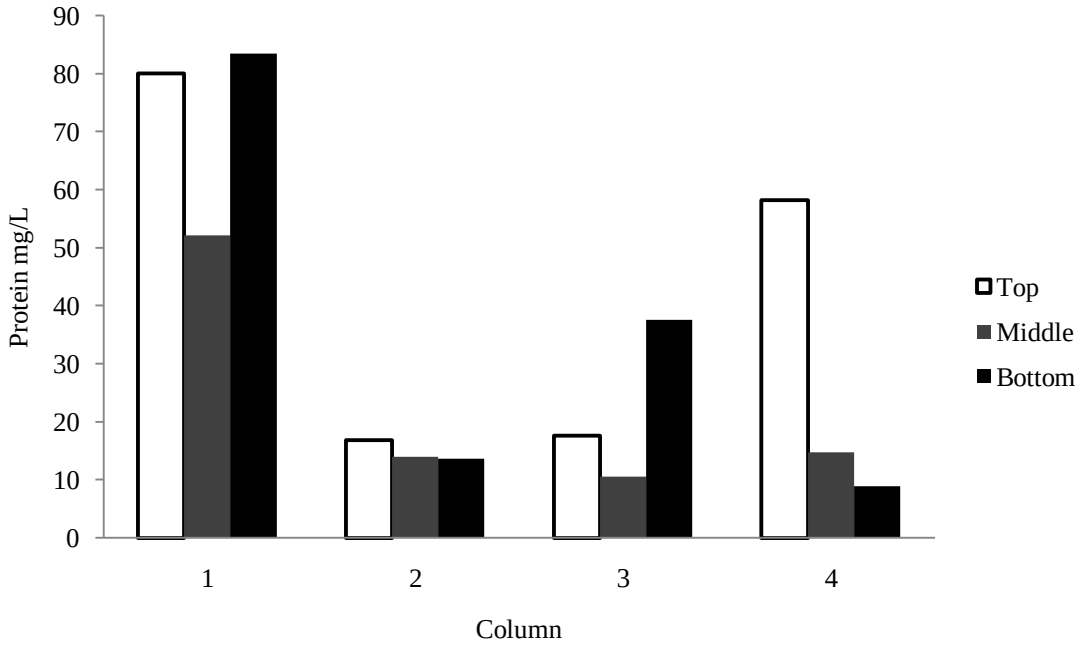

Figure 34. Protein concentrations taken from the four columns at the end of the study. The protein concentration was determined using a Pierce-Coomassie assay. The x-axis represents the column, samples were extracted from and the y-axis represents protein concentrations.

Discussion

Taking into consideration that there were no replicate studies for this experiment, and the columns were not set up in duplicate or triplicate (with the exception of columns 2 and 3, but they were not started at the same time nor run for the same duration), coupled with the contamination of the control column (discussed below); the data presented in this appendix is not reliable and should not be used for the drawing of conclusions about the effects of continuous flow conditions on the transformation of TNT

by *Y.* lipolytica AN-L15. Despite the aforementioned drawbacks to this experiment, there were some trends that may be inferred based on the previously discussed studies in this thesis and the data seen here. It is possible that the growth (OD_{600}) of *Y. lipolytica* AN-L15 was inhibited in columns 2 and 3 by the presence of TNT. It is also possible that the exposure time of TNT and its metabolites to *Y. lipolytica* AN-L15 had an effect on the dominance of the metabolite observed. This was seen in the study of differing initial pH; initially 3-H^--TNT was present in higher concentrations, but this eventually shifted to 4-HADNT being the most abundant metabolite. Column 2 showed similar results between the influent and effluent samples, which were separated by time of exposure based on the rate of flow of the medium.

The initial set up for the effluent silicon tubing may have been the source of contamination in column 4 and potentially led to contamination of the other columns, though this was harder to detect. The tubes were placed into an open beaker to collect waste, this was not a sterile technique, and bacteria or yeast possibly entered the effluent tube and traveled upstream into the column. This was confirmed by the protein assay showing much higher levels of protein at the top of column 4, 58 mg/L than in the middle or at the bottom, 15 mg/L and 10 mg/L, respectively. Additionally, column 4 showed detectable absorbance values throughout the study, indicating growth. On day seven, the set up was changed to a more sterile technique. The four effluent tubes were attached to glass tubes passing through a rubber stopper. The stopper was placed in the mouth of a 1000 mL Erlenmeyer flask and a 26-gauge needle was placed between the stopper and the flask to allow for off gassing from the waste beaker.

Despite the errors in techniques used throughout this study, it provided valuable information. The column set-up was not ideal, due to the volume of the column filled with glass beads and the flow rate of 5 mL/day later changed to 10 mL/day. The flow rate was changed from 5 mL/day to 10 mL/day during the study to decrease the time of exposure of TNT and TNT- metabolites to *Y. lipolytica* AN-L15 between the influent and effluent samples. However, this was still not ideal. A better set up would have been to use smaller volume glass columns set up in a series. This would have allowed for more sampling points along the flow path. Using glass columns would also have allowed for observation of possible biofilm inside the column while the experiment was running. Since the start of this thesis, a study was published by Dusane et al. (2008) showing the formation of a biofilm by *Y. lipolytica* NCIM 3589, a tropical marine strain.

Another recommended change to the column set up would be to place the influent sampling valve between the syringe pump and the in-line filter or add a second in-line filter between the sampling port and the column. This would allow for better monitoring of contamination from the medium source, while preventing *Y. lipolytica* AN-L15 from entering the sampling port. The set-up used in this thesis allowed *Y. lipolytica* AN-L15 to migrate to the sampling port, causing TNT transformation in the tubing before medium could enter the column.

APPENDIX B

DATA TABLE FOR THE STUDY OF TNT TRANSFORMATION BY *Y. LIPOLYTICA* AN-L15 WITH DIFFERENT INITIAL pH OF THE CULTURE MEDIUM

Fold change of YFT/YT

Time	pH 7.0	pH 6.5	pH 4.5
0	0.75	1.5	1.75
6	2	6.5	2.625
12	4.916667	19	10
24	10.875	26.5	8.6
36	15.86667	33.16667	5.892105
48	35.03175	31.3	4.725
72	23.80019	24.25556	3.067308
96	17.91279	13.49698	3.058059
120	23.11134	6.504	1.590345
194	16.1102	5.153792	1.012508
216	13.15788	5.165883	1.051645
240	10.94878	4.30437	0.843068

Absorbance for Treatment A OD_{600}

Time	Y pH 7.0 original	T pH 7.0 original	YT pH 7.0 original
0	0.202	0.001	0.201
6	0.324	0.001	0.225
12	0.414	0	0.29
24	0.623	0	0.31
36	0.76	0	0.339
48	0.843	0.003	0.458
72	1.428	0.001	0.668
96	1.475	0.004	1.23
120	1.64	0.001	1.49
194	1.764	0.002	1.807
216	1.802	0	1.817
240	1.812	0.004	1.811

Time	Y - pH 7.0	T - pH 7.0	YT - pH 7.0
0	0.003	0.001	0.003
6	0.003	0.001	0.001
12	0.008	0	0
24	0.027	0	0.004
36	0.086	0	0.006
48	0.261	0.002	0.007
72	0.523	0.003	0.019
96	0.788	0.003	0.043
120	0.928	0.008	0.034
194	1.445	0.005	0.08
216	1.471	0.005	0.117
240	1.458	0.004	0.132

Time	Y - pH 6.5	T - pH 6.5	YT - pH 6.5
0	0.002	0	0.002
6	0.01	0	0
12	0.031	0	0.001
24	0.075	0	0
36	0.146	0	0.003
48	0.243	0.004	0.006
72	0.47	0	0.018
96	0.678	0	0.05
120	0.763	0.185	0.109
194	1.187	1.596	0.237
216	1.284	1.234	0.26
240	1.374	1.363	0.312

Absorbance for Treatment B OD_{600}

Time	Y pH 7.0 original	T pH 7.0 original	YT pH 7.0 original
0	0.215	0.001	0.212
6	0.339	0.001	0.235
12	0.407	0	0.311
24	0.631	0	0.315
36	0.859	0	0.345
48	0.875	0.003	0.442
72	1.442	0.001	0.712
96	1.487	0.003	1.247
120	1.633	0.001	1.495
194	1.752	0.002	1.815
216	1.815	0	1.826
240	1.815	0	1.817

Time	Y - pH 7.0	T - pH 7.0	YT - pH 7.0
0	0.001	0.001	0.002
6	0.003	0.001	0.003
12	0.011	0	0.006
24	0.045	0	0.003
36	0.087	0	0.005
48	0.295	0.002	0.009
72	0.542	0	0.027
96	0.77	0.001	0.044
120	1.06	0.005	0.056
194	1.345	0.005	0.095
216	1.498	0.004	0.109
240	1.541	0.004	0.142

Time	Y - pH 6.5	T - pH 6.5	YT - pH 6.5
0	0.004	0.003	0.002
6	0.009	0	0.003
12	0.042	0.004	0.006
24	0.076	0.004	0.002
36	0.159	0.002	0.009
48	0.221	0	0.01
72	0.56	0.001	0.025
96	0.712	0	0.053
120	0.751	0.003	0.125
194	1.24	0	0.234
216	1.289	0.002	0.239
240	1.375	0.006	0.327

Absorbance for Treatment A OD_{600}

Time	Y - pH 4.5	T - pH 4.5	YT - pH 4.5
0	0.003	0	0.002
6	0.006	0	0.002
12	0.02	0	0.002
24	0.048	0	0.008
36	0.089	0	0.019
48	0.168	0	0.032
72	0.208	0.001	0.064
96	0.262	0.002	0.092
120	0.245	0	0.134
194	0.256	0.003	0.23
216	0.305		0.301
240	0.25	0.001	0.304

Absorbance for Treatment B OD_{600}

Time	Y - pH 4.5	T - pH 4.5	YT - pH 4.5
0	0.004	0	0.002
6	0.009	0	0.004
12	0.03	0	0.003
24	0.056	0.001	0.005
36	0.071	0	0.01
48	0.189	0.003	0.045
72	0.225	0	0.078
96	0.268	0	0.082
120	0.261	0.002	0.193
194	0.259	0.002	0.284
216	0.327	0.001	0.3
240	0.298	0	0.345

Average Absorbance OD_{600}

Time	Y pH 7.0 original	T pH 7.0 original	YT pH 7.0 original
0	0.2085	0.001	0.2065
6	0.3315	0.001	0.23
12	0.4105	0	0.3005
24	0.627	0	0.3125
36	0.8095	0	0.342
48	0.859	0.003	0.45
72	1.435	0.001	0.69
96	1.481	0.0035	1.2385
120	1.6365	0.001	1.4925
194	1.758	0.002	1.811
216	1.8085	0	1.8215
240	1.8135	0.002	1.814

Standard Deviation for Absorbance OD_{600}

Time	Y pH 7.0 original	T pH 7.0 original	YT pH 7.0 original
0	0.009192388	0	0.007778175
6	0.010606602	0	0.007071068
12	0.004949747	0	0.014849242
24	0.005656854	0	0.003535534
36	0.070003571	0	0.004242641
48	0.022627417	0	0.011313708
72	0.009899495	0	0.031112698
96	0.008485281	0.000707107	0.012020815
120	0.004949747	0	0.003535534
194	0.008485281	0	0.005656854
216	0.009192388	0	0.006363961
240	0.00212132	0.002828427	0.004242641

Time	Y - pH 7.0	T - pH 7.0	YT - pH 7.0
0	0.002	0.001	0.0025
6	0.003	0.001	0.002
12	0.0095	0	0.003
24	0.036	0	0.0035
36	0.0865	0	0.0055
48	0.278	0.002	0.008
72	0.5325	0.0015	0.023
96	0.779	0.002	0.0435
120	0.994	0.0065	0.045
194	1.395	0.005	0.0875
216	1.4845	0.0045	0.113
240	1.4995	0.004	0.137

Time	Y - pH 7.0	T - pH 7.0	YT - pH 7.0
0	0.001414214	0	0.000707107
6	0	0	0.001414214
12	0.00212132	0	0.004242641
24	0.012727922	0	0.000707107
36	0.000707107	0	0.000707107
48	0.024041631	0	0.001414214
72	0.013435029	0.00212132	0.005656854
96	0.012727922	0.001414214	0.000707107
120	0.093338095	0.00212132	0.015556349
194	0.070710678	0	0.010606602
216	0.019091883	0.000707107	0.005656854
240	0.058689863	0	0.007071068

Average Absorbance OD_{600}

Time	Y - pH 6.5	T - pH 6.5	YT - pH 6.5
0	0.003	0.0015	0.002
6	0.0095	0	0.0015
12	0.0365	0.002	0.0035
24	0.0755	0.002	0.001
36	0.1525	0.001	0.006
48	0.232	0.002	0.008
72	0.515	0.0005	0.0215
96	0.695	0	0.0515
120	0.757	0.094	0.117
194	1.2135	0.798	0.2355
216	1.2865	0.618	0.2495
240	1.3745	0.6845	0.3195

Time	Y - pH 4.5	T - pH 4.5	YT - pH 4.5
0	0.0035	0	0.002
6	0.0075	0	0.003
12	0.025	0	0.0025
24	0.052	0.0005	0.0065
36	0.08	0	0.0145
48	0.1785	0.0015	0.0385
72	0.2165	0.0005	0.071
96	0.265	0.001	0.087
120	0.253	0.001	0.1635
194	0.2575	0.0025	0.257
216	0.316	0.001	0.3005
240	0.274	0.0005	0.3245

Standard Deviation for Absorbance OD_{600}

Time	Y - pH 6.5	T - pH 6.5	YT - pH 6.5
0	0.001414214	0.00212132	0
6	0.000707107	0	0.00212132
12	0.007778175	0.002828427	0.003535534
24	0.000707107	0.002828427	0.001414214
36	0.009192388	0.001414214	0.004242641
48	0.015556349	0.002828427	0.002828427
72	0.06363961	0.000707107	0.004949747
96	0.024041631	0	0.00212132
120	0.008485281	0.128693434*	0.011313708
194	0.037476659	1.128542423*	0.00212132
216	0.003535534	0.871155554*	0.014849242
240	0.000707107	0.959543902*	0.010606602

Time	Y - pH 4.5	T - pH 4.5	YT - pH 4.5
0	0.000707107	0	0
6	0.00212132	0	0.001414214
12	0.007071068	0	0.000707107
24	0.005656854	0.000707107	0.00212132
36	0.012727922	0	0.006363961
48	0.014849242	0.00212132	0.009192388
72	0.012020815	0.000707107	0.009899495
96	0.004242641	0.001414214	0.007071068
120	0.011313708	0.001414214	0.0417193
194	0.00212132	0.000707107	0.038183766
216	0.015556349	0	0.000707107
240	0.25	0.001	0.304

* These samples may have been contaminated between ninety-six and 120 hours resulting in the higher absorbance measurements.

pH values for Treatment A

Time	Y pH 7.0 original	T pH 7.0 original	YT pH 7.0 original	Y - pH 7.0	T - pH 7.0	YT - pH 7.0
0	6.64	7	6.76	6.97	7	7
6	6.64	6.98	6.68	6.94	7	6.99
12	6.63	7.02	6.67	6.94	7.02	7.01
24	6.58	7.03	6.56	6.89	7.02	7.02
36	6.51	7	6.39	6.78	6.99	6.95
48	6.44	7	6.24	6.68	7	6.94
72	6.39	7	5.85	6.54	6.99	6.81
96	6.27	6.97	5.55	6.23	6.73	6.5
120	6.14	6.87	5.16	5.75	6.01	6.04
194	4.92	6.77	4.28	5.27	5.69	4.35
216	5.21	*	3.79	5.57	*	4.14
240	4.48	6.71	3.62	5.7	5.71	4.02

Time	Y - pH 6.5	T - pH 6.5	YT - pH 6.5	Y - pH 4.5	T - pH 4.5	YT - pH 4.5
0	6.65	6.65	6.62	4.55	4.65	4.5
6	6.63	6.65	6.58	4.52	4.24	4.59
12	6.66	6.66	6.59	4.15	4.24	4.6
24	6.67	6.65	6.48	3.75	4.26	4.47
36	6.6	6.65	6.31	3.54	4.32	4.23
48	6.53	6.64	6.4	3.44	4.51	3.99
72	6.12	6.65	6.39	3.37	4.6	3.67
96	5.09	6.63	6.09	3.26	5.3	3.44
120	4.21	5.87	6.25	2.92	5.51	3.07
194	3.04	4.28	4.56	2.81	5.44	2.82
216	2.91	*	5.2	2.62	*	2.68
240	2.94	4.76	4.82	2.67	5.55	2.82

* pH data missing for these samples.

pH values for Treatment B

Time	Y pH 7.0 original	T pH 7.0 original	YT pH 7.0 original	Y - pH 7.0	T - pH 7.0	YT - pH 7.0
0	6.89	7	6.86	7	7.02	7.01
6	6.71	7	6.71	6.99	7.01	6.99
12	6.63	7.02	6.67	6.95	7.03	7.01
24	6.59	7.01	6.45	6.91	7.02	6.94
36	6.47	7.02	6.21	6.75	7.01	6.93
48	6.43	7.01	6.14	6.6	7	6.89
72	6.41	7	5.75	6.51	6.79	6.83
96	6.33	6.97	5.19	6.18	6.56	6.67
120	6.18	6.97	5.16	5.62	6.01	6.12
194	5.02	9.99	4.11	5.35	5.5	4.95
216	5.11	9.84	3.84	5.21	*	4.26
240	4.32	6.86	3.55	5.5	5.51	4.15

Time	Y - pH 6.5	T - pH 6.5	YT - pH 6.5	Y - pH 4.5	T - pH 4.5	YT - pH 4.5
0	6.68	6.66	6.51	4.51	4.56	4.52
6	6.63	6.64	6.66	4.1	4.34	4.58
12	6.4	6.65	6.69	4.01	4.36	4.51
24	6.53	6.63	6.54	3.69	4.39	4.39
36	6.7	6.64	6.2	3.64	4.38	4.12
48	6.5	6.69	6.01	3.33	4.41	3.67
72	6.3	6.67	6.25	3.17	4.52	3.26
96	5.4	6.62	6.1	3.05	4.8	3.1
120	4.15	5.96	6.33	2.98	4.86	2.91
194	3.19	4.2	4.2	2.91	5.2	2.68
216	3.01	4.12	4.05	2.5	*	2.51
240	*	4.5	4.5	2.47	5.39	2.75

* pH data missing for these samples.

Average pH values

AVG

Time	Y pH 7.0 original	T pH 7.0 original	YT pH 7.0 original	Y - pH 7.0	T - pH 7.0	YT - pH 7.0
0	6.765	7	6.81	6.985	7.01	7.005
6	6.675	6.99	6.695	6.965	7.005	6.99
12	6.63	7.02	6.67	6.945	7.025	7.01
24	6.585	7.02	6.505	6.9	7.02	6.98
36	6.49	7.01	6.3	6.765	7	6.94
48	6.435	7.005	6.19	6.64	7	6.915
72	6.4	7	5.8	6.525	6.89	6.82
96	6.3	6.97	5.37	6.205	6.645	6.585
120	6.16	6.92	5.16	5.685	6.01	6.08
194	4.97	8.38	4.195	5.31	5.595	4.65
216	5.16	9.84	3.815	5.39	*	4.2
240	4.4	6.785	3.585	5.6	5.61	4.085

Time	Y - pH 6.5	T - pH 6.5	YT - pH 6.5	Y - pH 4.5	T - pH 4.5	YT - pH 4.5
0	6.665	6.655	6.565	4.53	4.605	4.51
6	6.63	6.645	6.62	4.31	4.29	4.585
12	6.53	6.655	6.64	4.08	4.3	4.555
24	6.6	6.64	6.51	3.72	4.325	4.43
36	6.65	6.645	6.255	3.59	4.35	4.175
48	6.515	6.665	6.205	3.385	4.46	3.83
72	6.21	6.66	6.32	3.27	4.56	3.465
96	5.245	6.625	6.095	3.155	5.05	3.27
120	4.18	5.915	6.29	2.95	5.185	2.99
194	3.115	4.24	4.38	2.86	5.32	2.75
216	2.96	4.12	4.625	2.56	*	2.595
240	2.94	4.63	4.66	2.57	5.47	2.785

* pH data missing for these samples.

Standard Deviations for pH

STDEV

Time	Y pH 7.0 original	T pH 7.0 original	YT pH 7.0 original	Y - pH 7.0	T - pH 7.0	YT - pH 7.0
0	0.176777	0	0.070711	0.021213	0.014142	0.007071
6	0.049497	0.014142	0.021213	0.035355	0.007071	0
12	0	0	0	0.007071	0.007071	0
24	0.007071	0.014142	0.077782	0.014142	0	0.056569
36	0.028284	0.014142	0.127279	0.021213	0.014142	0.014142
48	0.007071	0.007071	0.070711	0.056569	0	0.035355
72	0.014142	0	0.070711	0.021213	0.141421	0.014142
96	0.042426	0	0.254558	0.035355	0.120208	0.120208
120	0.028284	0.070711	0	0.091924	0	0.056569
194	0.070711	2.276884	0.120208	0.056569	0.13435	0.424264
216	0.070711	0	0.035355	0.254558	0	0.084853
240	0.113137	0.106066	0.049497	0.141421	0.141421	0.091924

Time	Y - pH 6.5	T - pH 6.5	YT - pH 6.5	Y - pH 4.5	T - pH 4.5	YT - pH 4.5
0	0.021213	0.007071	0.077782	0.028284	0.06364	0.014142
6	0	0.007071	0.056569	0.296985	0.070711	0.007071
12	0.183848	0.007071	0.070711	0.098995	0.084853	0.06364
24	0.098995	0.014142	0.042426	0.042426	0.091924	0.056569
36	0.070711	0.007071	0.077782	0.070711	0.042426	0.077782
48	0.021213	0.035355	0.275772	0.077782	0.070711	0.226274
72	0.127279	0.014142	0.098995	0.141421	0.056569	0.289914
96	0.219203	0.007071	0.007071	0.148492	0.353553	0.240416
120	0.042426	0.06364	0.056569	0.042426	0.459619	0.113137
194	0.106066	0.056569	0.254558	0.070711	0.169706	0.098995
216	0.070711	0	0.813173	0.084853	0	0.120208
240	0	0.183848	0.226274	0.141421	0.113137	0.049497

HPLC Data - Average(μM)

μM 7.0 original	10.6 +/- .2	15.2+/-.2	15.6 +/- .2	16.3+/-.2
Time	3-H-TNT	2-HADNT	TNT	4-HADNT
0	ND	ND	450.33143	ND
6	35.77852506	ND	380.8643365	7.599064238
12	54.02622455	16.79492764	294.4352827	17.09288724
24	139.4645604	31.85954213	125.0912983	21.01860309
30	119.587602	43.68738202	68.46338651	26.92720601
42	107.9833685	58.05624123	28.78595086	32.33507988
54	65.9393655	59.32675088	17.24446813	38.44397443
66	22.48377258	50.61468467	10.5607438	42.12934032
90	6.862438414	45.19989352	ND	43.57144002
114	ND	31.67804075	ND	39.26517009
138	ND	19.1846958	ND	28.46945152
212	ND	ND	ND	22.50076111
234	ND	ND	ND	14.74947524
258	ND	ND	ND	11.66498422

AVG

μM pH 7.0				
Ret time range 6.5	10.9 +/- .2	15.2 +/- .1	15.7 +/- .2	16.3 +/- .1
Time	3-H--TNT	2-HADNT	TNT	4-HADNT
0	ND	ND	450	ND
6	4.0535961	ND	394.7343829	ND
12	7.064466515	ND	376.9115614	ND
24	7.475039754	ND	366.7791598	ND
36	18.66478976	ND	360.0485238	ND
48	44.92192591	ND	293.5926046	ND
72	60.56281119	ND	224.4031238	ND
96	45.00013034	ND	105.5357173	ND
120	17.36789969	ND	49.88040364	ND
194	7.42290347	7.79589137	22.18031301	ND
216	2.189723938	21.41350868	14.25905902	14.80160335
240	ND	ND	ND	ND

ND - below detection limit

HPLC Data - Average(μM)

μM pH 6.5

Ret time range 6.5	10.9 +/- .2	15.2 +/- .1	15.7 +/- .2	16.3 +/- .1
Time	3-H--TNT	2-HADNT	TNT	4-HADNT
0	ND	ND	450	ND
6	0.97755533	ND	388.0303914	ND
12	1.831286984	ND	384.5449785	ND
24	7.149187977	ND	381.1973743	ND
36	16.77159094	ND	341.7955561	ND
48	39.26513907	ND	291.9868806	ND
72	63.5541305	ND	202.488137	ND
96	68.65240739	ND	98.77556926	19.37621176
120	29.92948568	25.44649339	55.33710317	28.80994728
194	11.32921457	29.56959973	50.31856789	40.54703649
216	ND	48.69077005	ND	49.17960551
240	ND	60.8029621	ND	48.7469756

AVG

μM pH 4.5

Ret time range 6.5	10.9 +/- .2	15.2 +/- .1	15.7 +/- .2	16.3 +/- .1
Time	3-H--TNT	2-HADNT	TNT	4-HADNT
0	ND	ND	450	ND
6	2.300513542	ND	400	ND
12	3.427960689	ND	383.3724557	ND
24	9.208571205	ND	375.7998649	ND
36	24.16581945	ND	346.2398883	ND
48	44.36146086	ND	245.9472744	ND
72	65.02046349	ND	193.47889	26.29428448
96	90.31307839	18.76119259	104.7874759	38.20362448
120	71.56356716	31.19403707	58.59857689	50.56161772
194	42.82604729	44.84596583	24.12342152	56.89083305
216	5.122389927	61.53501767	ND	57.38154753
240	ND	62.74502686	ND	52.2240382

ND - below detection limit

HPLC Data - Standard Deviations

AVG				
µM 7.0 original	10.6 +/- .2	15.2+/-.2	15.6 +/- .2	16.3+/-.2
Time	3-H-TNT	2-HADNT	TNT	4-HADNT
0	ND	ND	450.33143	ND
6	35.77852506	ND	380.8643365	7.599064238
12	54.02622455	16.79492764	294.4352827	17.09288724
24	139.4645604	31.85954213	125.0912983	21.01860309
30	119.587602	43.68738202	68.46338651	26.92720601
42	107.9833685	58.05624123	28.78595086	32.33507988
54	65.9393655	59.32675088	17.24446813	38.44397443
66	22.48377258	50.61468467	10.5607438	42.12934032
90	6.862438414	45.19989352	ND	43.57144002
114	ND	31.67804075	ND	39.26517009
138	ND	19.1846958	ND	28.46945152
212	ND	ND	ND	22.50076111
234	ND	ND	ND	14.74947524
258	ND	ND	ND	11.66498422

AVG				
µM pH 7.0				
Ret time range				
6.5	10.9 +/- .2	15.2 +/- .1	15.7 +/- .2	16.3 +/- .1
Time	3-H--TNT	2-HADNT	TNT	4-HADNT
0	ND	ND	450	ND
6	4.0535961	ND	394.7343829	ND
12	7.064466515	ND	376.9115614	ND
24	7.475039754	ND	366.7791598	ND
36	18.66478976	ND	360.0485238	ND
48	44.92192591	ND	293.5926046	ND
72	60.56281119	ND	224.4031238	ND
96	45.00013034	ND	105.5357173	ND
120	17.36789969	ND	49.88040364	ND
194	7.42290347	7.79589137	22.18031301	ND
216	2.189723938	21.41350868	14.25905902	14.80160335
240	ND	ND	ND	ND

ND - below detection limit

HPLC Data - Standard Deviations

STDEV

µM pH 6.5

Ret time range 6.5	10.9 +/- .2	15.2 +/- .1	15.7 +/- .2	16.3 +/- .1
Time	3-H--TNT	2-HADNT	TNT	4-HADNT
0	ND	ND	ND	ND
6	1.382472005	ND	2.728474026	ND
12	2.58983089	ND	0.738961715	ND
24	1.170492964	ND	0.081204584	ND
36	7.193462667	ND	6.59381223	ND
48	16.35925206	ND	15.80566025	ND
72	29.49273611	ND	16.67130112	ND
96	13.91411991	ND	2.525462566	0.254929619
120	10.62199324	4.36358911	4.450011209	3.45571261
194	2.08661108	4.008512741	5.245816134	6.231612903
216	ND	5.407428074	ND	4.730360704
240	ND	1.403193361	ND	3.608670381

STDEV

µM pH 4.5

Ret time range 6.5	10.9 +/- .2	15.2 +/- .1	15.7 +/- .2	16.3 +/- .1
Time	3-H--TNT	2-HADNT	TNT	4-HADNT
0	ND	ND	ND	ND
6	0.617504162	ND	2.828427125	ND
12	0.12903072	ND	7.379872604	ND
24	1.520719206	ND	6.707498648	ND
36	3.060793019	ND	22.4936698	ND
48	2.57139793	ND	12.27488493	ND
72	4.082900655	ND	0.763323091	0.40788739
96	1.179709444	0.213901427	4.417529376	3.030829912
120	1.281090725	0.684484566	2.013873686	4.532082111
194	1.369568933	2.280189211	0.649636673	2.379343108
216	1.050678724	0.812825422	ND	0.977230205
240	ND	3.978566541	ND	3.767293255

ND - below detection limit

Sums of hydrides and dihydrides treatment A (peak area)

pH 7.0

Time	Isomer of 3-H-TNT	3,5-2H-TNT H+	3,5-2H-TNT
6	ND	ND	ND
12	ND	ND	ND
24	ND	ND	ND
36	ND	ND	ND
48	ND	ND	ND
72	24	13.7	13.3
96	56.5	48.1	32.1
120	84.8	80.6	48
194	103.7	106.2	56.7
216	89.4	143.2	47.7
240	69.5	139.2	40.2

pH 6.5

	Isomer of 3-H-TNT	3,5-2H-TNT H+	3,5-2H-TNT
6	ND	ND	ND
12	ND	ND	ND
24	ND	ND	ND
36	ND	ND	ND
48	ND	ND	ND
72	22.8	102.7	12.7
96	55.5	247.6	33
120	93.8	374.3	49.1
194	126.4	470.9	55
216	37	497.7	25.9
240	14.6	453.8	10.6

pH 4.5

Time	Isomer of 3-H-TNT	3,5-2H-TNT H+	3,5-2H-TNT
6	ND	ND	ND
12	ND	ND	ND
24	ND	ND	ND
36	ND	ND	ND
48	ND	ND	ND
72	154	102.7	20.8
96	178.6	247.6	46.8
120	148.9	374.3	56.3
194	104.4	470.9	55.2
216	ND	497.7	ND
240	ND	453.8	ND

ND - below detection limit

Sums of hydrides and dihydrides treatment B (peak area)

pH 7.0

Time	Isomer of 3-H-TNT	3,5-2H-TNT H+	3,5-2H-TNT
6	ND	ND	ND
12	ND	ND	ND
24	ND	ND	ND
36	ND	ND	ND
48	ND	ND	ND
72	25.31	13	13
96	43.7	32.2	15.6
120	56.9	84.4	46.3
194	100	102.6	46.5
216	83.7	137.2	52.5
240	95.5	143.4	37.2

pH 6.5	Isomer of 3-H-TNT	3,5-2H-TNT H+	3,5-2H-TNT
6	ND	ND	ND
12	ND	ND	ND
24	ND	ND	ND
36	ND	ND	ND
48	ND	ND	ND
72	39.1	32.9	10.9
96	51.6	124.7	33.2
120	104.4	205.2	45
194	132.3	283.4	65.4
216	42.6	418.6	39.5
240	21.5	419.1	15.6

pH 4.5

Time	Isomer of 3-H-TNT	3,5-2H-TNT H+	3,5-2H-TNT
6	ND	ND	ND
12	ND	ND	ND
24	ND	ND	ND
36	ND	ND	ND
48	ND	ND	ND
72	170	102.5	21.6
96	173	232.1	45.8
120	179.6	381.1	57.9
194	100.4	477.7	55
216	ND	523.5	ND
240	ND	473.2	ND

ND - below detection limit

Sums of hydrides and dihydrides - Averages (peak area)

pH 7.0	AVG		
Time	Isomer of 3-H-TNT	3,5-2H-TNT H+	3,5-2H-TNT
6	ND	ND	ND
12	ND	ND	ND
24	ND	ND	ND
36	ND	ND	ND
48	ND	ND	ND
72	24.655	13.35	13.15
96	50.1	40.15	23.85
120	70.85	82.5	47.15
194	101.85	104.4	51.6
216	86.55	140.2	50.1
240	82.5	141.3	38.7

pH 6.5	AVG Isomer of 3-H-TNT	3,5-2H-TNT H+	3,5-2H-TNT
6	ND	ND	ND
12	ND	ND	ND
24	ND	ND	ND
36	ND	ND	ND
48	ND	ND	ND
72	30.95	67.8	11.8
96	53.55	186.15	33.1
120	99.1	289.75	47.05
194	129.35	377.15	60.2
216	39.8	458.15	32.7
240	18.05	436.45	13.1

pH 4.5	AVG		
Time	Isomer of 3-H-TNT	3,5-2H-TNT H+	3,5-2H-TNT
6	ND	ND	ND
12	ND	ND	ND
24	ND	ND	ND
36	ND	ND	ND
48	ND	ND	ND
72	162	102.6	21.2
96	175.8	239.85	46.3
120	164.25	377.7	57.1
194	102.4	474.3	55.1
216	ND	510.6	ND
240	ND	463.5	ND

ND - below detection limit

Sums of hydrides and dihydrides - Standard deviations (peak area)

pH 7.0	STDEV		
Time	Isomer of 3-H-TNT	3,5-2H-TNT H+	3,5-2H-TNT
6	ND	ND	ND
12	ND	ND	ND
24	ND	ND	ND
36	ND	ND	ND
48	ND	ND	ND
72	0.926309883	0.494974747	0.212132034
96	9.050966799	11.24299782	11.66726189
120	19.7282792	2.687005769	1.202081528
194	2.61629509	2.545584412	7.212489168
216	4.030508653	4.242640687	3.39411255
240	18.38477631	2.969848481	2.121320344

	STDEV		
pH 6.5	Isomer of 3-H-TNT	3,5-2H-TNT H+	3,5-2H-TNT
6	ND	ND	ND
12	ND	ND	ND
24	ND	ND	ND
36	ND	ND	ND
48	ND	ND	ND
72	11.52584053	49.35605333	1.272792206
96	2.757716447	86.90342341	0.141421356
120	7.495331881	119.5717567	2.899137803
194	4.171930009	132.5825215	7.353910524
216	3.959797975	55.93214639	9.616652224
240	4.87903679	24.53660531	3.535533906

pH 4.5	STDEV		
Time	Isomer of 3-H-TNT	3,5-2H-TNT H+	3,5-2H-TNT
6	ND	ND	ND
12	ND	ND	ND
24	ND	ND	ND
36	ND	ND	ND
48	ND	ND	ND
72	11.3137085	0.141421356	0.565685425
96	3.959797975	10.96015511	0.707106781
120	21.70817818	4.808326112	1.13137085
194	2.828427125	4.808326112	0.141421356
216	ND	18.24335495	ND
240	ND	13.71787156	ND

ND - below detection limit

APPENDIX C

DATA TABLE FOR THE STUDY OF TNT TRANSFORMATION BY *Y. LIPOLYTICA* AN-L15 IN THE PRESENCE OF FERRIHYDRITE

pH DATA

Treatments A

Time	YT	YF	FT	YFT
6	6.93	6.88	7.03	6.87
18	6.97	6.79	7.06	6.84
30	6.69	6.58	7.26	6.91
42	6.24	5.77	7.16	6.56
54	5.67	4.9	7.25	6.06
66	5.27	4.64	7.07	5.75
78	4.32	3.78	7.26	5.57
90	3.7	3.61	7.15	5.15
102	3.66	3.5	7.15	4.26

Treatments B

Time	YT	YF	FT	YFT
6	6.84	6.95	7.05	6.84
18	7.05	6.91	7.06	6.98
30	6.7	6.53	7.3	6.9
42	5.45	5.67	7.19	6.49
54	4.8	4.78	7.23	6.08
66	4.05	4.38	7.15	5.92
78	3.59	3.78	7.17	5.69
90	3.28	3.59	7.11	5.47
102	3.15	3.47	7.21	5.05

Treatments C

Time	YT	YF	FT	YFT
6	6.92	6.95	7.07	6.89
18	7.04	6.88	7.09	6.94
30	6.73	6.59	7.31	6.94
42	5.88	5.75	7.21	6.56
54	5.27	4.87	7.27	6.10
66	4.69	4.54	7.14	5.87
78	3.99	3.81	7.25	5.66
90	3.52	3.63	7.16	5.34
102	3.44	3.52	7.21	4.69

pH DATA

AVG

Time	YT	YF	FT	YFT
6	6.90	6.93	7.05	6.87
18	7.02	6.86	7.07	6.92
30	6.71	6.57	7.29	6.92
42	5.86	5.73	7.19	6.54
54	5.25	4.85	7.25	6.08
66	4.67	4.52	7.12	5.85
78	3.97	3.79	7.23	5.64
90	3.50	3.61	7.14	5.32
102	3.42	3.50	7.19	4.67

STDEV

Time	YT	YF	FT	YFT
6	0.05	0.04	0.02	0.02
18	0.04	0.06	0.02	0.07
30	0.02	0.03	0.03	0.02
42	0.40	0.05	0.02	0.04
54	0.44	0.06	0.02	0.02
66	0.61	0.13	0.04	0.09
78	0.37	0.02	0.05	0.06
90	0.21	0.02	0.03	0.16
102	0.26	0.02	0.03	0.40

PROTEIN DATA mg/L

Treatments
A

Time	YT	YF	FT	YFT
6	124.74	118.86	0	114.24
18	98.7	115.08	0	101.43
30	112.56	154.14	0	94.29
42	132.72	252.63	0	117.6
54	193.2	305.13	0	216.51
66	211.47	324.45	0	305.13
78	235.83	377.79	0	347.97
90	244.44	347.13	0	416.43
102	275.52	483.21	0	459.06

Treatments
B

Time	YT	YF	FT	YFT
6	112.98	137.55	0	111.72
18	82.11	117.81	0	89.46
30	101.85	203.07	0	90.72
42	86.94	321.72	0	38.64
54	222.81	345.03	0	267.33
66	194.46	378	0	363.72
78	230.37	430.29	0	399.42
90	266.07	341.46	0	435.309
102	330.33	513.24	0	509.46

Treatments
C

Time	YT	YF	FT	YFT
6	128.86	138.21	0.00	122.98
18	100.41	126.45	0.00	105.45
30	117.21	188.61	0.00	102.51
42	119.83	297.18	0.00	88.12
54	218.01	335.08	0.00	251.92
66	212.97	361.23	0.00	344.43
78	243.10	414.04	0.00	383.70
90	265.26	354.30	0.00	435.87
102	312.93	508.23	0.00	494.26
102	28.01	16.09	0.00	25.85

PROTEIN DATA mg/L

AVG

Time	YT	YF	FT	YFT
6	122.19	131.54	0.00	116.31
18	93.74	119.78	0.00	98.78
30	110.54	181.94	0.00	95.84
42	113.16	290.51	0.00	81.45
54	211.34	328.41	0.00	245.25
66	206.30	354.56	0.00	337.76
78	236.43	407.37	0.00	377.03
90	258.59	347.63	0.00	429.20
102	306.26	501.56	0.00	487.59

STDEV

Time	YT	YF	FT	YFT
6	8.24	10.98	0.00	5.91
18	10.11	5.93	0.00	8.32
30	7.87	25.14	0.00	6.04
42	23.61	35.02	0.00	39.90
54	15.89	20.77	0.00	26.06
66	10.28	27.39	0.00	29.86
78	6.39	26.88	0.00	26.36
90	12.26	6.43	0.00	11.07
102	28.01	16.09	0.00	25.85

Fe(II) DATA μM

Treatments A

Time	YT	YF	FT	YFT
6	0.00	0.00	0.00	64.46
18	0.00	87.74	0.00	79.68
30	0.00	24.17	0.00	110.12
42	0.00	76.10	42.97	198.75
54	0.00	89.53	39.39	183.53
66	0.00	149.51	86.84	240.82
78	0.00	123.55	46.55	231.87
90	0.00	126.23	27.75	239.03
102	0.00	136.08	42.97	229.19

Treatments B

Time	YT	YF	FT	YFT
6	0.00	0.00	0.00	59.09
18	0.00	91.32	0.00	94.90
30	0.00	31.33	18.80	112.80
42	0.00	62.67	56.40	195.17
54	0.00	89.53	39.39	256.94
66	0.00	122.65	68.93	223.81
78	0.00	179.95	46.55	213.97
90	0.00	114.59	35.81	251.57
102	0.00	101.16	43.87	254.25

Treatments C

Time	YT	YF	FT	YFT
6	0.00	0.00	0.00	68.04
18	0.00	94.90	0.00	93.55
30	0.00	33.12	17.64	117.73
42	0.00	74.75	57.92	218.62
54	0.00	94.90	47.63	241.90
66	0.00	161.15	86.12	253.98
78	0.00	176.81	54.79	244.58
90	0.00	145.48	40.02	266.97
102	0.00	143.69	51.66	263.38

Fe(II) DATA μM

AVG

Time	YT	YF	FT	YFT
6	0.00	71.08	0.00	63.86
18	0.00	91.32	0.00	89.38
30	0.00	29.54	12.15	113.55
42	0.00	71.17	52.43	204.18
54	0.00	91.32	42.14	227.45
66	0.00	144.43	80.63	239.54
78	0.00	160.10	49.30	230.14
90	0.00	128.77	34.53	252.52
102	0.00	126.98	46.17	248.94

STDEV

Time	YT	YF	FT	YFT
6	0.00	5.41	0.00	4.51
18	0.00	3.58	0.00	8.43
30	0.00	4.74	10.53	3.86
42	0.00	7.40	8.23	12.64
54	0.00	3.10	4.76	38.78
66	0.00	19.74	10.14	15.13
78	0.00	31.70	4.76	15.38
90	0.00	15.60	6.23	13.99
102	0.00	22.68	4.78	17.71

Fe total data μM

Treatment A

Time	YT	YF	FT	YFT
6	0.00	974.93	0.00	864.82
18	0.00	1034.91	0.00	1036.71
30	0.00	957.03	951.66	1202.33
42	0.00	1211.28	912.26	1016.11
54	0.00	1377.80	786.03	871.98
66	0.00	1524.62	785.14	1274.84
78	5.37	1766.34	773.50	1420.77
90	7.16	2119.96	786.03	1401.07
102	13.43	1526.41	736.79	563.12

Treatment B

Time	YT	YF	FT	YFT
6	0.00	1003.58	0.00	1021.49
18	0.00	1048.34	0.00	1031.33
30	0.00	941.81	1049.24	1022.38
42	0.00	1081.47	934.65	754.70
54	0.00	994.63	903.31	1354.52
66	0.00	700.09	865.71	746.64
78	0.00	1308.86	794.99	871.98
90	21.49	2184.42	834.38	2073.41
102	1.79	462.85	741.27	871.98

Treatment C

Time	YT	YF	FT	YFT
6	0.00	979.23	0.00	933.57
18	0.00	1009.85	0.00	1034.91
30	0.00	961.32	978.87	1167.59
42	0.00	1167.95	916.74	781.56
54	0.00	1291.67	918.89	1187.82
66	0.00	1454.79	852.28	1168.13
78	0.00	1533.39	798.57	1275.38
90	0.00	2170.10	796.78	1658.73
102	0.00	1169.92	738.59	816.65

Fe total data µM

AVG

Time	YT	YF	FT	YFT
6	0.00	985.91	0.00	939.96
18	0.00	1031.04	0.00	1034.32
30	0.00	953.39	993.26	1130.77
42	0.00	1153.57	921.22	850.79
54	0.00	1221.37	869.41	1138.11
66	0.00	1226.50	834.38	1063.21
78	1.79	1536.20	789.02	1189.38
90	9.55	2158.16	805.73	1711.07
102	5.07	1053.06	738.88	750.58

STDEV

Time	YT	YF	FT	YFT
6	0.00	15.45	0.00	78.53
18	0.00	19.54	0.00	2.74
30	0.00	10.26	50.36	95.46
42	0.00	66.09	11.84	143.80
54	0.00	201.03	72.63	245.08
66	0.00	457.22	43.17	279.30
78	3.10	228.75	13.56	284.32
90	10.94	33.85	25.38	339.21
102	7.29	541.33	2.25	164.69

HPLC DATA FOR TNT, 2-HADNT, 4-HADNT, 4-ADNT, 2-ADNT 3-H-TNT μM

ND - below detection limit

μmol/L

Treatment YTA

Time	2-HADNT	TNT	4-HADNT
6	10.56	355.77	36.16
18	20.12	203.42	36.04
30	50.03	75.59	121.85
42	64.99	13.72	157.95
54	64.56	ND	164.69
66	74.98	ND	195.58
78	70.09	ND	202.26
90	62.87	ND	183.32
102	59.59	ND	168.67

Treatment YTB

Time	2-HADNT	TNT	4-HADNT
6	9.91	341.44	29.73
18	18.91	214.33	29.91
30	44.67	64.27	102.60
42	73.25	6.46	180.01
54	71.34	19.41	188.47
66	71.60	ND	195.70
78	67.15	ND	188.22
90	62.74	ND	172.53
102	58.81	ND	157.82

Treatment YTC

Time	2-HADNT	TNT	4-HADNT
6	11.54	352.25	42.14
18	20.81	212.52	42.17
30	48.65	73.57	121.42
42	70.42	13.74	178.17
54	69.25	12.41	185.77
66	74.59	ND	204.83
78	69.92	ND	204.43
90	64.10	ND	187.12
102	60.49	ND	172.44

HPLC DATA FOR TNT, 2-HADNT, 4-HADNT, 4-ADNT, 2-ADNT 3-H$^-$-TNT μM

ND - below detection limit

μmol/L

Treatment YTA

2-ADNT	4-ADNT	3-H$^-$-TNT
ND	4.73	7.16
ND	7.35	17.45
ND	10.92	58.60
ND	11.82	23.74
ND	13.29	ND
ND	18.97	ND
5.22	21.46	ND
5.65	22.02	ND
6.58	24.15	ND

Treatment YTB

2-ADNT	4-ADNT	3-H$^-$-TNT
ND	4.55	3.08
ND	7.66	14.87
ND	9.75	58.89
ND	14.28	19.53
ND	16.90	ND
4.78	19.07	ND
5.26	20.23	ND
6.11	22.00	ND
6.76	23.24	ND

Treatment YTC

2-ADNT	4-ADNT	3-H$^-$-TNT
ND	5.22	5.86
ND	8.09	16.91
ND	10.92	59.49
ND	13.64	22.37
ND	15.68	ND
3.44	19.61	ND
5.63	21.43	ND
6.28	22.60	ND
7.07	24.28	ND

HPLC DATA FOR TNT, 2-HADNT, 4-HADNT, 4-ADNT, 2-ADNT 3-H-TNT μM

ND - below detection limit

Treatment YFTA

Time	2-HADNT	TNT	4-HADNT
6	ND	365.18	ND
18	ND	295.83	ND
30	23.49	221.06	23.60
42	57.29	102.68	83.66
54	49.47	60.64	72.38
66	41.86	17.30	54.24
78	34.25	ND	103.89
90	21.20	ND	77.23
102	17.57	ND	70.05

Treatment YFTB

Time	2-HADNT	TNT	4-HADNT
6	ND	361.63	ND
18	ND	290.29	ND
30	25.22	226.85	30.65
42	73.42	31.34	163.34
54	50.98	ND	68.95
66	41.56	17.10	36.28
78	33.73	18.78	88.81
90	22.80	9.98	76.18
102	17.00	24.80	66.01

Treatment YFTC

Time	2-HADNT	TNT	4-HADNT
6	ND	371.18	ND
18	ND	300.83	ND
30	25.65	231.73	36.93
42	66.65	74.79	133.31
54	51.52	37.89	80.47
66	43.01	24.97	55.07
78	35.29	16.96	106.15
90	23.29	12.56	86.51
102	18.58	19.97	77.84

HPLC DATA FOR TNT, 2-HADNT, 4-HADNT, 4-ADNT, 2-ADNT 3-H$^-$-TNT μM

ND - below detection limit

Treatment YFTA

2-ADNT	4-ADNT	3-H$^-$-TNT
ND	5.02	ND
ND	9.71	ND
ND	11.31	11.1701989
ND	14.66	ND
ND	14.87	ND
5.10	20.68	ND
5.02	20.17	ND
4.88	17.68	ND
5.24	18.70	ND

Treatment YFTB

2-ADNT	4-ADNT	3-H$^-$-TNT
ND	ND	ND
ND	7.72	ND
ND	10.51	14.33747817
ND	13.58	ND
ND	12.04	ND
4.80	18.82	ND
4.94	19.23	ND
5.02	19.54	ND
5.02	18.76	ND

Treatment YFTC

2-ADNT	4-ADNT	3-H$^-$-TNT
ND	7.93	ND
ND	11.67	ND
ND	14.01	11.6472459
ND	14.91	ND
ND	18.41	ND
4.99	21.52	ND
5.02	21.42	ND
4.99	19.79	ND
5.17	20.26	ND

HPLC DATA FOR TNT, 2-HADNT, 4-HADNT, 4-ADNT, 2-ADNT 3-H$^-$-TNT μM

Time	2-HADNT	TNT	4-HADNT
ND	ND	450	ND
6	10.67	349.82	36.01
18	19.94	210.09	36.04
30	47.78	71.14	115.29
42	69.55	11.31	172.04
54	68.38	10.61	179.64
66	73.72	ND	198.70
78	69.05	ND	198.30
90	63.24	ND	180.99
102	59.63	ND	166.31

STDEV

Time	2-HADNT	TNT	4-HADNT
6	0.82	7.47	6.21
18	0.96	5.85	6.13
30	2.78	6.04	10.99
42	4.20	4.20	12.24
54	3.48	9.83	13.02
66	1.84	ND	5.31
78	1.65	ND	8.80
90	0.75	ND	7.57
102	0.84	ND	7.59

AVG

2-ADNT	4-ADNT	3-H$^-$-TNT
ND	ND	ND
ND	4.83	5.36
ND	7.70	16.41
ND	10.53	58.99
ND	13.25	21.88
ND	15.29	ND
2.74	19.22	ND
5.37	21.04	ND
6.01	22.21	ND
6.80	23.89	ND

STDEV

2-ADNT	4-ADNT	3-H$^-$-TNT
ND	0.35	ND
ND	0.37	2.08
ND	0.68	1.36
ND	1.28	0.45
ND	1.84	2.15
2.47	0.34	ND
0.23	0.70	ND
0.32	0.34	ND
0.25	0.57	ND

HPLC DATA FOR TNT, 2-HADNT, 4-HADNT, 4-ADNT, 2-ADNT 3-H$^-$-TNT μM

Time	2-HADNT	TNT	4-HADNT
0	ND	450	ND
6	ND	365.99	ND
18	ND	295.65	ND
30	24.79	226.55	30.39
42	65.79	69.60	126.77
54	50.66	32.84	73.94
66	42.14	19.79	48.53
78	34.43	11.91	99.62
90	22.43	7.51	79.97
102	17.72	14.92	71.30

STDEV

Time	2-HADNT	TNT	4-HADNT
6	ND	4.83	ND
18	ND	5.27	ND
30	1.14	5.34	6.67
42	8.10	35.95	40.24
54	1.06	30.64	5.92
66	0.76	4.49	10.62
78	0.79	10.36	9.43
90	1.10	6.63	5.69
102	0.80	13.15	6.01

AVG

2-ADNT	4-ADNT	3-H$^-$-TNT
ND	ND	ND
ND	4.32	ND
ND	9.70	ND
ND	11.94	12.38497432
ND	14.38	ND
ND	15.10	ND
4.96	20.34	ND
4.99	20.27	ND
4.96	19.00	ND
5.14	19.24	ND

STDEV

2-ADNT	4-ADNT	3-H$^-$-TNT
ND	4.01	ND
ND	1.98	ND
ND	1.83	ND
ND	0.71	1.707658312
ND	3.19	ND
0.15	1.38	ND
0.05	1.10	ND
0.07	1.15	ND
0.11	0.89	ND

HYDRIDE DATA 476 nm (peak areas)

ND - below detection limit

Treatments YTA

Time	5.305 Isomer of 3-H⁻-TNT	5.611 3,5-2H⁻-TNT H+	5.71 3,5-2H⁻-TNT H+	6.207 3,5-2H⁻-TNT
0	ND	ND	ND	ND
6	ND	ND	ND	ND
18	ND	ND	ND	ND
30	10.8	21.1	ND	11.3
42	13.2	12.7	22.7	17.8
54	13.8	14.1	30.5	18.5
66	13.1	ND	36.2	15.6
78	18.9	ND	53.7	64.5
90	15.6	ND	46.8	58.6
102	ND	ND	45.2	ND

Treatments YTB

Time	Isomer of 3-H⁻-TNT	3,5-2H⁻-TNT H+	3,5-2H⁻-TNT H+	3,5-2H⁻-TNT
0	ND	ND	ND	ND
6	ND	ND	ND	ND
18	ND	ND	ND	ND
30	9.7	20.4	10.5	12.5
42	12.5	15.7	24.1	17.8
54	12.4	ND	38	17.4
66	16.2	ND	43.1	41.6
78	13	ND	39.8	41.7
90	ND	ND	42.2	ND
102	ND	ND	39.8	ND

Treatments YTC

Time	Isomer of 3-H⁻-TNT	3,5-2H⁻-TNT H+	3,5-2H⁻-TNT H+	3,5-2H⁻-TNT
0	ND	ND	ND	ND
6	ND	ND	ND	ND
18	ND	ND	ND	ND
30	10.45	20.85	8.25	14.9
42	13.05	14.3	26.4	20.8
54	13.3	7.15	37.25	20.95
66	14.85	ND	42.65	31.6
78	16.15	ND	49.75	56.1
90	8	ND	47.5	32.3
102	ND	ND	45.50	ND

HYDRIDE DATA 476 nm (peak areas)

ND - below detection limit

Treatment YTA

Time	6.336 Isomer of 3-H^--TNT	7.069 3,5-$2H^-$-TNT H+	9.921 3-H^--TNT	Sum of other 6 hydrides
0	ND	ND	ND	ND
6	ND	ND	54.9	6
18	ND	ND	133.9	18
30	12	10.1	449.6	95.3
42	14.4	21.3	182.1	144.1
54	13.3	34.7	ND	178.9
66	10.3	27.2	ND	168.4
78	ND	41.2	ND	256.3
90	ND	30.1	ND	241.1
102	ND	23.3	ND	170.5

Treatment YTB

Time	Isomer of 3-H^--TNT	3,5-$2H^-$-TNT H+	3-H^--TNT	Sum of other 6 hydrides
0	ND	ND	ND	ND
6	ND	ND	23.6	6
18	ND	ND	114.1	18
30	10.6	ND	451.8	93.7
42	14.9	27.5	149.8	154.5
54	11.7	35	ND	168.5
66	ND	35.2	ND	202.1
78	ND	33.4	ND	205.9
90	ND	26.7	ND	158.9
102	ND	23.6	ND	165.4

Treatment YTC

Time	Isomer of 3-H^--TNT	3,5-$2H^-$-TNT H+	3-H^--TNT	Sum of other 6 hydrides
0	ND	ND	ND	ND
6	ND	ND	44.95	ND
18	ND	ND	129.7	ND
30	11.5	7.05	456.4	73
42	14.85	26.4	171.65	115.8
54	12.7	36.85	ND	128.2
66	5.35	33.2	ND	127.65
78	ND	39.3	ND	161.3
90	ND	30.4	ND	118.2
102	ND	25.45	ND	70.95

HYDRIDE DATA 476 nm (peak areas)

ND - below detection limit

AVG YT

Time	Isomer of 3-H-TNT	3,5-2H-TNT H+	3,5-2H-TNT H+	3,5-2H-TNT
0	ND	ND	ND	ND
6	ND	ND	ND	ND
18	ND	ND	ND	ND
30	10.32	20.78	6.25	12.90
42	12.92	14.23	24.40	18.80
54	13.17	7.08	35.25	18.95
66	14.72	ND	40.65	29.60
78	16.02	ND	47.75	54.10
90	7.87	ND	45.50	30.30
102	ND	ND	43.50	ND

YT STDEV

Time	Isomer of 3-H$^-$-TNT	3,5-2H$^-$-TNT H+	3,5-2H$^-$-TNT H+	3,5-2H$^-$-TNT
0	ND	ND	ND	ND
6	ND	ND	ND	ND
18	ND	ND	ND	ND
30	0.56	0.35	5.53	1.83
42	0.37	1.50	1.87	1.73
54	0.71	7.05	4.13	1.82
66	1.55	ND	3.86	13.11
78	2.95	ND	7.16	11.53
90	7.80	ND	2.88	29.35
102	ND	ND	3.21	ND

HYDRIDE DATA 476 nm (peak areas)

ND - below detection limit

YT AVG

Time	Isomer of 3-H-TNT	3,5-2H-TNT H+	3-H-TNT	Sum of other 6 hydrides
0	ND	ND	ND	ND
6	ND	ND	41.15	4.00
18	ND	ND	125.90	12.00
30	11.37	5.72	452.60	87.33
42	14.72	25.07	167.85	138.13
54	12.57	35.52	ND	158.53
66	5.22	31.87	ND	166.05
78	ND	37.97	ND	207.83
90	ND	29.07	ND	172.73
102	ND	24.12	ND	135.62

YT STDEV

Time	Isomer of 3-H$^-$-TNT	3,5-2H$^-$-TNT H+	3-H$^-$-TNT	Sum of other 6 hydrides
0	ND	ND	ND	ND
6	ND	ND	15.99	3.46
18	ND	ND	10.43	10.39
30	0.71	5.18	3.47	12.44
42	0.28	3.31	16.48	20.03
54	0.81	1.16	ND	26.78
66	5.15	4.16	ND	37.28
78	ND	4.07	ND	47.53
90	ND	2.06	ND	62.61
102	ND	1.16	ND	56.06

HYDRIDE DATA 476 nm (peak areas)

ND - below detection limit

Treatment YFTA	5.305	5.611	5.71	6.207
Time	Isomer of 3-H⁻-TNT	3,5-2H⁻-TNT H+	3,5-2H⁻-TNT H+	3,5-2H⁻-TNT
0	ND	ND	ND	ND
6	ND	ND	ND	ND
18	ND	ND	ND	ND
30	ND	ND	ND	ND
42	5.3	ND	19.5	10.7
54	5.6	ND	31.6	11.4
66	5.1	ND	22.4	ND
78	ND	ND	26.3	ND
90	ND	ND	35.7	ND
102	ND	ND	35.8	ND

Treatment YFTB				
Time	Isomer of 3-H⁻-TNT	3,5-2H⁻-TNT H+	3,5-2H⁻-TNT H+	3,5-2H⁻-TNT
0	ND	ND	ND	ND
6	ND	ND	ND	ND
18	ND	ND	ND	ND
30	ND	ND	ND	ND
42	ND	ND	28.6	15
54	7.8	ND	31.5	13.9
66	6.8	ND	21.1	ND
78	6.2	ND	29.8	ND
90	ND	ND	30.3	ND
102	6.8	ND	31.7	ND

Treatment YFTC				
Time	Isomer of 3-H⁻-TNT	3,5-2H⁻-TNT H+	3,5-2H⁻-TNT H+	3,5-2H⁻-TNT
0	ND	ND	ND	ND
6	ND	ND	ND	ND
18	ND	ND	ND	ND
30	ND	ND	ND	ND
42	2.95	ND	25.05	14.3
54	7	ND	32.55	12.2
66	6.25	ND	22.75	ND
78	3.4	ND	29.05	ND
90	ND	ND	34	ND
102	3.7	ND	34.75	ND

HYDRIDE DATA 476 nm (peak areas)

ND - below detection limit

Treatment YFTA

Time	Isomer of 3-H^--TNT	3,5-$2H^-$-TNT H+	3-H^--TNT	Sum of other 6 hydrides
	6.336	7.069	9.921	
0	ND	ND	ND	ND
6	ND	ND	ND	6
18	ND	ND	ND	18
30	ND	ND	ND	30
42	ND	9.9	ND	87.4
54	ND	16.7	ND	119.3
66	ND	ND	ND	93.5
78	ND	13.4	ND	117.7
90	ND	17.8	ND	143.5
102	ND	19.8	ND	157.6

Treatment YFTB

Time	Isomer of 3-H^--TNT	3,5-$2H^-$-TNT H+	3-H^--TNT	Sum of other 6 hydrides
0	ND	ND	ND	ND
6	ND	ND	ND	6
18	ND	ND	ND	18
30	ND	ND	ND	30
42	ND	21.1	ND	106.7
54	ND	17.3	ND	124.5
66	ND	ND	ND	93.9
78	ND	11.6	ND	125.6
90	ND	9.2	ND	129.5
102	ND	39.9	ND	180.4

Treatment YFTC

Time	Isomer of 3-H^--TNT	3,5-$2H^-$-TNT H+	3-H^--TNT	Sum of other 6 hydrides
0	ND	ND	ND	ND
6	ND	ND	ND	ND
18	ND	ND	ND	ND
30	ND	ND	ND	ND
42	ND	19.5	ND	61.8
54	ND	21	ND	72.75
66	ND	ND	ND	29
78	ND	16.5	ND	48.95
90	ND	17.5	ND	51.5
102	ND	33.85	ND	72.3

HYDRIDE DATA 476 nm (peak areas)

ND - below detection limit

AVG

Time	Isomer of 3-H-TNT	3,5-2H-TNT H+	3,5-2H-TNT H+	3,5-2H-TNT
0	ND	ND	ND	ND
6	ND	ND	ND	ND
18	ND	ND	ND	ND
30	ND	ND	ND	ND
42	2.75	ND	24.38	13.33
54	6.80	ND	31.88	12.50
66	6.05	ND	22.08	ND
78	3.20	ND	28.38	ND
90	ND	ND	33.33	ND
102	3.50	ND	34.08	ND

STDEV

Time	Isomer of 3-H$^-$-TNT	3,5-2H$^-$-TNT H+	3,5-2H$^-$-TNT H+	3,5-2H$^-$-TNT
0	ND	ND	ND	ND
6	ND	ND	ND	ND
18	ND	ND	ND	ND
30	ND	ND	ND	ND
42	2.66	ND	4.59	2.31
54	1.11	ND	0.58	1.28
66	0.87	ND	0.87	ND
78	3.10	ND	1.84	ND
90	ND	ND	2.76	ND
102	3.40	ND	2.13	ND

HYDRIDE DATA 476 nm

ND - below detection limit

AVG

Time	Isomer of 3-H-TNT	3,5-2H-TNT H+	3-H-TNT	Sum of other 6 hydrides
0	ND	ND	ND	ND
6	ND	ND	ND	4.00
18	ND	ND	ND	12.00
30	ND	ND	ND	20.00
42	ND	16.83	85.00	85.30
54	ND	18.33	ND	105.52
66	ND	ND	ND	72.13
78	ND	13.83	ND	97.42
90	ND	14.83	ND	108.17
102	ND	31.18	ND	136.77

STDEV

Time	Isomer of 3-H$^-$-TNT	3,5-2H$^-$-TNT H+	3-H$^-$-TNT	Sum of other 6 hydrides
0	ND	ND	ND	ND
6	ND	ND	ND	3.46
18	ND	ND	ND	10.39
30	ND	ND	ND	17.32
42	ND	6.06	ND	22.52
54	ND	2.33	ND	28.50
66	ND	ND	ND	37.36
78	ND	2.48	ND	42.16
90	ND	4.88	ND	49.57
102	ND	10.31	ND	56.98

NITRITE AND NITRATE DATA µM

ND - below detection limit

NO2-

Treatments
A

Time	YT	YF	FT	YFT
6	53.91304348	0	ND	7.826086957
18	72.43478261	0	6.086956522	52.34782609
30	120.6521739	0	1.086956522	104.7826087
42	58.04347826	0	22.17391304	37.17391304
54	38.26086957	0	4.130434783	85.86956522
66	56.52173913	0	3.043478261	97.82608696
78	55.43478261	0	11.95652174	61.08695652
90	56.30434783	0	11.95652174	38.47826087
102	30.43478261	0	5.652173913	13.04347826

Treatments
B

Time	YT	YF	FT	YFT
6	33.91304348	0	ND	11.30434783
18	71.82608696	0	6.289855072	61.68115942
30	108.2608696	0	1.304347826	107.826087
42	28.69565217	0	19.56521739	20
54	50.2173913	0	3.695652174	99.7826087
66	41.08695652	0	8.47826087	105.6521739
78	31.95652174	0	17.17391304	84.34782609
90	30.65217391	0	15.2173913	54.56521739
102	31.30434783	0	4.565217391	25.43478261

Treatments
C

Time	YT	YF	FT	YFT
6	51.95652174	0	ND	17.17391304
18	80.17391304	0	8.144927536	64.62318841
30	122.5	0	3.152173913	113.9130435
42	51.41304348	0	22.82608696	36.19565217
54	52.2826087	0	5.869565217	100.4347826
66	56.84782609	0	7.717391304	109.3478261
78	51.73913043	0	16.52173913	80.32608696
90	51.52173913	0	15.54347826	54.13043478
102	38.91304348	0	7.065217391	26.84782609

NITRITE AND NITRATE DATA μM

NO_2^- μmol/L
AVG

Time	YT	YF	FT	YFT	
0	0	0	0	0	0
6	46.59	0.00	0.00	12.10	
18	74.81	0.00	6.84	59.55	
30	117.14	0.00	1.85	108.84	
42	46.05	0.00	21.52	31.12	
54	46.92	0.00	4.57	95.36	
66	51.49	0.00	6.41	104.28	
78	46.38	0.00	15.22	75.25	
90	46.16	0.00	14.24	49.06	
102	33.55	0.00	5.76	21.78	

STDEV

Time	YT	YF	FT	YFT	
6	11.03	0.00	0.00	4.72	
18	4.65	0.00	1.13	6.41	
30	7.74	0.00	1.13	4.65	
42	15.39	0.00	1.73	9.65	
54	7.57	0.00	1.15	8.23	
66	9.01	0.00	2.94	5.88	
78	12.62	0.00	2.84	12.43	
90	13.64	0.00	1.98	9.16	
102	4.66	0.00	1.25	7.59	

NITRITE AND NITRATE DATA μM

NO_3^- μmol/L

Treatment A

Time	YT	YF	FT	YFT
6	3.77	0.00	0.00	4.20
18	7.71	0.00	6.09	6.67
30	6.81	0.00	0.00	5.65
42	10.29	0.00	3.62	3.91
54	5.94	0.00	9.28	3.62
66	6.67	0.00	8.26	3.48
78	6.52	0.00	8.26	5.07
90	12.75	0.00	7.68	4.06
102	15.80	0.00	9.28	5.22

Treatment B

Time	YT	YF	FT	YFT
6	5.51	0.00	0.00	5.51
18	7.30	0.00	8.39	8.93
30	8.70	0.00	8.41	4.78
42	0.00	0.00	0.00	0.00
54	6.09	0.00	7.25	4.20
66	7.39	0.00	10.87	4.64
78	18.26	0.00	8.41	6.09
90	20.43	0.00	8.84	5.51
102	23.91	0.00	10.14	4.78

Treatment C

Time	YT	YF	FT	YFT
6	5.36	0.00	0.00	5.72
18	8.23	0.00	8.25	8.67
30	8.48	0.00	5.22	6.09
42	9.49	0.00	2.83	2.83
54	6.74	0.00	9.28	4.78
66	7.75	0.00	10.58	4.93
78	17.46	0.00	9.35	6.45
90	21.67	0.00	9.28	5.65
102	24.93	0.00	10.72	5.87

NITRITE AND NITRATE DATA μM

NO_3^- μmol/L
AVG

Time	YT	YF	FT	YFT
6	4.88	0.00	0.00	5.14
18	7.75	0.00	7.57	8.09
30	8.00	0.00	4.54	5.51
42	6.59	0.00	2.15	2.25
54	6.26	0.00	8.60	4.20
66	7.27	0.00	9.90	4.35
78	14.08	0.00	8.67	5.87
90	18.29	0.00	8.60	5.07
102	21.55	0.00	10.05	5.29

STDEV

Time	YT	YF	FT	YFT
6	0.96	0.00	0.00	0.82
18	0.46	0.00	1.29	1.24
30	1.03	0.00	4.24	0.66
42	5.72	0.00	1.90	2.02
54	0.42	0.00	1.17	0.58
66	0.55	0.00	1.43	0.77
78	6.56	0.00	0.59	0.71
90	4.83	0.00	0.82	0.88
102	5.00	0.00	0.73	0.55

APPENDIX D

DATA TABLE FOR THE STUDY OF TNT TRANSFORMATION BY *Y. LIPOLYTICA* AN-L15 UNDER CONSTANT FLOW CONDITIONS

BEAD PROTEIN ASSAY DATA - mg/L

C1T	1	80.02631579
C1M	2	52.13157895
C1B	3	83.44736842
C2T	1	16.86842105
C2M	2	13.97368421
C2B	3	13.71052632
C3T	1	17.65789474
C3M	2	10.55263158
C3B	3	37.65789474
C4T	1	58.18421053
C4M	2	14.76315789
C4B	3	8.973684211

COLUMN ABSORBANCE DATA - OD_{600}

time	Y in	YT in	YT in	T in
0	0.177	0.034		
17	0.088	0.03		
29	0.229	0.006		
41	0.385	0.019		
105	0.422	0	0.02	0
130	0.021	0	0.032	0.003
180	0.03	0	0.003	0.001
224	0.047	0.002	0	0.002
275	0.017	0.002	0.001	0.001
323	0.021	0.003	0.003	0
373	0.001	0.001	0.002	0
421	0.002	0	0	0
463	0	0.005	0	0.003

time	Y out	YT out	YT out	T out
0	0.014	0.031		
17	0.037	0.005		
29	0.096	0.011		
41	0.072	0.004		
105	0.107	0.027	0.015	0.016
130	0.092	0.015	0.012	0.003
180	0.11	0.033	0.02	0.027
224	0.071	0.024	0.08	0.083
275	0.148	0.083	0.07	0.058
323	0.176	0.047	0.048	0.019
373	0.139	0.042	0.059	0.041
421	0.085	0.037	0.113	0.043
463	0.063	0.135	0.04	0.093

pH DATA

time	Y in	YT in	YT in	T in
0	4.49	4.56		
17	4.46	4.49		
29	4.37	4.2		
41	4.28	4.27		
105	4.31	4.21	4.5	4.34
130	4.36	3.99	4.09	4.45
180	4.53	4.53	4.12	4.36
224	4.51	4.59	3.87	4.44
275	4.49	4.46	4.45	4.65
323	4.57	4.57	4.54	4.38
373	4.63	4.4	4.57	4.38
421	4.54	4.48	4.5	4.39
463	4.59	4.51	4.48	4.45

time	Y out	YT out	YT out	T out
0	4.54	4.45		
17	4.5	4.41		
29	4.43	4.33		
41	4.23	4.05		
105	4.21	3.45	4.41	4.57
130	4.33	3.23	4.37	4.59
180	4.12	3.19	4.12	4.49
224	4.19	3.08	3.51	4.31
275	4.24	3.15	3.22	4.33
323	4.17	3.11	3.05	4.23
373	4.23	3.09	3.09	4.14
421	4.25	3.17	3.17	4.12
463	4.18	3.02	3.1	3.99

HPLC DATA

ND - below detection limit

μmol/L
C-2 out
Ret time

range time	10.9 +/- .2 3-H-TNT	15.2 +/- .1 2-HADNT	15.7 +/- .2 TNT	16.4 +/- .1 4-HADNT
0	ND	ND	ND	ND
17	ND	ND	ND	ND
29	ND	ND	ND	ND
41	ND	ND	ND	ND
105	ND	ND	22.79	ND
130	ND	ND	ND	ND
180	ND	25.75	125.39	26.57
224	5.52	29.26	245.21	43.99
275	4.64	28.29	240.09	31.37
323	ND	ND	309.57	23.20
373	ND	ND	277.65	17.67
421	ND	ND	338.69	12.95
463	ND	ND	226.82	50.48

μmol/L
C-2 in
Ret time

range time	10.9 +/- .2 3-H-TNT	15.2 +/- .1 2-HADNT	15.7 +/- .2 TNT	16.4 +/- .1 4-HADNT
0	4.75	ND	169.86	24.52
17	6.27	36.88	115.03	33.78
29	3.56	37.79	114.30	33.70
41	7.01	31.80	133.89	30.17
105	0.77	ND	169.35	14.51
130	17.11	ND	283.73	17.99
180	6.27	ND	274.25	13.19
224	20.78	ND	419.70	ND
275	16.75	ND	257.32	ND
323	10.13	ND	291.66	ND
373	ND	ND	501.52	ND
421	ND	ND	431.72	ND
463	ND	ND	435.60	ND

HPLC DATA

ND - below detection limit

μmol/L
C-3 out

Ret time range time	10.9 +/- .2 3-H-TNT	15.2 +/- .1 2-HADNT	15.7 +/- .2 TNT	16.4 +/- .1 4-HADNT
0	ND	ND	ND	ND
17	ND	ND	ND	ND
29	ND	ND	ND	ND
41	ND	ND	ND	ND
105	ND	ND	ND	ND
130	ND	ND	ND	ND
180	ND	ND	ND	ND
224	ND	ND	ND	ND
275	ND	ND	ND	ND
323	ND	ND	ND	ND
373	ND	ND	ND	ND
421	ND	ND	ND	ND
463	ND	ND	ND	ND

μmol/L
C-3 in

Ret time range time	10.9 +/- .2 3-H-TNT	15.2 +/- .1 2-HADNT	15.7 +/- .2 TNT	16.4 +/- .1 4-HADNT
0	ND	ND	ND	ND
17	ND	ND	ND	ND
29	ND	ND	ND	ND
41	ND	ND	ND	ND
105	3.31	ND	130.08	15.23
130	4.64	ND	193.61	3.89
180	3.45	ND	179.09	25.40
224	11.15	ND	377.19	ND
275	11.67	ND	294.30	ND
323	13.08	ND	267.54	ND
373	ND	ND	436.38	ND
421	ND	ND	405.23	ND
463	ND	ND	11.56	ND

HPLC DATA

ND - below detection limit

μmol/L
C-4 out
Ret time

range Time	10.9 +/- .2 3-H-TNT	15.2 +/- .1 2-HADNT	15.7 +/- .2 TNT	16.4 +/- .1 4-HADNT
0	ND	ND	ND	ND
17	ND	ND	ND	ND
29	ND	ND	ND	ND
41	ND	ND	ND	ND
105	ND	ND	94.31	ND
130	22.60	ND	146.98	ND
180	ND	ND	251.92	ND
224	9.99	ND	276.86	12.67
275	ND	ND	288.37	11.26
323	ND	ND	287.66	6.38
373	ND	ND	282.88	7.94
421	ND	ND	264.85	8.70
463	ND	ND	189.93	38.14

μmol/L
C-4 in
Ret time

range time	10.9 +/- .2 3-H-TNT	15.2 +/- .1 2-HADNT	15.7 +/- .2 TNT	16.4 +/- .1 4-HADNT
	ND	ND	ND	ND
17	ND	ND	ND	ND
29	ND	ND	ND	ND
41	ND	ND	ND	ND
105	ND	ND	211.50	ND
130	ND	ND	431.33	ND
180	ND	ND	484.89	ND
224	ND	ND	427.24	ND
275	ND	ND	308.06	ND
323	ND	ND	345.46	ND
373	ND	ND	368.47	ND
421	ND	ND	345.54	ND
463	ND	ND	405.92	ND

REFERENCES CITED

1. Ahlers, P. M., A. Garofano, S. J. Kerscher, and U. Brandt. 2000. Application of the obligate aerobic yeast *Yarrowia lipolytica* as a eucaryotic model to analyse Leigh syndrome mutations in the complex I core subunits PSST and TYKY. Biochim. Biophys. Acta. 1459:258-265.

2. Army. 1976. Adverse health effects of selected explosives (TNT, RDX). Report no. USAEHH-32-049-75/76. Aberdeen Proving Ground: MD: U.S. Army Environmental Hygiene Agency.

3. Army. 1978. A literature review - problem definition studies on selected toxic chemicals. Volume3: Occupational health and safety aspects of 2,4,6-trinitrotoluene (TNT). Contract no. DAMD 17-77-C-7020. Frederick, MD: U.S. Army Medical Research and Development Command, Fort Detrick.

4. Beltz, L. A., D. R. Neira, C. A. Axtell, S. Iverson, W. Deaton, T. J. Waldschmidt, J. A. Bumpus, and C. G. Johnston. 2001. Immunotoxicity of explosives-contaminated soil before and after bioremediation. Archives of Environmental Contamination and Toxicology 40:311-317.

5. Blehert, D. S., B. G. Fox, and G. H. Chambliss. 1999. Cloning and sequence analysis of two *Pseudomonas* flavoprotein xenobiotic reductases. Journal of Bacteriology 181:6254-6263.

6. Borch, T., and R. Gerlach. 2004. Use of reversed-phase high-performance liquid chromatography-diode array detection for complete separation of 2,4,6-trinitrotoluene metabolites and EPA method 8330 explosives: influence of temperature and an ion-pair reagent. Journal of Chromatography A 1022:83-94.

7. Borch, T., W. P. Inskeep, and R. Gerlach. 2004. Iron (hydr)oxides and electron shuttles govern the fate of 2.4.6-trinitrotoluene by a soil bacterium. Geochimica Et Cosmochimica Acta 68:A451-A451.

8. Borch, T., W. P. Inskeep, J. A. Harwood, and R. Gerlach. 2005. Impact of ferrihydrite and anthraquinone-2,6-disulfonate on the reductive transformation of 2,4,6-trinitrotoluene by a gram-positive fermenting bacterium. Environmental Science & Technology 39:7126-7133.

9. Bruns-Nagel, D., S. Scheffer, B. Casper, H. Garn, O. Drzyzga, E. Von Low, and D. Gemsa. 1999. Effect of 2,4,6-trinitrotoluene and its metabolites on human monocytes. Environmental Science & Technology 33:2566-2570.

10. Caballero, A., A. Esteve-Nunez, G. J. Zylstra, and J. L. Ramos. 2005. Assimilation of nitrogen from nitrite and trinitrotoluene in *Pseudomonas putida* JLR11. Journal of Bacteriology 187:396-399.

11. Camper, A. K., M. W. LeChevallier, S. C. Broadaway, and G. A. McFeters. 1985. Evaluation of procedures to desorb bacteria from granular activated carbon. J. Microb. Meth. 3:187-198.

12. Croddy, E., and J. J. Wirtz. 2005. Weapons of mass destruction: and encyclopedia of worldwide policy, technology, and history. ABC-CLIO. Oxford, UK.

13. Daun, G., H. Lenke, M. Reuss, and H. J. Knackmuss. 1998. Biological treatments of TNT-contaminated soil. 1. Anaerobic cometabolic reduction and interaction of TNT and metabolites with soil components. Environmental Science & Technology 32:1956-1963.

14. Dilley, J. V., C. A. Tyson, R. J. Spanggord, D. P. Sasmore, G. W. Newell, and J. C. Dacre. 1982. Short-term oral toxicity of 2,4,6-trinitrotoluene in mice, rats, and dogs. Journal of Toxicology and Environmental Health 9:565-585.

15. Dujon, B., D. Sherman, G. Fisher, P. Durrens, S. Casaregola, I. Lafontaine, J. de Montigny, C. Marck, C. Neuveglise, E. Talla, N. Goffard, L. Frangeul, M. Aigle, V. Anthouard, A. Babour, V. Barbe, S. Barnay, S. Blanchin, J. M. Beckerich, E. Beyne, C. Bleykasten, A. Boisrame, J. Boyer, L. Cattolico, F. Confanioleri, A. de Daruvar, L. Despons, E. Fabre, C. Fairhead, H. Ferry-Dumazet, A. Groppi, F. Hantraye, C. Hennequin, N. Jauniaux, P. Joyet, R. Kachouri, A. Kerrest, R. Koszul, M. Lemaire, I. Lesur, L. Ma, H. Muller, J. M. Nicaud, M. Nikolski, S. Oztas, O. Ozier-Kalogeropoulos, S. Pellenz, S. Potier, G. F. Richard, M. L. Straub, A. Suleau, D. Swennen, F. Tekaia, M. Wesolowski-Louvel, E. Westhof, B. Wirth, M. Zeniou-Meyer, I. Zivanovic, M. Bolotin-Fukuhara, A. Thierry, C. Bouchier, B. Caudron, C. Scarpelli, C. Gaillardin, J. Weissenbach, P. Wincker, and J. L. Souciet. 2004. Genome evolution in yeasts. Nature 430:35-44.

16. Dusane, D. H., Y. V. Nancharaiah, V. P. Venugopalal, A. R. Kumar, and S. S. Zinjarde. 2008. Biofilm formation by a biotechnogically important tropical marine yeast isolate, *Yarrowia lipolytica* NCIM 3589. Water Science Technology. 58:1221-1229.

17. Elovitz, M. S., and E. J. Weber. 1999. Sediment mediated reduction of 2,4,6-trinitrotoluene and fate of the resulting aromatic (poly)amines. Environmental Science & Technology 33:2617-2625.

18. French, C. E., S. Nicklin, and N. C. Bruce. 1998. Aerobic degradation of 2,4,6-trinitrotoluene by *Enterobacter cloacae* PB2 and by pentaerythritol tetranitrate reductase. Applied and Environmental Microbiology 64:2864-2868.

19. Giles, J. 2004. Green explosives: Collateral damage. Nature 427:580-581.

20. Harkonen, H., M. Karki, A. Lahti, and H. Savolainen. 1983. Early equatorial cataracts in workers exposed to trinitrotoluene. American Journal of Ophthalmology 95:807-810.

21. Hathaway J. A. 1985. Subclinical effects of trinitrotoluene: A review of epidemiology studies. In: Rickett DE, ed. Toxicity of nitroaromatic compounds. New York, NY: Hemisphere Publishing Corporation, 255-274.

22. Hawari, J., A. Halasz, S. Beaudet, L. Paquet, G. Ampleman, and S. Thiboutot. 1999. Biotransformation of 2,4,6-trinitrotoluene with *Phanerochaete chrysosporium* in agitated cultures at pH 4.5. Applied and Environmental Microbiology 65:2977-2986.

23. Heiss, G., and H. J. Knackmuss. 2002. Bioelimination of trinitroaromatic compounds: immobilization versus mineralization. Current Opinion in Microbiology 5:282-287.

24. Hofstetter, T. B., C. G. Heijman, S. B. Haderlein, C. Holliger, and R. P. Schwarzenbach. 1999. Complete reduction of TNT and other (poly)nitroaromatic compounds under iron reducing subsurface conditions. Environmental Science & Technology 33:1479-1487.

25. Honeycutt, M. E., A. S. Jarvis, and V. A. McFarland. 1996. Cytotoxicity and mutagenicity of 2,4,6-trinitrotoluene and its metabolites. Ecotoxicology and Environmental Safety 35:282-287.

26. Huang, S. Q., P. A. Lindahl, C. Y. Wang, G. N. Bennett, F. B. Rudolph, and J. B. Hughes. 2000. 2,4,6-trinitrotoluene reduction by carbon monoxide dehydrogenase from *Clostridium thermoaceticum*. Applied and Environmental Microbiology 66:1474-1478.

27. Hughes, J. B., C. Wang, K. Yesland, A. Richardson, R. Bhadra, G. Bennett, and F. Rudolph. 1998. Bamberger rearrangement during TNT metabolism by *Clostridium acetobutylicum*. Environmental Science & Technology 32:494-500.

28. Hundal, L. S., J. Singh, E. L. Bier, P. J. Shea, S. D. Comfort, and W. L. Powers. 1997. Removal of TNT and RDX from water and soil using iron metal. Environmental Pollution 97:55-64.

29. Jain, M. R., S. S. Zinjarde, D. D. Deobagkar, and D. N. Deobagkar. 2004. 2,4,6-Trinitrotoluene transformation by a tropical marine yeast, *Yarrowia lipolytica* NCIM 3589. Marine Pollution Bulletin 49:783-788.

30. Jiang, Q. G., J. G. Sun, and X. F. Qin. 1991. The effects of trinitrotoluene on zinc and copper metabolism. Toxicology Letters 55:343-349.

31. Khan, H., R. J. Harris, T. Barna, D. H. Craig, N. C. Bruce, A. W. Munro, P. C. E. Moody, and N. S. Scrutton. 2002. Kinetic and structural basis of reactivity of pentaerythritol tetranitrate reductase with NADPH, 2-cyclohexenone, nitroesters, and nitroaromatic explosives. Journal of Biological Chemistry 277:21906-21912.

32. Klausen, J., S. P. Trober, S. B. Haderlein, and R. P. Schwarzenbach. 1995. Reduction of substituted nitrobenzenes by Fe(II) in aqueous mineral suspensions. Environmental Science & Technology 29:2396-2404.

33. Leibzon, V. N., A. P. Churilina, M. Y. Leonova, L. V. Mikhal'chenko, and A. K. Shakhnes. 2000. Regioselectivity of partial chemical and electroreduction of 2,4,6-trinitrotoluene. Russian Journal of Electrochemistry 36:170-173.

34. Lewis, T. A., D. A. Newcombe, and R. L. Crawford. 2004. Bioremediation of soils contaminated with explosives. Journal of Environmental Management 70:291-307.

35. Liu, Y. Y., M. Yao, J. L. Fang, and Y. W. Wang. 1995. Monitoring human risk and exposure to trinitrotoluene (TNT) using hemoglobin adducts as biomarkers. Conference proceedings. 281-287.

36. Lovley, D. R., and E. J. P. Phillips. 1986. Organic-matter mineralization with reduction of ferric iron in anaerobic sediments. Applied and Environmental Microbiology 51:683-689.

37. Lovley, D. R., and E. J. P. Phillips. 1987. Rapid assay for microbially reducible ferric iron in aquatic sediments. Applied and Environmental Microbiology 53:1536-1540.

38. Morton, A. R., M. V. Ranadive, and J. A. Hathaway. 1976. Biological effects of trinitrotoluene from exposure below threshold limit value. American Industrial Hygiene Association Journal 37:56-60.

39. Naumov, A. V., E. S. Suvorova, A. M. Boronin, S. K. Zaripova, and R. P. Naumova. 1999. Transformation of 2,4,6-trinitrotoluene into toxic hydroxylamino derivatives by lactobacilli. Microbiology 68:46-51.

40. Pak, J. W., K. L. Knoke, D. R. Noguera, B. G. Fox, and G. H. Chambliss. 2000. Transformation of 2,4,6-trinitrotoluene by purified xenobiotic reductase B from *Pseudomonas fluorescens* I-C. Applied and Environmental Microbiology 66:4742-4750.

41. Rieger, P. G., H. M. Meier, M. Gerle, U. Vogt, T. Groth, and H. J. Knackmuss. 2002. Xenobiotics in the environment: present and future strategies to obviate the problem of biological persistence. Conference proceedings. 101-123.

42. Rieger, P. G., V. Sinnwell, A. Preuss, W. Francke, and H. J. Knackmuss. 1999. Hydride-Meisenheimer complex formation and protonation as key reactions of 2,4,6-trinitrophenol biodegradation by *Rhodococcus erythropolis*. Journal of Bacteriology 181:1189-1195.

43. Schwarzenbach, R. P., R. Stierli, K. Lanz, and J. Zeyer. 1990. Quinone and iron poryphrin mediated reduction of nitroaromatic compounds in homogenous aqueous-solution. Environmental Science & Technology 24:1566-1574.

44. Smith, Q. C. 1918. Trinitrotoluenes and mono- and dinitrotoluenes their manufacture and properties. D. Van Norstrand Company. New York, NY.

45. Stumm, W. and J. J. Morgan. 1981. Aquatic Chemistry, 2nd ed. Wiley: New York, NY.

46. Timmis, K. N., and D. H. Pieper. 1999. Bacteria designed for bioremediation. Trends in Biotechnology 17:201-204.

47. Van Dillewijn, P., A. Caballero, J. A. Paz, M. M. Gonzalez-Perez, J. M. Oliva, and J. L. Ramos. 2007. Bioremediation of 2,4,6-trinitrotoluene under field conditions. Environmental Science & Technology 41:1378-1383.

48. van Dillewijn, P., R. M. Wittich, A. Caballero, and J. L. Ramos. 2008. Type II hydride transferases from different microorganisms yield nitrite and diarylamines from polynitroaromatic compounds. Applied and Environmental Microbiology 74:6820-6823.

49. Vanderberg, L. A., J. J. Perry, and P. J. Unkefer. 1995. Catabolism of 2,4,6-trinitrotoluene by *Mycobacterium-vacce*. Applied Microbiology and Biotechnology 43:937-945.

50. Vorbeck, C., H. Lenke, P. Fisher, and H. J. Knackmuss. 1994. Identification of a hydride-Meisenheimer complex as a metabolite of 2,4,6-trinitrotoluene by a *Mycobacterium* strain. Journal of Bacteriology 176:932-934.

51. Wang, C. Y., D. D. Zheng, and J. B. Hughes. 2000. Stability of hydroxylamino- and amino-intermediates from reduction of 2,4,6-trinitrotoluene, 2,4-dinitrotoluene, and 2,6-dinitrotoluene. Biotechnology Letters 22:15-19.

52. Williams, R. E., D. A. Rathbone, N. S. Scrutton, and N. C. Bruce. 2004. Biotransformation of explosives by the old yellow enzyme family of flavoproteins. Applied and Environmental Microbiology 70:3566-3574.

53. Wittich R., A. Haidour, P. van Dillewijn, and J. Ramos. 2008. OYE flavoprotein reductases initiate the condensation of TNT-derived intermediates to secondary diarylamines and nitrite. Environ. Sci. Technol. 42:734-739.

54. Wittich R., P. van Dillewijn, and J. Ramos. 2009. Microorganisms and explosives: mechanisms of nitrogen release from TNT for use as an N-source for growth. Environ. Sci. Technol. 43:2773-2776.

55. Zaripov, S. A., A. V. Naumov, E. V. Nikitina, and R. P. Naumova. 2002. Alternative pathways of the initial transformation of 2,4,6-trinitrotoluene by yeasts. Microbiology 71:558-562.

56. Zaripov, S. A., A. V. Naumov, E. S. Suvorova, A. V. Garusov, and R. P. Naumova. 2004. Initial stages of 2,4,6-trinitrotoluene transformation by microorganisms. Microbiology 73:398-403.

57. Zarlpov, S. A., A. V. Naumov, J. F. Abdrakhmanova, A. V. Garusov, and R. P. Naumma. 2002. Models of 2,4,6-trinitrotoluene (TNT) initial conversion by yeasts. Fems Microbiology Letters 217:213-217.

58. Ziganshin, A. M., R. Gerlach, T. Borch, A. V. Naumov, and R. P. Naumova. 2007. Production of eight different hydride complexes and nitrite release from 2,4,6-trinitrotoluene by *Yarrowia lipolytica*. Applied and Environmental Microbiology 73:7898-7905.